DOI:10.14753/SE.2019.2291

ROLE OF CANCER STEM CELLS AND CLAUDINS IN THE PATHOGENESIS OF HEPATOCELLULAR CARCINOMA AND METASTATIC LIVER CANCER

Doctoral thesis

Ágnes Holczbauer, M.D.

Pathology Doctoral School

Semmelweis University

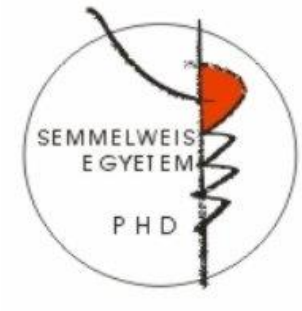

Supervisor: András Kiss, M.D., D.Sc.

Official reviewers: Veronika Papp, M.D., Ph.D.
János Nacsa, M.D., Ph.D.

Head of the Final Examination Committee:
Zoltán Sápi, M.D., D.Sc.

Members of the Final Examination Committee:
Krisztina Hagymási, M.D., Ph.D.
Károly Simon, M.D., Ph.D.

Budapest
2019

DOI:10.14753/SE.2019.2291

TABLE OF CONTENTS

DOI:10.14753/SE.2019.2291

DOI:10.14753/SE.2019.2291

DOI:10.14753/SE.2019.2291

LIST OF ABBREVIATIONS

ABC	ATP-binding cassette family of membrane transport proteins
AFP	alpha-fetoprotein
AH	adult hepatocyte
APC	adenomatous polyposis coli/allophycocyanin
BVES	blood vessel epicardial substance
CAG	chicken β-actin gene promoter/CMV enhancer
CCA	cholangiocarcinoma
CD	cluster of differentiation
CEA	carcinoembryonic antigen
CHC	combined hepatocellular and cholangiocarcinoma
CI	confidence interval
CK	cytokeratin
CLDN	claudin
c-Myc	avian myelocytomatosis viral oncogene homolog
CPE	*Clostridium perfringens* enterotoxin
CRC	colorectal cancer
CRLM	liver metastasis of colorectal adenocarcinoma
CSC	cancer stem cell
DDC	3,5-diethoxycarbonyl-1,4-dihydrocollidine
DMEM	Dulbecco's modified Eagle's medium
DNA	2’-deoxyribonucleic acid
DPPIV	dipeptidyl peptidase IV
EGF	epidermal growth factor
EGFP	enhanced green fluorescent protein
EMT	epithelial-mesenchymal transition
EpCAM	epithelial cell adhesion molecule
ESC	embryonic stem cell
FACS	fluorescence-activated cell sorting
FBS	fetal bovine serum
FerH	human ferritin heavy chain promoter/SV40 enhancer

FCM	flow cytometry
FDR	false discovery rate
FFPE	formalin-fixed, paraffin-embedded
Gapdh	glyceraldehyde-3-phosphate dehydrogenase
GSEA	gene set enrichment analysis
HB	hepatoblast
HBSS	Hanks' balanced salt solution
HBV	hepatitis B virus
HCC	hepatocellular carcinoma
HCV	hepatitis C virus
HEK	human embryonic kidney cells
HepPar-1	anti-hepatocyte paraffin 1
HIV	human immunodeficiency virus
HNF4a	hepatocyte nuclear factor 4 alpha
HPC	hepatic progenitor cell
H-Ras	Harvey rat sarcoma viral oncogene homolog
HRP	horseradish peroxidase
HSC	hepatic stem cell
ICC/IF	fluorescence immunocytochemistry
IHC-P	immunohistochemistry on FFPE sample
iPSC	induced pluripotent stem cell
IRES	internal ribosome entry site
JAM	junctional adhesion molecule
MACS	magnetic-activated cell sorting
MAGI	MAGUK with inverted orientation
MAGUK	membrane-associated guanylate kinase
MAPK	mitogen-activated protein kinase
MARVELD3	MAL and related proteins for vesicle trafficking and membrane link domain protein 3
miRNA	microRNA
MMP	matrix metalloproteinase
MUPP1	multi-PDZ domain protein 1

NES	normalized enrichment score
NIH	National Institutes of Health
NL	normal liver
NOD/SCID	non-obese diabetic/severe combined imunodeficient
PATJ	PALS1-associated tight junction protein
PBS	phosphate buffered saline
PDAC	pancreatic ductal adenocarcinoma
PE	phycoerythrin
PLC	primary liver cancer
PLM	liver metastasis of pancreatic adenocarcinoma
qRT-PCR	quantitative reverse transcription polymerase chain reaction
RNA	ribonucleic acid
Sca-1	stem cell antigen-1
sHCC	scirrhous HCC
shRNA	short hairpin RNA
SL	surrounding non-tumorous liver
SP	side population
SV40LT	simian virus 40 large T antigen
T-AH/T-HB/T-HPC	H-Ras-EGFP^{+}/SV40LT-mCherry^{+} AH/HB/HPC
TERT	telomerase reverse transcriptase
TGF-β	transforming growth factor beta
TIF	frequency of tumor-initiating cells
TJ	tight junction
TP53	cellular tumor antigen p53
v-H-Ras	constitutively active form of H-Ras
VSV-G	vesicular stomatitis virus G
WB	western blotting
Wnt	wingless-related integration site
ZO-1/-2/-3	zonula occludens-1/-2/-3

DOI:10.14753/SE.2019.2291

1. INTRODUCTION

1.1 Hepatocellular carcinoma

1.1.1 Epidemiology and risk factors

Primary liver cancer is the sixth most common cancer worldwide, with more than 850,000 new cases annually, and it is the second most common cause of cancer-related death. The prognosis is very poor, the overall ratio of mortality to incidence is 0.95.[1] Hepatocellular carcinoma (HCC) represents approximately 90 percent of primary liver cancer cases. HCC is more common in males, the male/female ratio is about 3-5/1.[2] The majority of cases occurs after the age of 40, and it reaches a peak at around the age of 70.[3] HCC incidence rates are the highest in areas with endemic hepatitis B virus (HBV) infection, such as Eastern Asia and sub-Saharan Africa (> 20 per 100,000).[4] In particular, China accounts for about 50 percent of all HCC cases worldwide.[1] Mongolia has the world's highest incidence of HCC with a rate of 78 per 100,000 individuals, about 8 times the global average.[5] Southern European countries have intermediate incidence rates of 10-20 per 100,000 individuals. Areas with low incidence (< 5 per 100,000) are found in South-Central Asia, North and South America, and Northern, Central, and Eastern Europe.[1, 4] Interestingly, HCC rates are increasing in the low-rate areas, which could be attributed to increases in chronic hepatitis C virus (HCV) infection, obesity, and type 2 diabetes. In contrast, HCC incidence is decreasing in many high-rate areas, most likely because of declining incidence of in HCV and HBV infection.[1]

Unlike most cancer types, HCC has well-established environmental and endogenous risk factors.[6] In approximately 70 percent of cases, HCC occurs on a background of hepatic cirrhosis, whereas in 15-20 percent of cases it develops in non-fibrotic liver or in livers with minimal portal fibrosis. Annual incidence rates of HCC in patients with cirrhosis are 2-6 percent.[7, 8] Major risk factors for developing cirrhosis are chronic HBV and HCV infection, half of all HCC cases are associated with HBV infection, with 25 percent associated with HCV infection.[9, 10] Aflatoxin B1, a mycotoxin present in a variety of food commodities in Asia and sub-Saharan Africa, acts in synergism with HBV.[11] Heavy alcohol intake (> 60 g/day) also increases the risk of HCC through the development of

cirrhosis and has a synergistic effect with HCV and HBV infection.[4] The prevalence of metabolic syndrome, a collection of problems, including insulin resistance, obesity, hyperlipidemia, and hypertension, is increasing worldwide. It has recently been recognized as a risk factor for HCC because of the associated non-alcoholic fatty liver disease and non-alcoholic steatohepatitis.[12] Other risk factors include anabolic steroids, oral contraceptives, autoimmune hepatitis, cholestatic liver diseases, hypothyreosis, hereditary hemochromatosis, and α-1 antitrypsin deficiency.[5]

1.1.2 Morphology and histology

Hepatocarcinogenesis is a multistep process that usually takes place in the context of liver cirrhosis. Cirrhosis is characterized by an exhaustion of the regenerative capacity of the liver, and the replacement of normal liver tissue by fibrous tissue. The first step of HCC development in cirrhotic liver is the appearance of microscopic dysplastic foci (< 1 mm in diameter). Dysplastic foci are composed of dysplastic hepatocytes and display a spectrum of cytologic abnormalities, among which small cell change is regarded as premalignant. Dysplastic nodules are macroscopically detectable, distinctly nodular lesions (> 1 mm in diameter) that may also appear in chronic liver disease without cirrhosis. Dysplastic nodules are classified as low-grade and high-grade dysplastic nodules according to the degree of cellular atypia and can be difficult to distinguish from large regenerative nodules. High-grade dysplastic nodules are characterized by moderate cytologic or architectural atypia and an increased risk of malignant transformation.[8, 13]

Based on clinicopathological studies, HCCs can be divided into early and progressed carcinomas. Early HCCs are small (< 2 cm), vaguely nodular, well-differentiated lesions that consist of small neoplastic cells arranged in irregular, thin trabeculae and pseudoglandular structures. Invasion into portal tracts and fibrous septa is frequently observed; however, early HCC does not show vascular invasion. Progressed HCCs are larger than 2 cm or small (< 2 cm), but moderately differentiated, distinctly nodular lesions (**Figure 1**).[13, 14] By gross appearance, progressed HCC can be classified as nodular, massive (large tumor with irregular demarcation) and diffuse (many small nodules in a lobe or the whole liver). Tumors are generally soft because of lack of a desmoplastic stroma. Fibrous capsule formation and the presence of unpaired arteries within the tumor

nodule are characteristic features of progressed HCC. Vascular invasion with involvement of portal veins is also frequently seen.

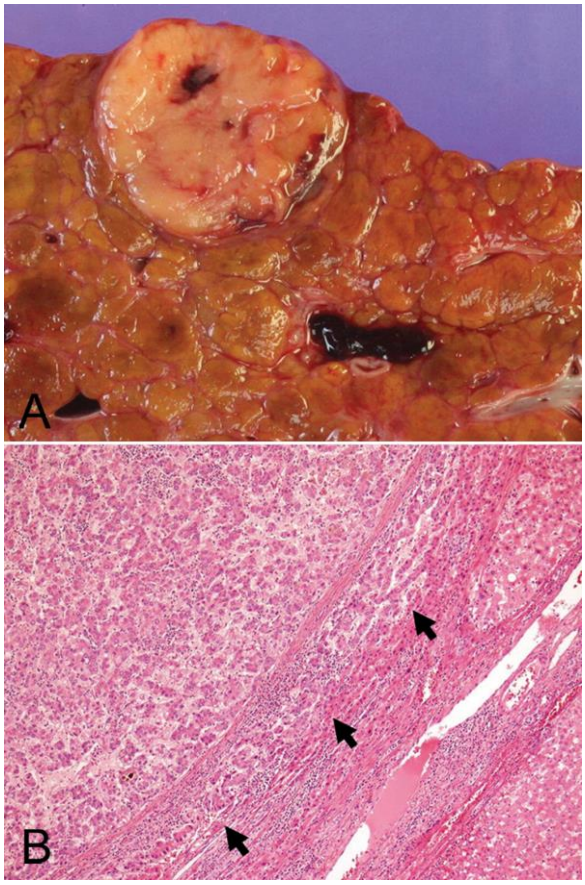

Figure 1. Progressed, small hepatocellular carcinoma. Adapted from Park.[13] (A) Macroscopic features of progressed, small hepatocellular carcinoma. Note the distinctively nodular appearance with tumor capsule in cirrhosis. (B) Microscopic features of moderately differentiated, progressed, small hepatocellular carcinoma. Arrows indicate invasion of the tumor capsule. Hematoxylin-eosin stain, original magnification ×200.

The WHO describes several histologic patterns of HCC: trabecular (micro- and macrotrabecular), acinar (pseudoglandular), solid (compact), and scirrhous. Clear cell HCC and fibrolamellar HCC are recognized as rare variants. The most common growth pattern is trabecular, where thick cords of neoplastic cells are separated by sinusoids, resembling the cell plates and sinusoids of normal liver. Acinar pattern is characterized by gland-like structures formed by dilated bile canaliculi that may contain bile or proteinaceous material. Scirrhous HCC (sHCC) is composed of small tumor nests divided by abundant desmoplastic stroma. Fibrolamellar HCC has clinicopathologic features distinct

from classic HCC. It typically occurs in young adults in a non-cirrhotic liver, has no gender predilection and no known risk factors. Tumor cells in HCC are usually polygonal, have eosinophilic, finely granular cytoplasm and hyperchromatic nuclei with prominent nucleoli. Mallory-Denk bodies, pale bodies, lipid deposition, glycogen, and bile can also be present within the tumor cells.[8, 15]

1.1.3 Diagnosis

In early stages, HCC is usually asymptomatic making clinical diagnosis difficult. The majority of patients are diagnosed at an advanced stage with large, symptomatic tumors and/or portal vein invasion. Symptoms and signs include abdominal discomfort, jaundice, ascites, hepatic encephalopathy, splenomegaly, fever, anorexia, weight loss, and malaise.[16, 17] Current clinical guidelines recommend surveillance of HCC in patients at risk for HCC. Surveillance involves the repeated application of screening tools to detect the disease at an early stage in order to reduce mortality. Surveillance of HCC is recommended in all cirrhotic patients and in some non-cirrhotic patients with chronic liver disease, especially in HBV carriers with serum viral load > 10^4 copies/mL or HCV infected patients with bridging fibrosis. Surveillance of patients at risk should be carried out by abdominal ultrasound every 6 months.[16, 18] The measurement of alpha-fetoprotein (AFP) or other serum biomarkers alone or in combination with ultrasound is not recommended for surveillance.[5]

In cirrhotic patients, hepatic nodules smaller than 1 cm are followed by ultrasound until further progression, since the likelihood that these small lesions are HCC is low. Hepatic nodules larger than 1 cm in diameter are investigated further with multiphase contrast-enhanced computed tomography or magnetic resonance imaging. For nodules of 1-2 cm in diameter, diagnosis is based on characteristic radiological findings (so called ‘non-invasive criteria’) or biopsy. Nodules larger than 2 cm in diameter can be diagnosed as HCC based on characteristic findings on one imaging modality. Typical hallmark of HCC is a robust arterial phase enhancement with washout in the portal venous or delayed phases. Biopsy is recommended to confirm the diagnosis for cases with inconclusive or atypical imaging appearance in cirrhotic livers and for all nodules that occur in non-cirrhotic livers.[17, 19, 20] Core liver biopsy is superior to fine needle aspiration, because both

architectural and cytologic features can be evaluated in biopsy specimen.[21] Negative biopsy result may warrant a second sample if the suspicion of HCC is suffciently strong. Pathological diagnosis of HCC is based on the recommendations of the International Consensus Group for Hepatocellular Neoplasia.[19, 21] They recommend immunostainings for a combination of different markers (glypican 3, heat schock protein 70, and glutamine synthetase) to differentiate high grade dysplastic nodules from early HCC. Additional immunostainings for cytokeratin 19 (CK19), epithelial cell adhesion molecule (EpCAM), or CD34 can be performed to detect progenitor cell features or assess neovascularisation.

1.1.4 Molecular pathogenesis

1.1.4.1 Genetic and epigenetic alterations

HCC is a complex, genetically and phenotypically heterogeneous malignancy. The development of HCC is a slow, multistep process during which genetic and epigenetic changes in cellular proto-oncogenes and tumor suppressor genes, and subsequent disruption of specific pathways progressively alter the hepatocellular phenotype.[22] Oncogene activation can arise through mutations, copy number alterations, chromosome rearrangements, or epigenetic changes; inactivation of tumor suppressor genes can result from mutations, loss of heterozygosity, or epigenetic silencing (**Table 1**).[5, 23]

Elucidating the early and late events of hepatocarcinogenesis has gathered momentum by recent advances in molecular biological techniques, the latest being the next-generation sequencing technologies. A major goal of large-scale genome sequencing studies has been to find cancer driver genes. A cancer driver would be a cell-autonomous or non-cell-autonomous alteration that contributes to tumor evolution at any stage by promoting proliferation, survival, invasion, or immune evasion.[24] Cancer driver genes are defined as those for which the rate of non-silent mutations is significantly greater than a background (or passanger) mutation rate estimated from silent mutations.[25] Exome sequencing analysis of 243 HCCs revealed a median of 64 non-silent and 21 silent mutations per tumor (ranging from 1 to 706 mutations), corresponding to a mean somatic mutation rate of 1.3 mutations per megabase in coding sequences.[26] By integration of mutations, focal amplifications, and homozygous deletions, 161 putative driver genes were identified. The genetic alterations centered on *CTNNB1*, *AXIN1*, and *TP53*, forming three major clusters. Eleven pathways were recurrently altered in ≥ 5% of HCCs: telomerase

reverse transcriptase (TERT) promoter mutations activating telomerase expression, Wnt/β-catenin, PI3K-AKT-mTOR, TP53/cell cycle, mitogen-activated protein kinase (MAPK), hepatic differentiation, epigenetic regulation, chromatin remodeling, oxidative stress, IL-6/JAK-STAT, and transforming growth factor beta (TGF-β).[26]

Table 1. Major genetic alterations observed in advanced hepatocellular carcinoma. Adapted from Llovet et al.[5]

Pathway(s)	Gene(s)	Alteration	Frequency in HCC
Telomere maintenance	*TERT*	Promoter mutation	54-60%
		Amplification	5-6%
Cell cycle control	*TP53*	Mutation or deletion	12-48%
	RB1	Mutation or deletion	3-8%
	CCND1	Amplification	7%
	CDKN2A	Mutation or deletion	2-12%
Wnt-β-catenin signalling	*CTNNB1*	Mutation	11-37%
	AXIN1	Mutation or deletion	5-15%
Oxidative stress	*NFE2L2*	Mutation	3-6%
	KEAP1	Mutation	2-8%
Epigenetic and chromatin remodelling	*ARID1A*	Mutation or deletion	4-7%
	ARID2	Mutation	3-18%
	KMT2A (*MLL1*), *KMT2B* (*MLL4*), *KMT2C* (*MLL3*), and *KMT2D* (*MLL2*)	Mutation	2-6%
AKT-mTOR-MAPK signalling	*RPS6KA3*	Mutation	2-9%
	TSC1 and *TSC2*	Mutation or deletion	3-8%
	PTEN	Mutation or deletion	1-3%
	FGF3, *FGF4*, and *FGF19*	Amplification	4-6%
	PI3KCA	Mutation	0-2%
Angiogenesis	*VEGFA*	Amplification	3-7%

ARID, AT-rich interaction domain; *AXIN1*, axin 1; *CCND1*, cyclin D1; *CDKN2A*, cyclin-dependent kinase inhibitor 2A; *CTNNB1*, β-catenin; *FGF*, fibroblast growth factor; HCC, hepatocellular carcinoma; *KEAP1*, kelch like ECH associated protein 1; *KMT*, lysine (K)-specific methyltransferase; MAPK, mitogen-activated protein kinase; *MLL*, myeloid/lymphoid or mixed-lineage leukaemia (trithorax homologue, *Drosophila*); mTOR, mammalian target of rapamycin; *NFE2L2*, nuclear factor, erythroid 2 like 2; *PI3K*, phosphoinositide 3-kinase; *PTEN*, phosphatase and tensin homologue; *RB1*, retinoblastoma 1; *RPS6KA3*, ribosomal protein S6 kinase, 90kDa, polypeptide 3; *TERT*, telomerase reverse transcriptase; *TP53*, cellular tumor antigen p53; *TSC*, tuberous sclerosis; *VEGFA*, vascular endothelial growth factor A; Wnt, wingless-related integration site.

The Cancer Genome Atlas Research Network has recently published the results of the first large-scale multi-platform analysis of HCC.[27] The most common somatic mutation was *TERT* promoter mutation, found in 44 percent of all HCC cases. In total, 26 cancer driver genes were identified, of which 18 were previously reported in various studies, including *TP53*, *CTNNB1*, *ALB*, *AXIN1*, *APOB*, *KRAS*, and *NRAS*.[5, 26] The most frequent chromosomal arm alterations included copy number gains in 1q and 8q, and copy number losses in 8p and 17p. Twenty-eight significantly reoccurring focal amplifications and 36 deletions were identified in the tumors. The focal amplifications contained previously described driver oncogenes such as *MCL1* (1q21.3), *MYC* (8q24.21), *CCND1* and *FGF19* (11q13.3), *MET* (7q31.2), and *VEGFA* (6p21.1). Amplification of *TERT* (5p15.33) was found in 10 percent of HCCs. Among the deletions, 13q14.2 (*RB1*), 9p21.3 (*CDKN2A*), 1p36.23 (*ERRFI1*), and 17p11.2 (*NCOR1*) were significant.[27]

Epigenetic mechanisms, including covalent modification of DNA and histone proteins that changes gene expression without affecting the DNA sequence, are frequently deregulated in HCC. Similarly to other cancer types, HCC is characterized by a global loss of DNA methylation and selective hypermethylation of gene promoters. Demethylation largely affects the intergenic and intronic regions of the DNA leading to genomic instability. Hypermethylation of CpG islands within gene promoters usually leads to gene silencing. Frequent hypermethylation of *APC* (81.7%), *GSTP1* (76.7%), *RASSF1A* (66.7%), *CDKN2A* (48.3%), *PTGS2* (35%), *CDH1* (33.3%), *DLC1* (24%), and *TP53* (14.2%) have been described.[28-30] Moreover, Villanueva et al. identified IGF, PI3K, TGF-β, and Wnt signaling pathways as clearly deregulated by DNA methylation in HCC.[31] Histone modifications, such as methylation, phosphorylation, acetylation, and ubiquitination are complex alterations on the amino-terminal tails that can regulate gene expression by altering chromatin structure or recruiting histone modifiers.

Significant associations between risk factors and mutations were observed. HCCs related to alcohol abuse are significantly enriched in *TERT*, *CTNNB1*, *CDKN2A*, *SMARCA2*, and *HGF* alterations.[26] Hepatitis B virus can induce mutagenesis by inserting viral DNA into the genome of hepatocytes.[32] Integration of HBV DNA most frequently occurs within the *TERT* promoter and activates telomerase and other oncogenes, including *KMT2B* (*MLL4*), *CCNE1*, and *SENP5*.[33] Aflatoxin B1 exposure, in cooperation with

HBV infection, induces DNA adducts and the occurrence of frequent mutations, particularly in *TP53*.[26] In contrast, HCV infection and metabolic syndrome are not associated with genetic alterations.

Genetic alterations associated with the multistep development of HCC have also been intensively studied. Marquardt et al. found that the number of exonic somatic mutations with a potentially damaging effect was low in low-grade dysplastic nodules (5), high-grade dysplastic nodules (4), and early HCC (2) but drastically increased during conversion to progressed HCC (110). Activation of prognostically adverse signaling pathways occurred only late during hepatocarcinogenesis and was centered on key oncogenic drivers, such as *TGFB1*, *MYC*, *MET*, *WNT1*, *NOTCH1*, and pro-metastatic/epithelial-mesenchymal transition (EMT) genes.[34] Similarly, Schulze et al. described progressive accumulation of mutations and chromosome aberrations during progression, with chromosome aberrations appearing later than gene mutations.[26] *TERT* activation, that allows uncontrolled hepatocyte proliferation, was identified as the earliest recurrent genetic event in cirrhotic preneoplastic nodules.

1.1.4.2 Molecular classification

Gene expression profiling and analysis of genetic and epigenetic alterations provided basis for molecular classification of HCC with prognostic implications and potential targets for targeted therapies. Integration of molecular subclasses reported by different investigators revealed that HCCs can be divided into proliferation and non-proliferation subtypes, each representing about 50 percent of patients (**Figure 2**).[35-38]

Proliferation subclass is characterized by activation of signaling pathways related to cell proliferation and cell cycle progression and is associated with a more aggressive phenotype. These pathways include RAS/MAPK, AKT/mTOR, MET, TGF-β, IGF, and NOTCH signaling. Notably, this class is also enriched in progenitor cell markers, such as EpCAM and AFP. HCCs related to HBV infection predominantly belong to the proliferation subclass. In the non-proliferation subclass, up to 25 percent of cases are characterized by activation of canonical Wnt signaling and *CTNNB1* mutations, whereas other cases display predominantly inflammation-related traits. Gene expression profiles of tumors in this subclass resemble that of normal hepatocytes. Non-proliferative HCCs are less aggressive and frequently associated with human immunodeficiency virus (HIV) infection or alcohol abuse.

DOI:10.14753/SE.2019.2291

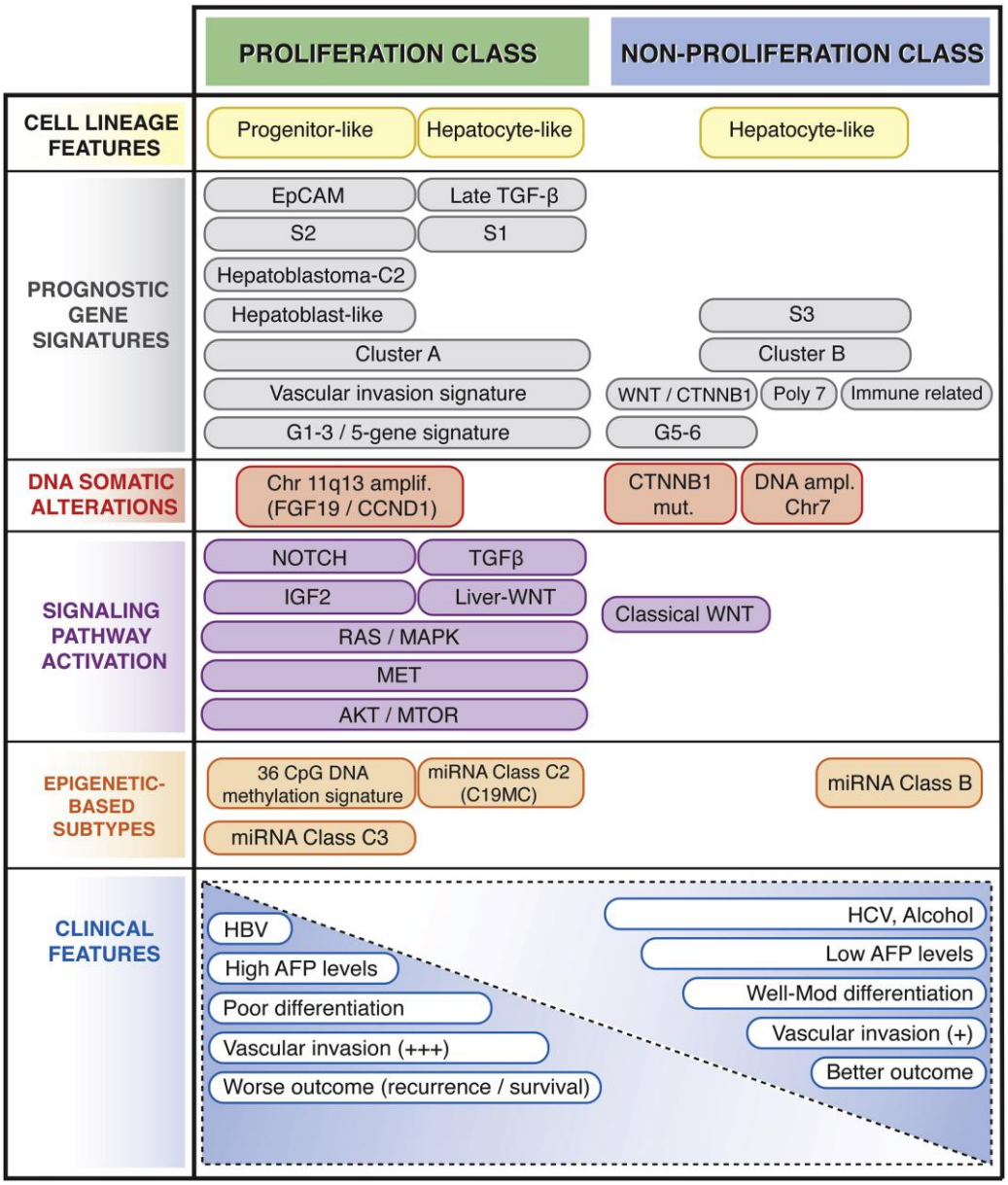

Figure 2. Molecular classification of hepatocellular carcinoma. Adapted from Zucman-Rossi et al.[38] Proliferation and non-proliferation classes are depicted based on transcriptome profiling with overlapping genetic, epigenetic, and clinical features. AFP, alpha-fetoprotein; EpCAM, epithelial cell adhesion molecule; HBV, hepatitis B virus; HCV, hepatitis C virus; IGF2, insulin-like growth factor 2; MET, hepatocyte growth factor receptor; RAS, rat sarcoma viral oncogene homolog; TGF-β, transforming growth factor beta.

DOI:10.14753/SE.2019.2291

1.2 Secondary liver cancer

The liver is one of the most common sites for metastasic disease, which confers a bad prognosis, as metastatic lesions disrupt the function of the liver, leading to hepatic failure.[39] Secondary liver cancers are far more frequent than primary liver cancers, representing 95 percent of all hepatic malignancies.[40] In the majority of secondary liver cancer cases, the primary tumors originate from the gastrointestinal tract because of the venous drainage of gastrointestinal organs through the hepatic portal system. Other common sites of primary tumors include breast, lung, and genitourinary system.[41, 42] Histologically, adenocarcinomas are the most frequent subtype of liver metastases, followed by squamous cell carcinomas and neuroendocrine carcinomas. Adenocarcinomas are also the most frequent cancer type found in the liver in patients with neoplasms of unknown primary site.[43, 44]

1.2.1 Metastatic process

The capability to invade adjacent tissues and metastasize is one of the hallmarks of cancer.[45] The basic steps of metastasis formation has been excessively studied over the past century. These include local invasion, intravasation into adjacent vessels, survival of the cells in the circulation, extravasation into the surrounding tissue, and initiation and growth of metastatic tumors.[46, 47] Cancer cells that escaped from the primary tumor can enter the liver through the hepatic artery or the portal vein. The arterial and portal blood mixes within the hepatic sinusoids, where metastatic cells encounter the liver unique immune defence mechanisms.[48] This immune surveillance includes Kupffer cells, liver-specific natural killer cells, and hepatic sinusoidal endothelial cells. Kupffer cells are liver-specific macrophages that reside in the wall of the sinusoids.[49] Hepatic natural killer cells (known as ‘pit cells’ in the rat liver) show morphological similarity to large granular lymphocytes and exert cytotoxic activity.[50, 51] The interactions with Kupffer cells, natural killer cells, and hepatic sinusoidal endothelial cells lead to the death of over 90 percent of metastatic cells, whereas the surviving cells adhere to the endothelial cells and migrate through the hepatic endothelium. Tumor cell invasion into the extrasinusoidal space trigger the activation of hepatic stellate cells and Kupffer cells. Activated hepatic stellate cells release various factors, including growth factors and matrix metalloproteinases

(MMPs), produce excessive extracellular matrix proteins, and contribute to neoangiogenesis and metastasic growth.[52]

Secondary liver cancer classically presents as multiple, well-demarcated, white-yellow lesions, however, single massive nodules or infiltrative lesions can also be found. A fibrous capsule around the metastatic tumor or microcalcifications are infrequently present.[53] Necrotic areas are often found in the center of large metastatic tumors.

1.2.2 Colorectal cancer liver metastases

Colorectal cancer (CRC) is a common and lethal disease. Globally, it is the third most common cancer and the fourth leading cause of cancer-related deaths.[54] In Hungary, CRC is the second leading cause of cancer death.[55] Approximately 20 percent of patients have synchronous liver metastasis at the time of diagnosis, and up to 40 percent of patients develop metachronous liver metastases.[56-58] Development of liver metastases confers a poor prognosis, about 90 percent of patients who die from CRC have liver metastases.[59]

Histologically, over 90 percent of CRCs are adenocarcinomas, variants of which include mucinous and signet-ring cell adenocarcinomas.[60] Histological subtype has been suggested to influence the metastatic pattern of CRC. Mucinous and signet-ring cell adenocarcinoma were more frequently associated with peritoneal than liver metastases.[61, 62] Well and moderately differentiated, columnar shaped metastatic CRC cells form glandular structures, poorly differentiated liver metastases show almost entirely solid growth pattern. Metastatic cells from mucinous or signet-ring cell carcinoma produce abundant mucin.

1.2.3 Pancreatic cancer liver metastases

Pancreatic cancer is the fourth most fatal cancer worldwide, as well as in Hungary.[55, 63] Pancreatic ductal adenocarcinoma (PDAC) arises from the ductal epithelium and represents 95 percent of pancreatic cancer cases.[64] It has very poor prognosis, the incidence and mortality rates are nearly equal. Approximately 50 percent of the patients are initially diagnosed with distant metastases. The most common site of metastasis is the liver, followed by the peritoneum and lung. At autopsy, about 60 percent of patients had hepatic metastases, even small (< 2 cm) tumors were associated with metastatic disease.[42,

[65] Microscopically, poorly differentiated metastatic tumors are more frequent than well-differentiated duct-forming carcinomas. The extensive fibrosis termed desmoplasia that occur in primary carcinomas are also observed in metastatic lesions.[66]

1.2.4 Differential diagnosis of HCC and metastatic adenocarcinoma

Differentiating HCC from metastatic adenocarcinoma, especially moderately and poorly differentiated HCC from poorly differentiated metastatic adenocarcinoma, and identifying the site of origin for metastatic adenocarcinoma can be challenging for pathologists. Diagnosis often requires additional immunohistochemical work-up besides routine histopathology. Tumor samples can be obtained through image-guided sampling using fine needle aspiration and needle core biopsy techniques or surgical resection. Several studies aimed to find the most effective immunohistochemical panel that aids in the differential diagnosis (**Table 2**). Ideally, this panel would consist of as few markers as possible with high sensitivity and specificity.[8, 44, 67]

The most commonly used antibody to identify benign or malignant hepatocytes is hepatocyte paraffin 1 (HepPar-1), a monoclonal antibody that recognizes an antigen specific for hepatocyte mitochondria.[68] The sensitivity and specificity of HepPar-1 for HCC is over 80 percent.[69, 70] However, 50 percent of poorly differentiated sHCCs are negative and 20-30 percent of lung, esophageal and gastric adenocarcinomas are positive for HepPar-1. Polyclonal anti-carcinoembryonic antigen (CEA) antibody is highly sensitive for HCC and exhibits a specific bile canalicular staining pattern. Alike HepPar-1, it has a lower sensitivity in poorly differentiated sHCCs. On the contrary, glypican-3, a cell surface heparan sulfate proteoglycan, shows a higher sensitivity in poorly differentiated sHCCs compared to well and moderately differentiated tumors.[71] Expression of AFP is observed in approximately 30 percent of HCCs but lacking in metastatic adenocarcinomas.[69] Villin and CD10, similarly to polyclonal anti-CEA, display a bile canalicular staining pattern specific for HCC. Lack of staining with monoclonal anti-CEA antibody is also characteristic of HCCs. Thyroid transcription factor 1 is highly sensitive for HCC and exhibits a specific cytoplasmic pattern.[72] A monoclonal antibody directed against Ep-CAM, MOC-31, is highly sensitive and specific for metastatic adenocarcinomas of various origin, while HCCs are uniformly negative.[70, 73] Caudal type homeobox 2 is an intestine-specific transcription factor that has been identified as a highly sensitive and specific

marker for intestinal adenocarcinomas.[43] Cytokeratins are keratin proteins found in intermediate filaments of epithelial cells. Cytokeratins exhibit highly tissue-specific expression patterns in normal organs and tumors, thus they are useful markers for diagnostic histopathology.[8, 11] Cytokeratin 7 and CK19 positivity is characteristic of liver metastases of pancreatic adenocarcinomas (PLMs), while CK20 is expressed in 70 percent of liver metastases of colorectal adenocarcinomas (CRLMs). Most HCC are negative for CK7, CK19, and CK20.

Table 2. Differential diagnosis of HCC from metastatic adenocarcinoma. Modified from Centeno.[44]

Immunohistochemical markers	Tumor type	
	HCC	Metastatic adenocarcinoma
HepPar-1	+	-
Glypican-3[71]	+/-	-/rarely +
AFP	+/-	-
CD34[70]	+	-
TTF-1[70, 72, 74]	+	-
Bile	+	-
CD10[69, 70, 74, 75]	+ (canalicular)	+
Villin[69, 70]	+ (canalicular)	+
Polyclonal anti-CEA	+ (canalicular)	+
Monoclonal anti-CEA[69, 75]	-	+
CK7/19	-/rarely +	+/-
CK20	-	+/-
CK8/18	+	+/-
CDX2	-	+
MOC-31	-	+
Mucin	-	+

-, absent; +/-, may be present; +, usually present. CDX2, caudal type homeobox 2; CEA, carcinoembryonic antigen; CK, cytokeratin; HepPar-1, hepatocyte paraffin 1; MOC-1, anti-EpCAM antibody; TTF-1, thyroid transcription factor 1**.**

1.3 Cancer stem cells

The cancer stem cell (CSC) model emerged in the 1990s when John Dick discovered that in human acute myeloid leukemia, only a small subset of cells was capable

of initiating leukemia when injected into immunocompromised mice. These leukemic cells appeared to be abnormal versions of normal adult hematopoietic stem cells that differentiate into mature blood cells. Thus, it was suggested that acut myeloid leukemia is organized as a hierarchy with many similarities to normal hematopoiesis.[76, 77] Other research groups subsequently reported rare populations of cells with tumor-initiating capacity in a variety of solid tumors, such as brain, lung, breast, ovarian, colon, pancreatic, and liver cancers.[78-85]

The classical CSC model of tumor heterogeneity proposes that tumors are organized in a rigid cellular hierarchy that is often reminiscent of the hierarchy in the tissue of origin (**Figure 3**). The bulk of tumor cells that are at the bottom of the hierarchy are only capable of transient proliferation, therefore do not contribute to long-term tumor growth and eventually die off. At the top, rare, tipically quiescent CSCs, also known as tumor-initiating cells, have the capacity to self-renew (that is, to regenerate themselves) and to differentiate into the heterogeneous non-tumorigenic cancer cell types that constitute the bulk of the tumor.

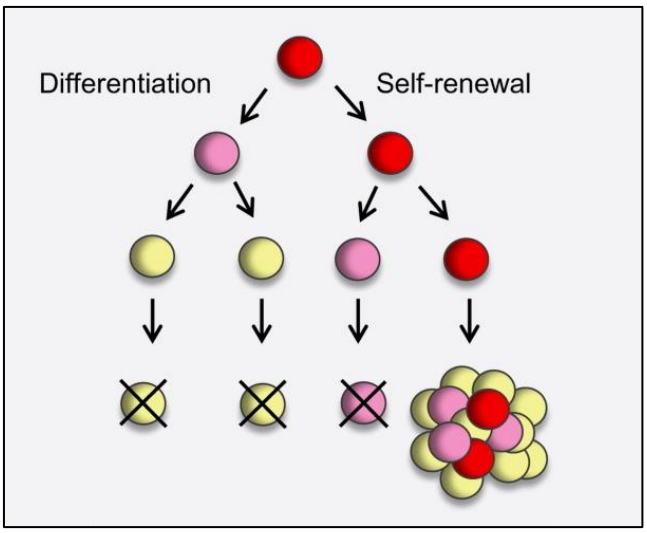

Figure 3. The classical cancer stem cell (CSC) model of tumor heterogeneity. Adapted from Sugihara and Saya.[86] The CSC model states that tumors are composed of a hierarchy of cell types, with only a small subset of cancer cells at the top being responsible for tumor growth. Upon asymmetric division, CSCs (red) give rise to one CSC and one transit-amplifying cell (pink). The latter rapidly amplifies the pool of differentiated cells (yellow) but is not capable of self-renewal.

Cancer stem cells have been hypothesized to be the subpopulation that disseminates from the primary tumor, intravasates into the circulation, and metastasizes to distant sites.[87-90] This is supported by accumulating evidence that CSCs express markers of EMT, a developmental program frequently activated during cancer invasion and metastasis. Furthermore, induction of EMT in transformed epithelial cells promotes the formation of CSCs.[91, 92] Cancer stem cells are resistant to conventional cancer treatments, such as chemotherapeutic agents and radiation, partly because these treatments selectively kill rapidly dividing non-CSCs - a characteristic that explains relapse after treatment. Thus, the CSC theory has important implications for cancer therapy. Development of novel therapeutic strategies that target CSCs has become a key goal in the challenge to achieve complete eradication of cancer.[93, 94]

Various cell surface markers have been associated with CSCs. None of these markers are expressed exclusively by CSCs, they can also be present on embryonic stem cells (ESCs) (SSEA-1, CD90, CD133, EpCAM, CD24, CD49f, CD29, and CD117), adult stem/progenitor cells (LGR5, SSEA-1, CD117, EpCAM, CD133, CD90, CD24, CD29, CD49f, and CD44), and normal tissue cells (CD20, CD96, CD29, and CD44).[95] CD133 (Prominin-1), a glycosylated protein with five transmembrane domains, is one of the most frequently studied CSC surface marker in solid cancers. It has identified CSCs in liver, pancreatic, colon, breast, ovary, prostate, brain, lung, and head and neck cancers in transplantation studies where $CD133^+$ cells generate tumors in immunocompromised mice more efficiently than $CD133^-$ cells.[96] Importantly, antigenic approaches have several shortcomings, such as lack of specificity, cross-reactivity, and antibody-dependent toxicity. Thus, CSCs cannot be defined based solely on surface markers, marker expression has to be linked to functional assays.[88]

1.4 Intercellular junctions and claudins

1.4.1 Intercellular junctions

Intercellular junctions connect plasma membranes of adjacent cells together. Four kinds of intercellular junctions occur in vertebrates: tight junctions, adherens junctions, gap junctions, and desmosomes. Adherens junctions are cadherin-based adhesions closely associated with actin filaments. Gap junctions are clusters of protein channels that allow

the exchange of small metabolites, ions, and second messengers between adjacent cells. Desmosomes provide a connection between intermediate filaments of neighboring cells conferring stability to tissues that experience mechanical stress.[97]

Tight junctions (TJ), the apicalmost part of intercellular junctions, form a circumferential belt at the boundary between the apical and basolateral plasma membrane domains.[98] By transmission electron microscopy, TJs appear as a series of close focal contacts or 'kissing points' between plasma membranes of adjacent cells. Freeze-fracture electron microscopy has revealed a network of continuous, anastomosing TJ strands on the protoplasmic face of the plasma membrane with complementary vacant grooves on the exoplasmic face (**Figure 4**).

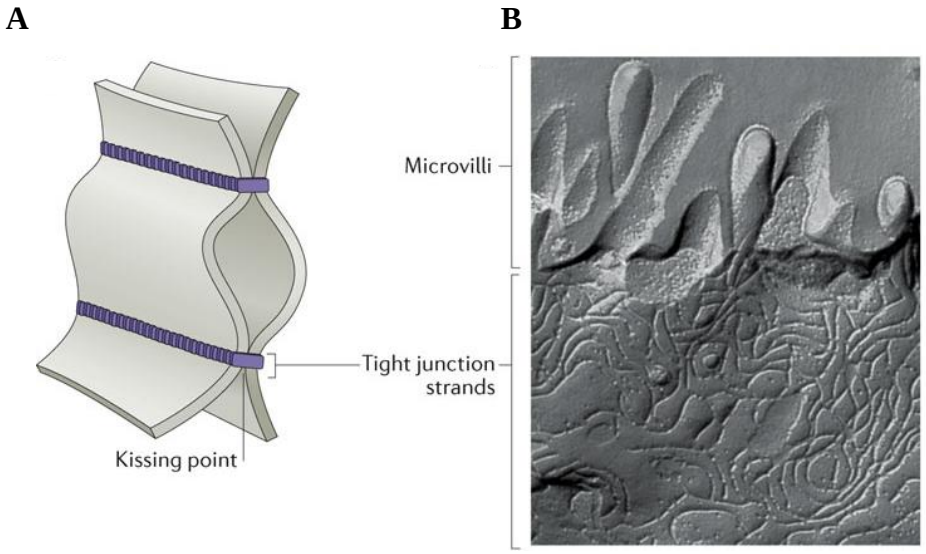

Figure 4. Tight junctions. Adapted from Zihni et al.[99] (A) Schematic three-dimensional structure of tight junctions. Each tight-junction strand associates with another tight-junction strand in the opposing membrane of an adjacent cell to occlude the intercellular space (kissing point). (B) Freeze-fracture electron microscopy image of tight junction strands along the apical membrane of intestinal epithelial cells.

The number and complexity of TJ strands depend greatly on the cell type and correlate with barrier function.[100] Tight junctions are composed of a complex assembly of transmembrane and peripheral proteins. The main transmembrane proteins are claudins (CLDNs), occludin, tricellulin, and MARVELD3 that all contain four transmembrane do-

mains. Other transmembrane components include a three-transmembrane-domain protein, BVES, and a large group of immunoglobulin-type adhesion proteins with a single transmembrane domain including JAMs, angulins, and CAR. Tricellulin and angulins are localized mainly at the tricellular TJs that occur where three cells intersect.[99, 101, 102]

Tight junction-associated peripheral membrane proteins function as a bridge between the transmembrane proteins and the actin cytoskeleton. They include a vast number of adaptor proteins that contain multiple protein-protein interaction domains. The most important TJ adaptor proteins are members of the MAGUK protein family, ZO-1, ZO-2, and ZO-3. MAGUK proteins are recognized for having structurally conserved PDZ, GK, and SH3 domains. Other examples of TJ adaptor proteins are cingulin, MUPP1, PATJ, and the MAGUK inverted proteins named MAGI. Signaling proteins, such as atypical protein kinase C, the Rho family guanosine triphosphatases CDC42, Rac, and RhoA and their regulators control the establishment and function of TJs.[98, 99]

The two major physiological roles of TJs are the gate and fence functions. By constituting semipermeable gates that restrict paracellular diffusion of ions, water, and macromolecules, TJs are essential for the maintenance of homoeostasis in organs and tissues. Fence function refers to maintenance of cell polarity by blocking free diffusion of proteins and lipids between the apical and basolateral plasma membrane domains. Apart from their barrier functions, TJs send signals to the cell interior through various signaling pathways to regulate cell proliferation, differentiation, and apoptosis.[99] Despite being heavily cross-linked structures, TJs undergo continuous remodeling at steady state, which modulates their different functions.[103] Disturbances of TJ function have been shown in various diseases. Some of these are inherited diseases, such as velocardiofacial syndrome, familial hypercholanemia, or pseudohypoaldosteronism type II. Viral and bacterial pathogenes that target TJ proteins include hepatitis C virus, coxsackieviruses, adenoviruses, *Clostridium perfringens*, *Vibrio cholerae*, and *Helicobacter pylori*. Chronic inflammatory diseases and cancer have also been linked to TJ dysfunction, however, it is unclear whether the observed changes are primary or secondary to disease pathogenesis.[104, 105]

1.4.2 Claudins

The demonstration that knockout mice for occludin possessed physiologically and structurally normal TJs led to the discovery that the backbones of TJ strands were constituted by claudin proteins.[106] Claudins comprise a large gene family, to date, 26 members in humans and 27 in mice have been identified.[99] Claudin genes are typically small with few introns, and many of them lack introns all together. Interestingly, several pairs of *CLDN* genes that are sequence-wise very similar to each other are located close together on the same chromosome, suggesting that their evolution was driven by gene duplication.[107] Phylogenetic analyses revealed close relationships among several claudin proteins. High common sequence similarity was detected among CLDN-1-10, -14, -15, -17, and -19 in mice, these CLDNs were therefore named 'classic' CLDNs.[108]

Claudins contain four transmembrane domains, two extracellular loops and short intracellular amino-terminal and carboxy-terminal tails (**Figure 5**). Generally, the amino-terminal domain consists of 4-5 residues followed by the first extracellular loop of 60 residues, a short 20-residue intracellular loop, the second extracellular loop of approximately 24 residues, and a carboxy-terminal tail of 21-63 residues. The amino acid sequences of the first and fourth transmembrane domains are highly conserved, whereas the second and third exhibit more variability.[107] The first extracellular loop determines the charge selectivity of paracellular transport because of its charged amino acids.[109] The two highly conserved cysteine residues in the first extracellular loop form an intramolecular disulfide bond to increase protein stability.[110, 111] The second extracellular loop has been implicated in the formation of dimers between CLDNs of opposing cell membranes by virtue of its helix-turn-helix motif conformation.[112] The second extracellular loop of several CLDNs, including CLDN-3, -4, and -7, also act as a receptor for *Clostridium perfringens* enterotoxin (CPE).[113] The carboxy-terminal tail shows the most sequence and size heterogeneity among CLDNs. At positions -3, -2, -1, and 0, most CLDNs contain a PDZ-binding motif that allows them to directly interact with TJ adaptor proteins ZO-1, -2, -3, and MUPP1.[114, 115] Post-translational modifications, such as palmitoylation and phosphorylation by serine/threonine and tyrosine kinases, target the carboxy-terminal tail and regulate localization and function of CLDNs.[116] For example, phosphorylation of CLDN-3 and CLDN-4 by protein kinase A and C, respectively, increases paracellular permeability.[117, 118]

Claudins exhibit tissue- and cell-type-specific expression patterns. Multiple CLDNs expressed simultaneously at the TJ establish homotypic and heterotypic interactions that allows strand pairing between adjacent cells.[119] Heterotypic interactions are restricted to specific combinations of CLDNs. Although CLDN-3 and CLDN-4 are heteromerically compatible, they do not heterotypically interact. On the other hand, heterotypic interaction has been demonstrated for claudins 1↔3, 2↔3, and 3↔5.[120] Claudins frequently locate outside the TJ at the lateral membrane, in the cytoplasm, or in the nucleus. Their non-TJ functions include interaction with cell surface receptors, formation of unconventional adhesive cell contacts, and intracellular signaling.[121]

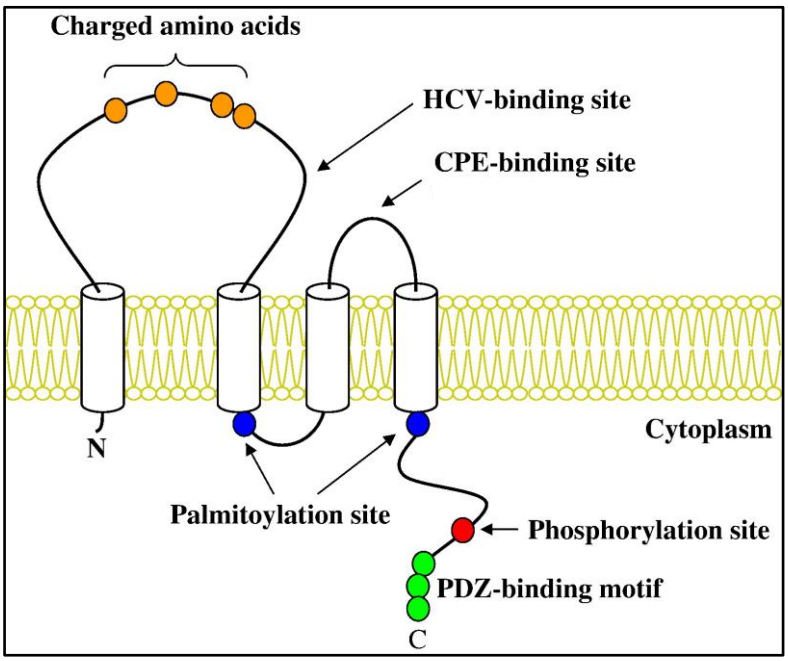

Figure 5. Scheme of claudin structure. Modified from Chiba et al.[100] Claudin proteins consist of four transmembrane domains, two extracellular domains, and short intracellular amino- and carboxy-terminal tails. They interact with tight junction-associated adapter proteins that contain PDZ domain through their carboxy-terminal tail. CPE, *Clostridium perfringens* enterotoxin.

Claudins determine the charge and size selectivity of paracellular transport by forming paracellular pores. Permeability properties of a given tissue are largely dependent on the combination of CLDNs that are expressed.[122] Claudins can be functionally grouped according to their barrier- and channel-forming characteristics. Barrier-forming CLDNs (CLDN-1, -3, -4, -5, -8, -11, -14, and -19) seal the paracellular space to restrict the passage

of water and solutes. Channel-forming CLDNs form paracellular cation pores (CLDN-2, -7, -10B, -15, and 16) or anion pores (CLDN-10A).[108, 123] Claudins play a key role in the pathogenesis of several human diseases. Mutations in four claudin genes (CLDN-1, -14, -16, and -19) have been reported to cause hereditary diseases involving ionic imbalance in various body compartments.[100] Alteration in CLDN expression has been demonstrated in various cancer types (**Table 3**). In particular, CLDN-1, -3, -4, and -7 are among the most frequently altered members of the claudin family.[124]

Table 3. Dysregulated claudin expression in human cancers. Modified from Osanai et al.[124]

Cancer origin	CLDN 1	CLDN 2	CLDN 3	CLDN 4	CLDN 5	CLDN 7	CLDN 10	CLDN 16	CLDN 18	CLDN 23
Skin, SCC[125]	↓	↑				↑				
Skin, melanoma[126]	↑									
Thyroid, FTC[127]	↑									
Breast	↑↓		↑↓	↑↓		↓				
Lung, SCLC[128]		↓	↑	↑		↑				
Lung, AC[128]	↓	↓	↑	↑	↑	↑				
Lung, SCC[128]	↑	↓	↓	↓	↓	↑				
Esophagus, SCC[129]	↑↓			↓		↑↓				
Esophagus AC[130]		↑	↑	↑						
Stomach	↑		↑	↑↓		↑			↑↓	↓
Large intestine	↑↓	↑	↑	↑↓	↑	↑↓				
Liver, HCC[131]	↑↓	↑			↑	↑↓	↑			
Biliary tract[132]	↓	↓	↓	↑		↑↓	↓		↑	
Pancreas, DAC[133]	↑↓	↑	↑	↑	↑				↑	
Pancreas, NEC[133]			↑			↑				
Bladder				↑↓						
Kidney	↑		↑	↑		↑				
Prostate	↑		↑	↑	↓	↑				
Ovary, EOC	↓		↓	↑	↑	↑		↑		
Uterine cervix	↓	↓		↓		↓				
Uterine corpus			↑	↑		↓				

AC, adenocarcinoma; CLDN, claudin; DAC, ductal adenocarcinoma; EOC, epithelial ovarian cancer; FTC, follicular thyroid carcinoma; NEC, neuroendocrine carcinoma; SCC, squamous cell carcinoma; SCLC, small cell lung cancer.

DOI:10.14753/SE.2019.2291

2. OBJECTIVES

In this thesis, I aimed to explore the role that two interconnected concepts recently emerged in the field of cancer research - cancer stem cells and altered tight junction pattern - play in the development of HCC, and metastatic liver cancer. The aim of the first part of the thesis was to investigate whether the differentiation stage of cells from which liver CSCs evolve affects the acquisition of stemness traits and contributes to the genetic and phenotypic heterogeneity of HCC. In the second part of the thesis, I aimed to characterize the claudin expression profiles in HCC, and liver metastases of colorectal adenocarcinoma and pancreatic adenocarcinoma. My objectives were as follows:

- To assess the ability of mouse hepatic lineage cells at distinct differentiation stages (i.e., bipotential hepatic progenitor cells, hepatocyte lineage-committed hepatoblasts, and adult hepatocytes) to become cancer stem cells.

- To explore the influence of cell-of-origin on the phenotype of mouse liver tumors derived from distinct mouse hepatic lineage cells.

- To identify common and cell-of-origin-specific gene expression signatures in mouse liver tumors derived from distinct mouse hepatic lineage cells.

- To investigate the role of c-Myc in the acquisition of cancer stem cell properties in adult mouse hepatocytes.

- To characterize the mRNA and protein expression of claudin-1, -2, -3, -4, and -7 in human HCC, and liver metastases of colorectal adenocarcinoma and pancreatic adenocarcinoma.

DOI:10.14753/SE.2019.2291

3. METHODS

3.1 Plasmid constructs

I used two lentiviral vectors carrying oncogenes to transform primary hepatic progenitor cells (HPCs), hepatoblasts (HBs), and adult hepatocytes (AHs). Lentiviral vectors are very efficient gene transfer tools that integrate into non-dividing and dividing cells.[134] The pSico.FerH-v-H-Ras-IRES-Luc2-EGFP bicistronic lentiviral vector (referred to as H-Ras-EGFP) that constitutively expresses oncogenic H-Ras and firefly luciferase/enhanced green fluorescent protein (EGFP) double reporter was constructed by Dr. Dominic Esposito (Leidos Biomedical Research, Frederick, MD, USA). The v-H-Ras oncogene is a highly transforming ras gene, whose encoded protein is constitutively active and differs from normal H-Ras protein only at amino acids 12 and 59.[135] Bicistronic vectors that contain internal ribosome entry site (IRES) element allow the simultaneous expression of two proteins separately but from the same messenger RNA.[136] The fusion protein of firefly Luciferase2 and EGFP (Luc2-EGFP) combines advantages of a bioluminescent (luciferase) and a fluorescent (EGFP) reporter. Successfully transduced cells can be identified by fluorescence microscopy or flow cytometry, and cells expressing luciferase can be tracked *in vivo* by bioluminescence imaging.[137] The third-generation HIV-1-based lentiviral plasmid pSico (Addgene, Cambridge, MA, USA) was modified for MultiSite Gateway recombinational cloning (Thermo Fisher Scientific, Waltham, MA, USA).[138] A cassette containing IRES2-Luc2-EGFP was constructed and introduced into the modified pSico vector. A ubiquitous FerH promoter (human ferritin heavy chain promoter/SV40 enhancer) was then inserted allowing ubiquitous, stable expression of v-H-Ras and Luc2-EGFP.[137] The oncogenic H-Ras open reading frame was subcloned from pBW1423 plasmid.[135]

I constructed the pRRLSIN.cPPT.CAG-SV40LT-IRES-mCherry bicistronic lentiviral vector (referred to as SV40LT-mCherry) to constitutively express simian virus 40 large T antigen (SV40LT) and red fluorescent protein mCherry. Simian virus 40 large T antigen, an oncoprotein derived from the polyomavirus SV40, elicits cellular transformation primarily via inhibition of the p53 and Rb family of tumor suppressors.[139-141] The PGK-EGFP cassette was removed from the third-generation lentiviral plasmid

pRRLSIN.cPPT.PGK-GFP.WPRE (Addgene), and CAG promoter was inserted.[142-144] Simian virus 40 large T antigen was subcloned from pBabe-puro largeTcDNA (Addgene), and an IRES-mCherry cassette was inserted.[145]

The pRS retroviral vectors expressing mouse c-Myc short hairpin RNA (shRNA) and scrambled negative control shRNA under the U6 polymerase III promoter were kind gifts from Dr. James Manley (Columbia University, New York, NY, USA).[146] To produce viral particles, a second generation packaging vector psPAX2 and an envelope vector pCMV-VSV-G were purchased from Addgene.[147]

3.2 Production of lenti- and retroviruses

Lenti- and retroviral expression vectors were propagated in One Shot Stbl3 Chemically Competent *Escherichia coli* (Thermo Fisher Scientific) using 100 µg/mL carbenicillin at 30°C. Plasmids pCMV-VSV-G and psPAX2 were propagated in DH5α Chemically Competent *Escherichia coli* (Thermo Fisher Scientific) at 37°C. Transfection quality plasmid DNA was isolated by using Plasmid Midi- or Maxi Kit (Qiagen, Valencia, CA, USA). Plasmid DNA was verified by agarose gel electrophoresis and restriction analysis, and concentrations were determined by spectrophotometry.

Human embryonic kidney (HEK) 293T/17 (American Type Culture Collection, Manassas, VA, USA) and HEK 293-GP (Takara Bio, Mountain View, CA, USA) cells were used for the production of lenti- and retroviral vector particles, respectively. Cells were maintained in high glucose (4.5 g/L) Dulbecco's modified Eagle's medium (DMEM; Corning, Corning, NY, USA) supplemented with 4 mM L-glutamine (Thermo Fisher Scientific), 100 units/mL penicillin/streptomycin (Thermo Fisher Scientific), and 10% fetal bovine serum (FBS; Corning) in a humidified incubator in an atmosphere of 5% CO_2 and 95% air at 37°C. To produce H-Ras-EGFP and SV40LT-mCherry lentiviral vector particles pseudotyped with VSV-G envelope, HEK 293T/17 cells were seeded at a density of 4×10^6 cells per 10-cm tissue culture dish (BD, Franklin Lakes, NJ, USA) and cultured for 24 hours (**Figure 6**). Lentiviral expression vectors (4 µg of each construct) were co-transfected with pCMV-VSV-G (1.3 µg) and psPAX2 (2.7 µg) by using 24 µL of LipoD293 transfection reagent (SignaGen Laboratories, Rockville, MD, USA) in the presence of high glucose DMEM supplemented with 4 mM L-glutamine, 10% FBS, and 100 units/mL penicillin/streptomycin for 16 hours. Vector supernatants were harvested 60

hours later, filtered through a 0.45 µm filter, and concentrated by ultracentrifugation at 20,000 rpm for two hours at 4°C. Virus pellet was resuspended in William's E medium (Thermo Fisher Scientific) or DMEM supplemented with 10% FBS and stored at -80°C until use.

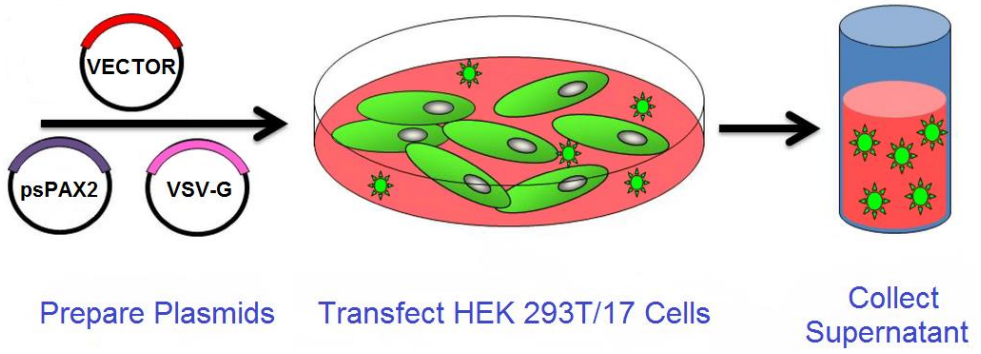

Figure 6. Production of lentiviral vectors by transient transfection. Modified from Shaw and Cornetta.[148] Human embryonic kidney (HEK) 293T/17 cells were co-transfected with lentiviral expression vectors H-Ras-EGFP and SV40LT-mCherry, packaging vector psPAX2, and envelope vector pCMV-VSV-G. Culture supernatants were collected 60 hours later, filtered, and concentrated by ultracentrifugation.

To determine the biological titer of concentrated lentiviral vectors, HeLa cells (American Type Culture Collection) were plated at 5×10^4 cells per well in 6-well plates (BD) in high glucose DMEM containing 2 mM L-glutamine, 100 units/mL penicillin/streptomycin, and 10% FBS.[149] Twenty-four hours later, the number of viable cells in two wells was assessed by trypan blue (Thermo Fisher Scientific) exclusion test, and cells in the remaining duplicate wells were transduced with various volumes (0.5 µL, 1 µL, 2 µL, 5 µL, and 10 µL) of lentiviral vector preparations in the presence of 8 µg/mL hexadimethrine bromide (Merck, Kenilworth, NJ, USA). After 4 days, cells were detached and analyzed on an LSR II flow cytometer (BD) for EGFP or mCherry fluorescence. Dilutions yielding 1-20% EGFP- or mCherry-positive cells were chosen for titer calculations. Titers were calculated as transducing unit/mL using the following equation, where 1 transducing unit is equal to 1 infectious particle:

$$\text{Titer} = \frac{\text{number of target HeLa cells} \times \%\ \text{of EGFP}^+ \text{ or mCherry}^+ \text{ cells}}{\text{volume of lentivirus (in mL)} \times 100}$$

To produce VSV-G-pseudotyped retroviral vectors, 3.6×10^6 HEK 293-GP cells per 10-cm tissue culture dish were seeded and cultured for 24 hours. HEK 293-GP is a 293-based cell line stably expressing large quantities of the Moloney murine leukemia virus Gag and Pol proteins. Retroviral expression vectors were co-transfected with pCMV-VSV-G using LipoD293 transfection reagent in the presence of high glucose DMEM, 4 mM L-glutamine, 10% FBS, and 100 units/mL penicillin/streptomycin. Medium was replaced 16 hours after transfection. Vector supernatant was harvested 24 and 48 hours later, filtered through a 0.45 µm filter, pooled, and used directly upon collection, without freeze and thaw.

3.3 Isolation and transduction of mouse hepatic lineage cells

I isolated HPCs, HBs, and AHs from C57BL/6NCr mice (Leidos Biomedical Research). Genetically labeled AHs were isolated from B6.Cg-*Gt(ROSA)26Sor*$^{tm14(CAG-tdTomato)Hze}$/J mice (The Jackson Laboratory, Bar Harbor, ME, USA). All procedures were performed according to protocols approved by the Animal Care and Use Committee at the National Institutes of Health (NIH; Bethesda, MD, USA).

To induce HPCs, 9-week-old male mice were given a diet containing 0.1% 3,5-diethoxycarbonyl-1,4-dihydrocollidine (DDC; Bio-Serv, Flemington, NJ, USA) for 2 weeks.[150] Non-parenchymal cells from DDC livers were obtained by a modified two-step collagenase perfusion method.[151] Liver perfusion catheter was inserted through the right atrium into the superior vena cava, and livers were perfused with Hank's balanced salt solution (HBSS; Thermo Fisher Scientific) for 5 minutes followed by Williams' E medium containing 0.05% collagenase type IV (Worthington, Lakewood, NJ, USA) for 10 minutes at 37°C. Digested livers were removed, minced, and incubated in Williams' E medium containing 0.05% collagenase type IV, 0.05% pronase E (Worthington), and 0.005% DNase I (Worthington) for 30 minutes at 37°C. Cells were then centrifuged twice at 500 rpm for 2 minutes to remove hepatocytes and incubated in hemolysis buffer (16.5 mM Tris base, 0.1M NH_4Cl) containing 10% FBS for 3 minutes on ice. Cell suspensions were incubated with a biotinylated antibody against EpCAM (**Table 4**) and APC Mouse Lineage Antibody Cocktail (**Table 4**) for 30 minutes on ice followed by incubation with streptavidin-PE.[152, 153] The Lineage Antibody Cocktail was used to exclude cells of hem-

atopoietic origin. EpCAM$^+$/Lineage Coctail$^-$ HPCs were sorted with a FACSVantage instrument (BD) and plated in a collagen type I coated 96-well plate (BD) at a density of 10^5 cells/cm^2 in a basal growth medium supplemented with 50 ng/mL hepatocyte growth factor (PeproTech, Rocky Hill, NJ, USA) and 20 ng/mL epidermal growth factor (EGF; PeproTech).[152] Sorted HPCs from three mice were pooled to form one sample, and four

Table 4. List of primary antibodies

Antibody	Company	Application (Dilution)
anti-actin	Merck	WB (1:30000)
anti-AFP	Agilent Technologies (Santa Clara, CA, USA)	ICC/IF (1:500)
anti-albumin	Bethyl Laboratories (Montgomery, TX, USA)	ICC/IF (1:100)
anti-A6	Gift from Dr. V. M. Factor[154]	FCM (1:100) IHC-P (1:40)
anti-CD29-APC	Thermo Fisher Scientific	FCM (1:160)
anti-CD44-APC-Cy7	BD	FCM (1:333)
anti-CD49f-APC	Thermo Fisher Scientific	FCM (1:333)
anti-CD90.2-APC	Thermo Fisher Scientific	FCM (1:333)
anti-CD133-APC	Thermo Fisher Scientific	FCM (1:160)
anti-CLDN-1	Thermo Fisher Scientific	IHC-P (1:100)
anti-CLDN-2	Thermo Fisher Scientific	IHC-P (1:100)
anti-CLDN-3	Thermo Fisher Scientific	IHC-P (1:100)
anti-CLDN-4	Thermo Fisher Scientific	IHC-P (1:100)
anti-CLDN-7	Thermo Fisher Scientific	IHC-P (1:100)
anti-c-Myc	Cell Signaling Technology (Danvers, MA, USA)	WB (1:1000)
anti-E-cadherin	Takara Bio	ICC/IF (1:100) MACS (1:40)
anti-EpCAM	BD	FCM (1:50)
anti-EpCAM-biotin	Gift from Dr. A. Miyajima[152]	FCM (1:50)
anti-HNF4a	Santa Cruz Biotechnology (Dallas, TX, USA)	IHC-P (1:50)
anti-CK18	Developmental Studies Hybridoma Bank (Iowa City, IA, USA)	FCM (1:3) ICC/IF (1:100)
anti-CK19	Developmental Studies Hybridoma Bank	FCM (1:43) IHC-P (1:200)
anti-laminin	Abcam (Cambridge, MA, USA)	IHC-P (1:50)
anti-Sca-1-APC	Thermo Fisher Scientific	FCM (1:333)
anti-SV40LT	Abcam	WB (1:1000) IHC-P (1:50)
anti-v-H-Ras	Thermo Fisher Scientific	WB (1:1000) IHC-P (1:50)
anti-vimentin	Abcam	IHC-P (1:200)
APC Mouse Lineage Antibody Cocktail	BD	FCM (1:5)

APC, allophycocyanin; BD, Becton Dickinson; FCM, flow cytometry; HNF4a, hepatocyte nuclear factor 4 alpha; ICC/IF, fluorescence immunocytochemistry; IHC-P, immunohistochemistry on formalin-fixed, paraffin-embedded sample; MACS, magnetic-activated cell sorting; SV40LT, simian virus 40 large T antigen; v-H-Ras, Harvey rat sarcoma viral oncogene homolog (constitutively active form); WB, western blotting.

and three biological replicates were collected for microarray and quantitative reverse transcription polymerase chain reaction (qRT-PCR) analysis, repectively.

Hepatoblasts were isolated from timed pregnant mice at embryonic day 16.5 by magnetic-activated cell sorting (MACS; Miltenyi Biotec, Auburn, CA, USA) using anti-E-cadherin antibody, clone ECCD2 (**Table 4**).[155, 156] The gestational age of the embryos was determined by the number of days after the appearance of the vaginal plug; noon of the day on which the vaginal plug was found the embryos were aged 0.5 days.[157] Livers from littermate embryos were pooled and minced with a scalpel. Minced livers were incubated in 1 U/mL dispase II (Stemcell Technologies, Vancouver, BC, Canada) for 1 hour at 37°C with gentle agitation followed by incubation with ACK lysing buffer (Thermo Fisher Scientific) and 0.01% DNase I. Up to 10^7 cells were blocked with 5% normal goat serum and incubated with 5 μg of rat anti-mouse E-cadherin antibody for 15 minutes at 4 ^oC in MACS buffer containing 1% bovine serum albumin (Thermo Fisher Scientific) in phosphate buffered saline (PBS; Thermo Fisher Scientific). After washing, cells were mixed with 20 μl of goat anti-rat IgG microbeads (Miltenyi Biotec) in a total volume of 100 μl and incubated at 4 ^oC for 15 minutes. Microbeads labeled cell suspension was then loaded onto the MS separation column followed by washing twice with MACS buffer. Finally, the column was removed from the magnetic field, and E-cadherin$^+$ HBs retained in the column were eluted twice with 1 mL MACS buffer as the positively selected fraction. The number of viable HBs was assessed by trypan blue exclusion test. Hepatoblasts were plated in collagen type I coated 6-well plates (BD) at a density of 10^5 cells/cm^2 in fresh growth medium (DMEM supplemented with 2 mM L-glutamine, 1 mM sodium pyruvate, 100 units/mL penicillin/streptomycin, and 10% FBS) mixed 1:1 with conditioned medium. Conditioned medium was collected from fetal liver cells cultured without the separation of hepatoblasts and non-parenchymal cells, centrifuged at 1000 rpm for 5 minutes, filtered through a 0.22 μm syringe filter, and stored at −80°C in aliquots. Hepatoblasts isolated from littermate embryos formed one sample, and four and three biological replicates were collected for microarray and qRT-PCR analysis, repectively.

Adult hepatocytes were isolated from 3-month-old C57BL/6NCr and B6.Cg-*Gt(ROSA)26Sor*$^{tm14(CAG-tdTomato)Hze}$/J male mice by a modified two-step collagenase perfusion procedure.[158] Six days prior to hepatocyte isolation, I administered 200 μL of Ad-CMV-iCre, a Cre recombinant adenovirus (Vector BioLabs, Malvern, PA, USA) at a con-

centration of 10^{10} plaque-forming units/mL intravenously via tail vein injection into B6.Cg-*Gt(ROSA)26Sor*$^{tm14(CAG-tdTomato)Hze}$/J reporter mice to induce hepatocyte-specific expression of tdTomato.[159] Livers were perfused with HBSS for 5 minutes followed by Williams' E medium containing 0.05% collagenase type I (Worthington) for 15 minutes at 37°C. After discoloration of the liver (from dark red to pink) and two-fold increase in liver size, digested livers were removed and hepatocytes were combed out in cold hepatocyte growth medium.[160] After washing, cell suspension was gently overlaid onto equal volume of 90% isotonic Percoll solution (Merck) and centrifuged at 1000 rpm for 10 minutes to separate dead cells from the living ones. Supernatant was discarded, and hepatocytes were washed with hepatocyte growth medium. Viable cells were counted using trypan blue exclusion test and seeded at a density of 10^4 cells/cm^2 in hepatocyte growth medium supplemented with 10% FBS. After 4 hours of attachment, the medium was replaced with fresh hepatocyte growth medium. Hepatocytes isolated from one C57BL/6NCr mouse formed one sample, and four and three biological replicates were collected for microarray and qRT-PCR analysis, repectively.

Primary cells were co-transduced with concentrated lentiviruses H-Ras-EGFP and SV40LT-mCherry at a multiplicity of infection of 5 (HPCs and HBs) or 10 (AHs) in the presence of 6 µg/mL hexadimethrine bromide 24 hours after plating for 12 hours at 37°C. Multiplicity of infection is defined as the ratio of infectious virus particles (transducing units) to target cells in a culture. Transduced cells were maintained in their respective culture medium for 6 days after lentiviral transduction, then cultured for 3 weeks in high glucose DMEM containing 2 mM L-glutamine, 1 mM sodium pyruvate, 100 units/mL penicillin/streptomycin, and 10% FBS to collect a sufficient number of transduced cells from low-frequency HPCs for *in vitro* and *in vivo* experiments. H-Ras-EGFP$^+$/SV40LT-mCherry$^+$ HPCs, HBs, and AHs, referred hereafter as T-HPCs, T-HBs, and T-AHs, were then sorted with a FACSVantage instrument using the same gating parameters to ensure comparable viral loads. To obtain single cell-derived clones, T-AHs were serially diluted to 10 cells/mL and plated in 96-well plates (BD) at 100 µL/well. Twenty-four hours after plating, wells containing single cells were identified and marked. Colonies derived from single cells were expanded, and the growth of 15 clonal lines was established.

For long-term knockdown of c-Myc, T-AHs were transduced with pRS retroviral vectors expressing c-Myc shRNA or scrambled shRNA for 16 hours at 37°C. Transduced cells were selected with 9 μg/mL puromycin (Merck) for 10 days. Cells transduced with c-Myc shRNA vector were sorted into individual wells of a 96-well plate (1 cell/well) with a FACSVantage instrument. Expression of c-Myc protein was analyzed by western blotting. The following sense shRNA sequences were used: scrambled shRNA, 5'-GAGGCTTCTTATAAGTGTTTACTCGAGTAAACACTTATAAGAAGCCTCTTTT T-3'; c-Myc shRNA, 5'-CGGACACACAACGTCTTGGAACTCGAGTTCCAAGACG TTGTGTGTCCGTTTTT-3'.[146]

3.4 Transplantation mouse models

I used male non-obese diabetic/severe combined imunodeficient (NOD/SCID) mice between 6 and 9 weeks of age for cell transplantation experiments. Mice were anesthetized for 3 minutes with 5% isoflurane (Baxter, Deerfield, IL, USA) in oxygen and kept at 2% isoflurane throughout the procedures. All procedures were performed at the NIH in accordance with the guidelines of the NIH Animal Care and Use Committee.

3.4.1 Subcutaneous transplantation

For limiting dilution analysis, T-HPCs, T-HBs, and T-AHs (10^1, 10^2, or 10^3 cells of each) were mixed 1:1 in DMEM/Matrigel (BD) and injected subcutaneously into both flanks (4 mice per group). Tumor formation was monitored weekly by palpation and using an external caliper. Mice were euthanized by cervical dislocation 5 weeks after transplantation. Liver, brain, and lungs were removed from each animal and subjected to *ex vivo* bioluminescence imaging. Three million normal HPCs that were injected subcutaneously as described above served as negative control. To assess the effect of c-Myc knockdown on tumor growth, 10^2 T-AHs expressing c-Myc shRNA or scrambled shRNA were injected subcutaneously as described earlier (5 mice per group). Animals were monitored weekly to detect tumor onset and growth. Tumor dimensions were measured by an external caliper, and tumor volume (V) was determined using the following formula: $V = l \times w^2/2$ where length (l) > width (w).

3.4.2 Orthotopic transplantation via direct intrahepatic injection and establishment of tumor-derived cell lines

To assess orthotopic growth and establish tumor-derived cell lines, T-HPCs, T-HBs, and T-AHs (1.5×10^5 cells in 40 µl HBSS) were injected into the left liver lobe (5 mice per group). Surgicel absorbable hemostat (Johnson & Johnson, New Brunswick, NJ, USA) was placed over the puncture site, and gentle pressure was applied with a cotton-tipped applicator to achieve complete hemostasis and prevent leakage of tumor cells. Wounds were closed in two layers using 3-0 silk suture and surgical clips. Mice were subjected to *in vivo* bioluminescence imaging twice a week and were euthanized at the same time when any of the mice displayed tumor related symptoms. Liver, brain, and lungs were removed from each animal and subjected to *ex vivo* bioluminescence imaging.

Primary grafted liver tumors (4 tumors per cell type) were macrodissected and washed three times with cold PBS 100 units/mL containing penicillin/streptomycin. Tumors tissues were then finely minced using a sterile scalpel, washed with HBSS supplemented with 1 M HEPES (Thermo Fisher Scientific) and 0.2 M EGTA (Merck), and incubated in a shaking water bath at 37°C for 15 minutes. Supernatants were discarded, and cell fragments were incubated in collagenase IV for 20 minutes at 37°C followed by a digestion with 0.25% trypsin-EDTA (Thermo Fisher Scientific) for 15 minutes. Single cell suspensions were diluted in regular culture medium, centrifuged, and plated in 10 cm culture dishes (BD). H-Ras-EGFP$^+$/SV40LT-mCherry$^+$ cancer cells were FACS-sorted after 3 days of culture. Cells at passage 2 to 5 were used for all *in vitro* assays.

3.4.3 Orthotopic transplantation via intrasplenic injection

I generated tumor samples for immunochistochemistry and microarray analysis by injecting T-HPCs, T-HBs, and T-AHs (10^5 cells in 20 µl HBSS) intrasplenically to ensure tumor formation in the liver from engraftment of a single cell. To calculate the probability of tumor initiation by transduced hepatic stem cells (HSCs), we transplanted a low number of non-sorted, H-Ras/SV40LT-transduced primary AHs (10^3 cells) after a short-term (1-day) culture. Spleens were removed 30 seconds after the intrasplenic injection was performed. Wounds were closed in two layers using 3-0 silk suture and surgical clips. Tumor growth was monitored by *in vivo* bioluminescence imaging twice a week.

All mice were euthanized by cervical dislocation when any of the mice displayed symptoms of disease, and individual liver tumors were macrodissected.

3.4.4 Bioluminescence imaging

D-luciferin (Biosynth, Itasca, IL, USA) was dissolved in PBS (15 mg/mL) and sterile-filtered through a 0.22 µm syringe filter. Mice were anesthetized, injected intraperitoneally with 10 µL of luciferin solution per gram of body weight, and placed in the imaging chamber of a Xenogen-IVIS-200 Imaging System (PerkinElmer, Waltham, MA, USA). Images were acquired 5 minutes after luciferin injection and analyzed using Living Image Software v3.0 (PerkinElmer). Bioluminescent signal was expressed as total flux (photons per second). After mice were euthanized by cervical dislocation, liver, lungs, and brain were dissected and subjected to *ex vivo* bioluminescence imaging 10 minutes after luciferin injection.

3.5 Flow cytometry

3.5.1 Analysis of cancer stem cell and hepatic lineage markers

I analyzed the expression of hepatic lineage (A6, CK19, and EpCAM) and CSC (CD29, CD44, CD49f, CD133, CD90, and Sca-1) markers in normal and H-Ras-EGFP^{+}/SV40LT-mCherry^{+} mouse hepatic lineage cells, and tumor-derived cell lines using antibodies and corresponding isotype controls (**Table 4**). Viability was assessed by staining cells with 4',6-diamidino-2-phenylindole (Thermo Fisher Scientific). Twenty thousand events were recorded on an LSR II flow cytometer configured with FACSDiva software (BD). Data analysis was performed with FlowJo software (BD). Each staining was performed in triplicate. Data are expressed as mean percentage ± standard deviation.

3.5.2 Side population analysis

The side population (SP) assay is a flow cytometry method based on the ability of CSCs to exclude the Hoechst 33342 dye via the ATP-binding cassette (ABC) family of membrane transport proteins.[161] Normal and H-Ras-EGFP^{+}/SV40LT-mCherry^{+} mouse hepatic lineage cells, and tumor-derived cell lines were incubated in a shaking water bath

at 37°C for 90 minutes with 15 µg/mL of Hoechst 33342 dye (Thermo Fisher Scientific) in the presence or absence of 50 µmol/l fumitremorgin C (Merck), an ABCG2 inhibitor, to identify the SP gate.[162] One hundred thousand events were collected on an LSR II flow cytometer configured with FACSDiva software. Data analysis was performed with FlowJo software. Each assay was performed in triplicate. Data are expressed as mean percentage ± standard deviation.

3.5.3 Nuclear ploidy test

Nuclear ploidy of normal mouse HPCs, HBs, AHs, and tumor-derived cell lines was determined using Cycletest Plus DNA Reagent Kit (BD). Briefly, 5.0×10^5 cells were incubated with trypsin-EDTA and ribonuclease A (Merck) at room temperature. Nuclear chromatin was stabilized with spermine. Isolated nuclei were stained with cold propidium iodide solution at 4°C. Spleen cells from normal adult mice were stained simultaneously as a diploid reference. Fifty thousand data events were collected on a FACSCalibur flow cytometer (BD) configured with CellQuest Pro software (BD). Data analysis was performed with ModFit (Verity Software House, Topsham, ME, USA). Each assay was performed in triplicate.

3.6 Sphere formation assay

Sphere formation assays are widely used *in vitro* assays that identify normal stem cells and CSCs based on their capacity to self-renew and differentiate.[79] A tumorsphere is a solid, spherical structure derived from a single CSC. By serial passage of tumorsphere cultures, this assay can be used to estimate the frequency of CSCs within a population of cancer cells. I tested the ability of normal and H-Ras-EGFP$^+$/SV40LT-mCherry$^+$ mouse hepatic lineage cells, and tumor-derived cell lines to form spheroids in adherent-free, serum-free conditions. For each cells type, I seeded 500 cells/well in 10 wells in ultra-low attachment 96-well plates (Corning) in serum-free growth medium containing 1% methylcellulose (Bio-Techne, Minneapolis, MN, USA), 2% B27 (Thermo Fisher Scientific), 2 mM L-glutamine, 20 ng/mL EGF, and 20 ng/mL basic fibroblast growth factor. The growth factors were added fresh every 2 days. The tumorsphere cultures were subjected to serial passage every 7 days for 6 weeks. Spheroids were pooled and dissociated

with 0.25% Trypsin-EDTA. Viable cells were counted and reseeded in a new 96-well plate as described above. Average number and diameters (d_1; d_2) of spheroids were calculated using ImageJ software (NIH). Spheroid volumes (V) were calculated (in μm^3) using the following equation: $V = d_1 \times d_2^2/2$, where d_2 designates the shorter diameter. Spheroids smaller than 50 µm in diameter were excluded from analysis. Data are presented as the mean ± standard error of mean of triplicate experiments.

3.7 Western blot

Whole cell lysates were prepared from mouse cells using M-PER Mammalian Protein Extraction Reagent (Thermo Fisher Scientific) containing Complete Protease Inhibitor Cocktail (Roche, Indianapolis, IN, USA). The amount of total proteins was determined with Pierce BCA Protein Assay Kit (Thermo Fisher Scientific). Proteins (10 or 50 µg) were separated by sodium dodecyl sulfate-polyacrylamide gel electrophoresis and transferred onto polyvinylidene difluoride membranes. The membranes were blocked in 5% non-fat milk in Tris-buffered saline (Thermo Fisher Scientific) containing 0.1% Tween 20 (Thermo Fisher Scientific) for 1 hour and then incubated with primary antibodies against v-H-Ras, SV40LT, and c-Myc overnight at 4°C (**Table 4**). The secondary antibodies were horseradish peroxidase (HRP)-conjugated anti-rat, anti-mouse, and anti-rabbit (Thermo Fisher Scientific). Immunoreactive bands were visualized using ECL Plus Western Blotting Detection Reagent (GE, Chicago, IL, USA). Equal protein loading was assessed by probing the same membrane with anti-actin antibody (**Table 4**).

3.8 Tissue specimens

3.8.1 Human tissues

Formalin-fixed, paraffin-embedded samples from 20 surgically removed HCCs, and liver metastases of 20 colorectal adenocarcinomas and 15 pancreatic adenocarcinomas with paired surrounding non-tumorous liver tissues were enrolled in the present study with the permission of the Regional Ethical Committee of the Semmelweis University (#137/2008). Samples were collected at the 2nd Department of Pathology at Semmelweis University over an 8-year period. Diagnoses were reevaluated and confirmed by expert

pathologists and further supported by clinical data specific to the location of the primary tumor. The median age and female to male ratio in the patient groups were as follows: 65 years, 7:13 (HCC); 65 years, 7:13 (CRLM) and 58 years, 9:6 (PLM). Five normal liver samples from patients who died in accidents were obtained from the Department of Forensic Medicine at Semmelweis University.

3.8.2 Mouse tissues

I generated liver tumors by intrasplenic injection of T-HPCs, T-HBs, and T-AHs into NOD/SCID mice as described earlier. Individual tumors (>3 mm in diameter) were macrodissected and divided into two portions. One portion of each tumor was frozen in liquid nitrogen and stored at -80°C, the remainder was fixed in formalin and embedded in paraffin. Semiquantitative histological evaluation and immunohistochemical stainings were performed on formalin-fixed, paraffin-embedded tumors (14 HPC-, 28 HB-, and 28 AH-derived). Frozen tumors were used for microarray analysis (10 HPC-, 20 HB-, and 20 AH-derived), qRT-PCR (6 samples of each tumor group), and western blotting (2 AH-derived).

3.9 Immunostainings and morphometry

3.9.1 Immunofluorescence stainings

To assess the purity of primary mouse HBs, cells were fixed in 4% paraformaldehyde (Merck) in PBS for 30 minutes at room temperature. After washing with PBS, cells were incubated with PBS containing 1% bovine serum albumin and 0.1% Triton X-100 (Merck) for 1 hour at room temperature, followed by overnight incubation with primary antibodies including E-cadherin, albumin, AFP, and CK18 (**Table 4**). Alexa Fluor 594-conjugated rabbit anti-goat IgG, Alexa Fluor 594-conjugated goat anti-rabbit IgG, or Alexa 488-conjugated goat anti-rat IgG (Thermo Fisher Scientific) were used as secondary antibodies for 30 minutes at room temperature. Nuclei were counterstained with 4’,6-diamidino-2-phenylindole. Cells were covered with Fluoromount-G mounting medium (Thermo Fisher Scientific), and images were acquired on Zeiss LSM 510 NLO (Zeiss, Dublin, CA, USA) or Zeiss LSM 710 NLO (Zeiss) confocal laser scanning microscopes.

3.9.2 Immunohistochemistry on formalin-fixed, paraffin-embedded samples

Tissues samples were fixed in 10% neutral buffered formalin overnight, embedded in paraffin (FFPE), cut, and stained with hematoxylin and eosin (Merck) for histological evaluation. Immunohistochemical detection of CLDN-1, -2, -3, -4, and -7, v-H-Ras, SV40LT, hepatocyte nuclear factor 4 alpha (HNF4a), CK19, laminin, vimentin, and A6 was performed on 3-to-4-μm-thick FFPE sections (**Table 4**). Immunoreactions for CLDNs were carried out using the Ventana ES automatic immunostainer (Roche) with the streptavidin-biotin-peroxidase technique.[128, 163-165] Primary antibodies bound to v-H-Ras, SV40LT, HNF4a, CK19, laminin, vimentin, or A6 were detected with polymeric HRP-conjugated secondary antibodies: Rat-on-Mouse HRP-Polymer Kit (Biocare Medical, Concord, CA, USA) or Dako EnVision+ System-HRP (anti-mouse or anti-rabbit) (Agilent Technologies). All immunoreactions were visualized by 3,3'-diaminobenzidine (Merck). For negative controls, specific antibodies were omitted, and either the antibody diluent alone or isotype control were used. Positive controls for CLDNs were normal human skin epithelium (CLDN-1), human colon mucosa (CLDN-2, -3, and -4), and human breast ductal cells (CLDN-7). Biliary epithelial cells in normal mouse liver served as positive control for CK19 and A6, whereas hepatocytes served as positive control for HNF4a.

3.9.3 Morphometric analysis

Reactions of CLDN-1, -2, -3, -4, and -7 in 20 HCCs, 20 CRLMs, and 15 PLMs, paired surrounding non-tumorous livers and 5 normal liver samples were subjected to morphometrical analysis. Ten non-overlapping images of each FFPE slide were captured (×60 objective) using an Olympus BX50 microscope (Olympus Corporation, Tokyo, Japan). Morphometric analysis of the digital images was performed using Leica QWin 3.0 morphometrical software (Leica Microsystems Imaging Solutions, Cambridge, UK). Claudin expression was measured as percentage of immunopositive pixels relative to the total area, which correlates with both the presence and strength of the staining.[166] A.H. and V.M.F. evaluated semiquantitatively the mean percentage of tumor areas occupied

by HCC-, cholangiocarcinoma (CCA)-, and EMT-like phenotypes on hematoxylin-eosin-stained FFPE sections of 14 HPC-, 28 HB-, and 28 AH-derived tumors.

3.10 Gene expression studies

3.10.1 RNA extraction

I used High Pure RNA Paraffin Kit (Roche) to isolate total RNA from manually dissected FFPE tissue blocks of 20 HCCs, 20 CRLMs, 15 PLMs, and 5 normal liver samples. Tumorous and non-tumorous samples were processed separately. I isolated total RNA from 16 HPC-, 26 HB-, and 26 AH-derived tumors, and freshly isolated primary mouse HPCs, HBs, and AHs (7 samples each) using TRIzol reagent (Thermo Fisher Scientific) in combination with RNeasy Mini Kit (Qiagen). Tumors were histologically verified prior to RNA isolation to ensure that tumor cells comprised the majority of the sample. Quantity and purity of total RNA was determined using a Nanodrop ND-1000 Spectrophotometer (Thermo Fisher Scientific). I assessed RNA integrity by Agilent 2100 Bioanalyzer (Agilent Technologies).

3.10.2 Quantitative RT-PCR

To measure the relative mRNA expression of CLDN-1, -2, -3, -4, and -7, total RNA was reverse transcribed using High Capacity RNA-to-cDNA Kit (Thermo Fisher Scientific). Quantitative polymerase chain reaction was perfomed using SYBR Green PCR Master Mix (Thermo Fisher Scientific) on an ABI Prism 7000 qPCR machine (Thermo Fisher Scientific). Oligonucleotide primers were designed with Primer Express software (Thermo Fisher Scientific; **Table 5**). Relative quantification of target gene expression was performed using the formula $2^{\Delta Ct}$, where $\Delta Ct = Ct_{reference} - Ct_{target}$, and β-actin was used as a reference.

Validation of microarray results was carried out on an independent set of frozen HPC-, HB-, and AH-derived tumors (6 samples of each tumor group), and primary HPCs, HBs, and AHs (3 samples each cell type). Total RNA was reverse transcribed using SuperScript III reverse transcriptase (Thermo Fisher Scientific) and random hexamers.

SYBR Green-based qPCR was performed using the Bio-Rad iCycler Thermal Cycler with iQ5 Multicolor Real-Time PCR Detection System (Bio-Rad, Hercules, CA, USA). Oligonucleotide primers (**Table 5**) were obtained from Primer Bank (Harvard University, Cambridge, MA, USA) or designed using Primer3 software.[167] Relative quantification of target gene expression was performed using the above formula, glyceraldehyde-3-phosphate dehydrogenase (Gapdh) was used as a reference.

Table 5. Primers used for quantitative PCR

Gene symbol	Forward primer (5' - 3')	Reverse primer (5' - 3')
ACTB	CCTGGCACCCAGCACAAT	GGGCCGGACTCGTCATAC
CLDN1	GTGCGATATTTCTTCTTGCAGG	TTCGTACCTGGCATTGACTGG
CLDN2	CTCCCTGGCCTGCATTATCTC	ACCTGCTACCGCCACTCTGT
CLDN3	CTGCTCTGCTGCTCGTGTCC	TTAGACGTAGTCCTTGCGGTCGTAG
CLDN4	GGCTGCTTTGCTGCAACTGTC	GAGCCGTGGCACCTTACACG
CLDN7	CATCGTGGCAGGTCTTGCC	GATGGCAGGGCCAAACTCATAC
Gapdh	CCACCCAGAAGACTGTGGAT	CACATTGGGGGTAGGAACAC
Afp	CCAGGAAGTCTGTTTCACAGAAG	CAAAAGGCTCACACCAAAGAG
Alb	AGCACAAGCCCAAGGCTAC	TGCATCTAGTGACAAGGTTTGG
Ednra	AGTATGCCTGAGACTTCCAG	GTCATCACTGTAGGAGAAACTG
Flt1	GAGGAGGATGAGGGTGTCTATAGGT	GTGATCAGCTCCAGGTTTGACTT
Mmp12	CATGAAGCGTGAGGATGTAGAC	TGGGCTAGTGTACCACCTTTG
Mmp13	CTATCCCTTGATGCCATTACCAG	ATCCACATGGTTGGGAAGTTC
Pdgfra	GGAGACTCAAGTAACCTTGCAC	TCAGTTCTGACGTTGCTTTCAA
Pdgfrb	GACTTGGAGTGACAGTGAGT	CTTCCTCTCATTGCCCATCT
Vim	CTTGAACGGAAAGTGGAATCCT	GTCAGGCTTGGAAACGTCC
Zeb2	AAAGCGTTCAAACACAAACACC	CCGCTTGCAGTAGGAGTACC

Human gene symbols are italicized written in all uppercase letters, mouse gene symbols are italicized, with only the first letter in upper case. *ACTB*, β-actin; *Alb*, albumin; *Ednra*, endothelin receptor type A; *Flt1*, Fms-related tyrosine kinase 1; *Gapdh*, glyceraldehyde-3-phosphate dehydrogenase; *Mmp*, matrix metalloproteinase; *Pdgfr*, platelet-derived growth factor receptor; *Vim*, vimentin; *Zeb2*, zinc finger E-box-binding protein 2.

3.10.3 Microarray

Ten HPC-, 20 HB-, and 20 AH-derived tumors, and their normal counterparts (4 samples each) were subjected to microarray analysis. Linear amplification of 400 ng RNA was performed using Illumina TotalPrep RNA Amplification Kit (Thermo Fischer Scientific). Reactions were incubated at 37ºC for 16 hours for *in vitro* transcription. Biotinylated complementary RNA (750 ng/sample) was then hybridized onto MouseRef-8 v2.0 Expression BeadChips for 18 hours at 58ºC (Illumina, San Diego, CA, USA). Following

washing and staining with Cy3-Streptavidin conjugate (GE Healthcare), BeadChips were scanned on an Illumina iScan System (Illumina).

3.11 Statistical analysis

Lilliefors and Pearson normality tests were used to assess the normality of data. Non-parametric tests were used to analyze non-normal data. Significant differences in the number of spheres formed by normal and H-Ras-EGFP$^+$/SV40LT-mCherry$^+$ mouse hepatic lineage cells were evaluated by Poisson generalized linear model. Frequency of tumor-initiating cells in T-AHs, T-HBs, and T-HPCs was calculated and compared using Poisson distribution statistics 5 weeks after transplantation. The probability of tumor initiation by transduced HSCs was calculated using binomial distribution. Significant differences in the proportion of HCC-, CCA-, and EMT-like phenotypes in mouse liver tumors were calculated by one-way analysis of variance and Tukey post hoc test. Effect of c-Myc knockdown on the kinetics of subcutaneous tumor growth and sphere formation was evaluated by Student's t-test and Poisson generalized linear model, respectively. Kruskal-Wallis and post hoc tests were conducted to compare the protein and mRNA expression of individual claudins in the different groups; the surrounding non-tumorous livers were treated as one group. Statistical analysis was performed using Statistica 8.0 software (Dell, Round Rock, TX, USA), GraphPad Prism 5.0 software (GraphPad Software, La Jolla, CA, USA) or L-Calc software (Stemcell Technologies). $P < 0.05$ was considered significant in all the analyses described above.

Microarray image analysis and data extraction were performed using Illumina GenomeScan software (Illumina). Gene expression values were adjusted by subtracting background noises in each spot and normalized by quantile normalization method with GenomeStudio software (Illumina). All microarray data were submitted to GEO (accession number GSE41312) and are accessible at http://www.ncbi.nlm.nih.gov/geo/. Transcriptomic similarities between tumors and their normal counterparts were identified using bioequivalence test.[168] Significant differences in gene expression (fold change > ±2; $P < 0.001$) between tumors and their corresponding cell-of-origin were determined by bootstrap t-test with 5,000 repetitions.[169] Overlap of differentially expressed genes in HPC-, HB-, and AH-derived tumors with a core embryonic stem cell module map consisting of 335 genes was evaluated.[170] Functional annotation and network analyses were

performed by Ingenuity Pathway Analysis tool 8.7 (Qiagen). Gene set enrichment analysis (GSEA) was performed using GSEA software provided by the Broad Institute (Cambridge, MA, USA). Gene set enrichment analysis is a commonly applied method that determines whether an *a priori* defined gene set shows statistically significant, concordant differences between two biological states.[171] Statistical significance of the enrichment score for a single gene set was estimated by nominal *P* value. False positives were calculated by the false discovery rate (FDR). Gene sets with a nominal P value < 0.05 and FDR < 0.25 were considered significantly enriched. Enrichment of a 35-gene EMT signature, a hepatocyte-derived induced pluripotent stem cell (iPSC) signature of 786 genes, and 229 Myc E-box target genes was tested in HPC-, HB-, and AH-derived tumors.[172-174] Mann-Whitney U test was used to analyze the expression of genes selected for validation by qRT-PCR from microarray analyses.

DOI:10.14753/SE.2019.2291

4. RESULTS

4.1 Contribution of distinct mouse hepatic lineage cells to the evolution of liver cancer stem cells and heterogeneity of HCC

4.1.1 H-Ras/SV40LT reprogram mouse hepatocyte lineage cells into cancer stem cells

Activation of Ras pathway and disruption of p53 and retinoblastoma pathways frequently occur in rodent and human HCCs.[175-177] Thus, my experimental approach was as follows: isolation of primary mouse hepatic lineage cells at different stages of differentiation, followed by co-transduction with oncogenic H-Ras-Luciferase/EGFP and SV40LT-mCherry lentiviral vectors.

Hepatic progenitor cells are considered to be the progeny of adult hepatic stem cells that differentiate into hepatocytes and cholangiocytes in severely injured liver. They express markers in common with cholangiocytes, and fetal and adult hepatocytes.[178] I isolated HPCs from livers of DDC-treated mice by FACS using anti-EpCAM antibody (**Figure 7**).

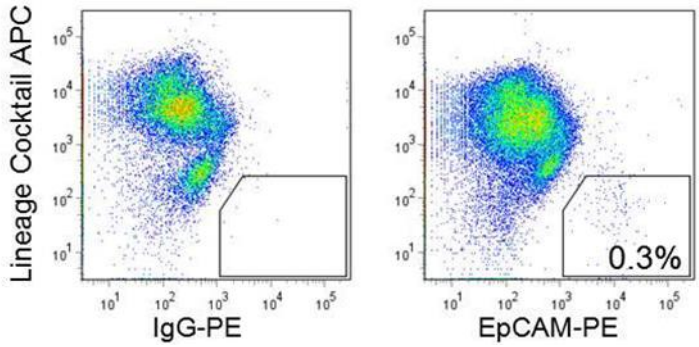

Figure 7. Purification of primary mouse hepatic progenitor cells. High purity, epithelial cell adhesion molecule $(EpCAM)^{+}$/Lineage Antibody $Cocktail^{-}$ hepatic progenitor cells were isolated by fluorescence-activated cell sorting. PE, phycoerythrin.

Hepatoblasts are common progenitors of hepatocytes and cholangiocytes in the fetus.[179] In mice, the majority of hepatoblasts are committed towards hepatocyte lineage after embryonic day 15.[180] I isolated hepatoblasts from fetal mouse liver at embryonic day

16.5 by MACS using a monoclonal antibody against E-cadherin, a specific surface marker of immature hepatocytes. I obtained fully differentiated adult hepatocytes from 3 month-old male mice using a two-step collagenase perfusion method. Next, I analyzed the purity of freshly isolated HBs, HPCs, and AHs. Over 99% of the isolated HBs expressed E-cadherin, AFP, an early marker of hepatocytic differentiation, and albumin, another specific marker of hepatic lineage cells (**Figure 8**).[156, 181] Reflecting high purity, only isolated HBs expressed AFP, whereas AHs exhibited the highest levels of albumin, as measured by qRT-PCR (**Figure 9**).

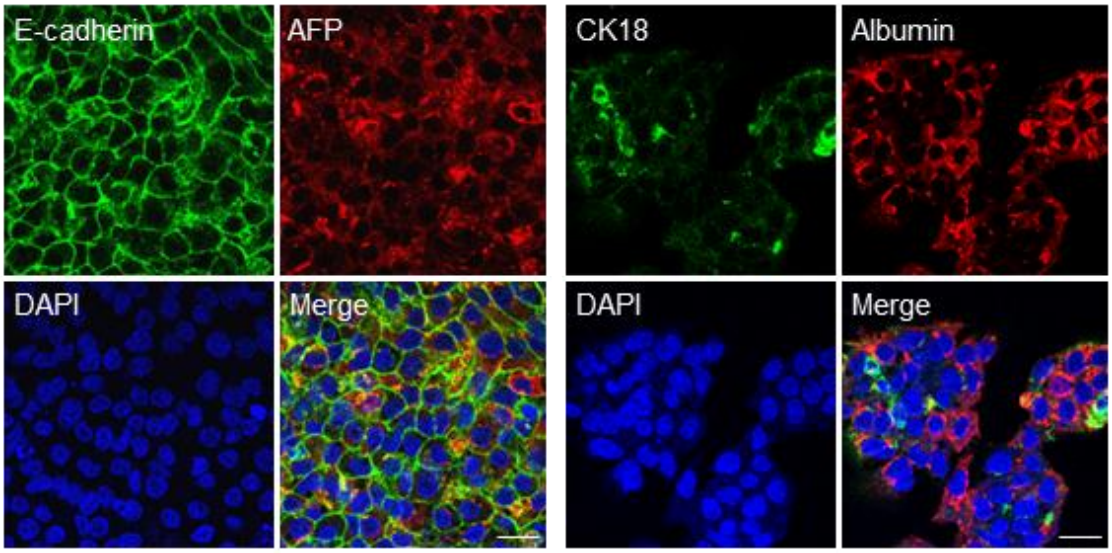

Figure 8. Immunostaining of primary mouse hepatoblasts after magnetic cell sorting. Purity of purified hepatoblasts was determined by fluorescence immunocytochemistry for E-cadherin, AFP, albumin, and CK18 after overnight incubation of primary cultures. Nuclei were counterstained with 4',6-diamidino-2-phenylindole (DAPI). Scale bar = 20 µm.

I co-transduced the cells with H-Ras-EGFP and SV40LT-mCherry lentiviruses 24 hours after isolation. The infection efficiency was measured by flow cytometry as the percentage of EGFP and mCherry double positive cells 10 days after infection. To test the properties of the resulting cell populations both *in vitro* and *in vivo*, $EGFP^+/mCherry^+$ HPCs, HBs, and AHs were FACS sorted using the same gating parameters to ensure comparable viral load and transgene expression (**Figures 10** and **11**).

DOI:10.14753/SE.2019.2291

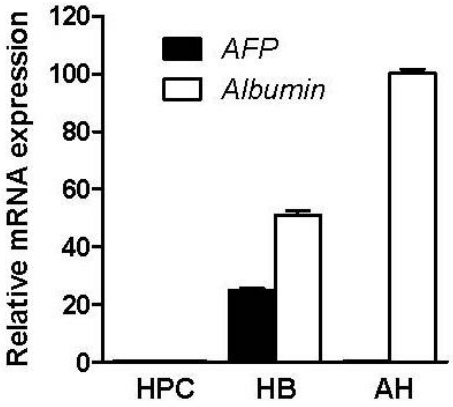

Figure 9. Quantitative RT-PCR analysis with primers specific to hepatic lineage cells. Data are presented as mean expression levels ± standard deviation of AFP and albumin in freshly isolated primary cells relative to glyceraldehyde-3-phosphate dehydrogenase. All experiments were performed in duplicate using three independent cell isolations. AH, adult hepatocyte; HB, hepatoblast; HPC, hepatic progenitor cell.

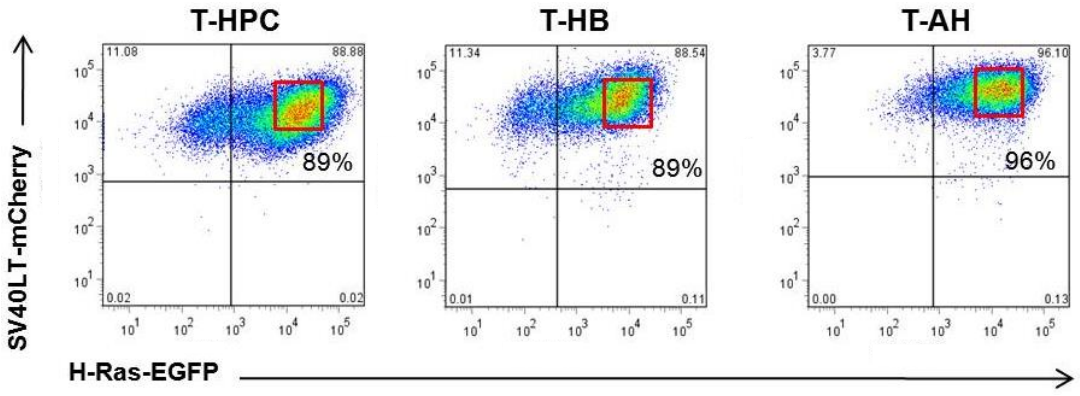

Figure 10. Efficient transduction of primary mouse hepatic lineage cells with H-Ras-EGFP and SV40LT-mCherry lentiviral vectors. Primary HPCs, HBs, and AHs were co-transduced with H-Ras-EGFP and SV40LT-mCherry lentiviruses 24 hours after plating. Transduction efficiency was measured by flow cytometry as the percentage of $EGFP^+/mCherry^+$ cells 10 days after co-transduction. Transduced cells were sorted using the same gating parameters (boxed areas) for further analysis. EGFP, enhanced green fluorescent protein; T-AH/T-HB/T-HPC, H-Ras-$EGFP^+$/SV40LT-$mCherry^+$ AH/HB/HPC.

DOI:10.14753/SE.2019.2291

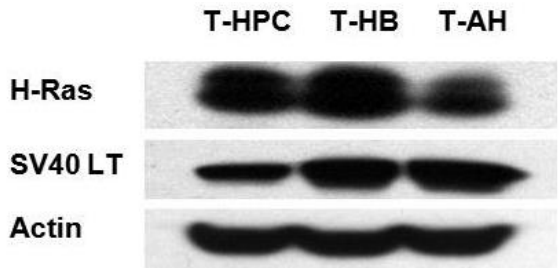

Figure 11. Western blot analysis of H-Ras and SV40LT protein expressions in H-Ras-EGFP$^+$/SV40LT-mCherry$^+$ mouse hepatic lineage cells. Primary HPCs, HBs, and AHs were *ex vivo* co-transduced with H-Ras-EGFP and SV40LT-mCherry lentiviruses. EGFP$^+$/mCherry$^+$ cells were sorted 10 days after co-transduction and subjected to western blot analysis. Actin was used as loading control.

All three types of hepatic lineage cells were effectively transformed by H-Ras/SV40LT and acquired CSC properties as defined by an increase and/or acquisition of SP fraction, CD133 expression, and ability to grow as self-renewing spheres (**Figures 12** and **13**).[80, 83, 92]

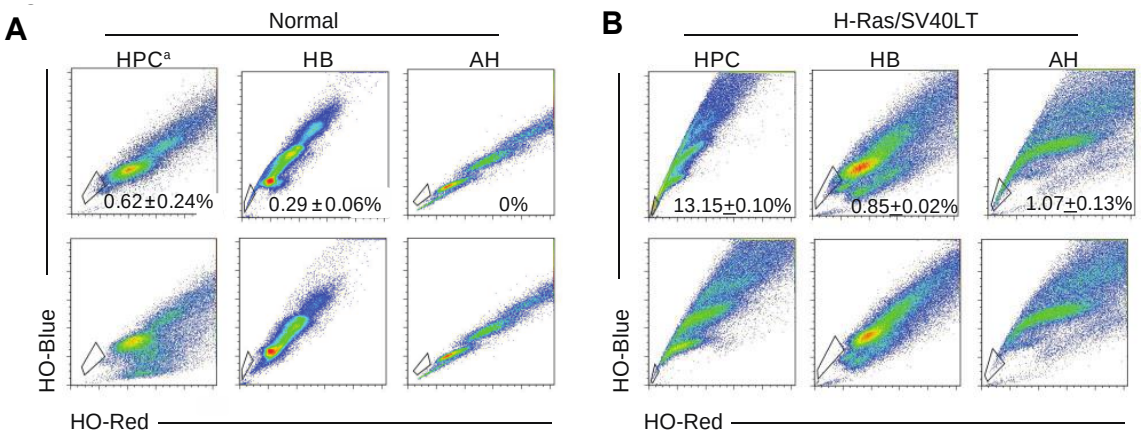

Figure 12. Flow cytometric analysis of side population cells in normal and H-Ras-EGFP$^+$/SV40LT-mCherry$^+$ mouse hepatic lineage cells. Side population (SP) cells were identified in (A) normal and (B) transduced HPCs, HBs, and AHs by Hoechst 33342 (HO) staining. SP gates were drawn by using fumitremorgin C (dot plots at the bottom). Data represent mean ± standard deviation of three experiments. [a]Cultured HPCs at passage 5.

DOI:10.14753/SE.2019.2291

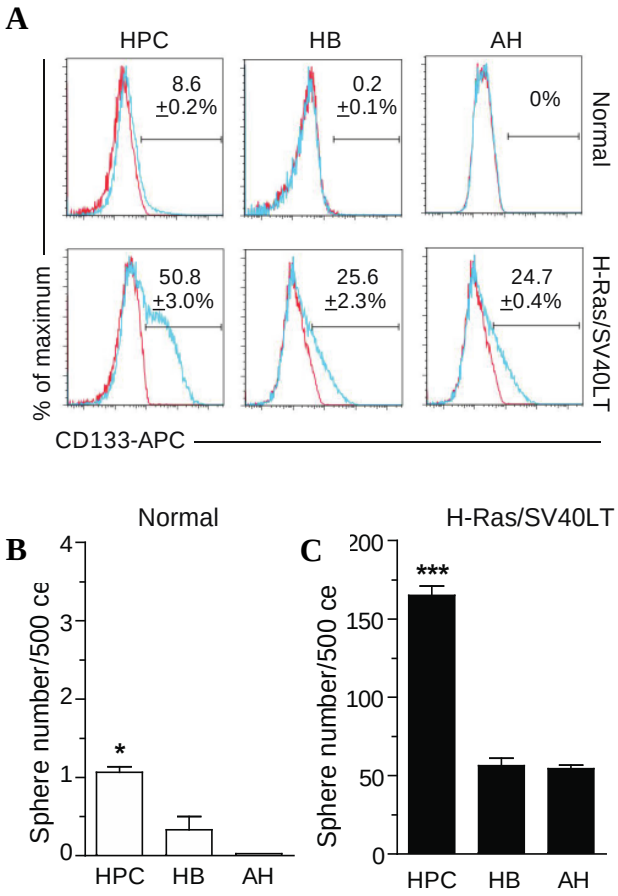

Figure 13. Analysis of CD133 expression and sphere forming ability in normal and H-Ras-EGFP^{+}/SV40LT-mCherry^{+} mouse hepatic lineage cells. (A) CD133 expression was measured by flow cytometry. Blue line indicates APC-conjugated anti-CD133 antibody, red line indicates isotype control. Data represent mean ± standard deviation percentages of positive cells in three experiments. (B and C) Spheroid forming ability. Freshly isolated normal (B) and transduced (C) mouse hepatic lineage cells were cultured in 1% methylcellulose in 96-well ultra-low attachment plates at low density. Spheroids were counted on day 7. Data represent mean ± standard deviation of four experiments. Significant differences were evaluated by Poisson generalized linear model and one-way analysis of variance; $P < 0.05$ was considered statistically significant. *$P < 0.05$; ***$P < 0.001$.

To quantify the frequency of tumor-initiating cells in each transduced cell population, I next performed a limiting dilution assay. The frequency of tumor initiating cells within each transplanted cell population was calculated based on the number of palpable tumors per number of injections at each transplant dose. Interestingly, the frequency of tumor-initiating cells was significantly higher in T-HPCs as compared to T-HBs and T-AHs. As few as 10 T-HPCs produced tumors in 6 of 8 injections compared to T-HBs (2/8)

and T-AHs (0/8) by 5 weeks after subcutaneous transplantation (**Table 6**). In contrast, subcutaneous injection of 3 million normal HPCs did not generate tumors after 6 months. *Ex vivo* bioluminescence imaging revealed that tumors initiated by T-HPCs, T-HBs, and T-AH were very aggressive and gave rise to multiple metastatic foci throughout liver, lungs, and brain with a slightly higher frequency in the recipients of T-HPCs (**Figure 14**, **Table 7**).

Table 6. Limiting dilution analysis

Transformed cell type	Number of injected cells			TIF	95% CI	*P* (comparison with HPC)
	1000	100	10			
HPC	8/8	8/8	6/8	1/7	1/3 – 1/17	-
HB	8/8	8/8	2/8	1/26	1/11 – 1/62	0.04
AH	8/8	8/8	0/8	1/42	1/19 – 1/91	0.003

H-Ras-EGFP$^+$/SV40LT-mCherry$^+$ HPCs, HBs, and AHs were sorted and injected subcutaneously into both flanks of NOD/SCID mice (4 mice/group). Frequency of tumor-initiating cells (TIF) was calculated 5 weeks after transplantation based on the number of palpable tumors per number of injections at each transplant dose. Significant differences were evaluated using Poisson distribution statistics; $P < 0.05$ was considered statistically significant. CI, confidence interval.

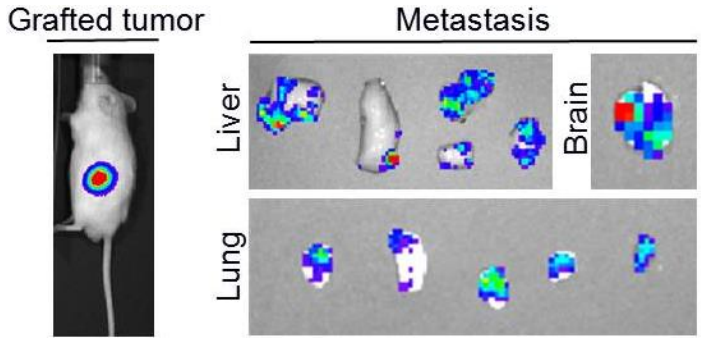

Figure 14. Subcutaneous tumor growth and metastatic ability. One hundred cells of H-Ras-EGFP$^+$/SV40LT-mCherry$^+$ HPCs, HBs, and AHs were injected subcutaneously into both flanks of NOD/SCID mice (4 mice/group). (Left panel) Representative *in vivo* bioluminescence image of a mouse 5 weeks after injection of hepatic progenitor cells. (Right panel) *Ex vivo* bioluminescence images of liver, lungs, and brain from the same mouse.

DOI:10.14753/SE.2019.2291

Table 7. Incidences of primary grafted and metastatic tumors 5 weeks after subcutaneous transplantation

Transformed cell type	Tumor incidence	Metastasis		
		Intrahepatic	Lung	Brain
HPC	8/8 (100%)	4/4 (100%)	2/4 (50%)	3/4 (75%)
HB	8/8 (100%)	4/4 (100%)	2/4 (50%)	3/4 (75%)
AH	8/8 (100%)	4/4 (100%)	3/4 (75%)	3/4 (75%)

One hundred cells of H-Ras-EGFP$^+$/SV40LT-mCherry$^+$ HPCs, HBs, and AHs were injected subcutaneously into both flanks of NOD/SCID mice (4 mice/group). Metastases were identified using *ex vivo* bioluminescence imaging 5 weeks after injection.

I obtained similar results in an independent orthotopic transplantation experiment when I injected transduced cells of each genotype into the left liver lobe of immunodeficient mice (**Figure 15**, **Table 8**).

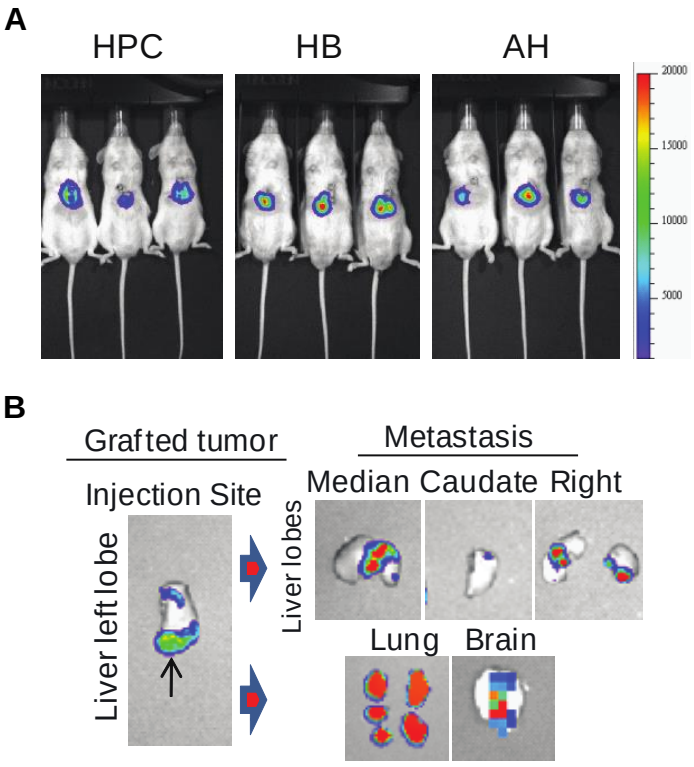

Figure 15. Orthotopic tumor growth and metastatic ability. (A) Representative *in vivo* bioluminescence images of mice 11 days after orthotopic transplantation of 1.5×10^5 cells of H-Ras-EGFP$^+$/SV40LT-mCherry$^+$ HPCs, HBs, and AHs into the left liver lobe of NOD/SCID mice (5 mice/group). (B) *Ex vivo* bioluminescence imaging of the liver, lungs, and brain 16 days after transplantation.

Table 8. Incidences of primary grafted and metastatic tumors in the orthotopic transplantation model

Transformed cell type	Grafted tumor	Metastasis		
		Intrahepatic	Lung	Brain
HPC	5/5 (100%)	5/5 (100%)	5/5 (100%)	3/5 (60%)
HB	5/5 (100%)	4/5 (80%)	5/5 (100%)	2/5 (40%)
AH	5/5 (100%)	4/5 (80%)	4/5 (80%)	3/5 (60%)

H-Ras-EGFP$^+$/SV40LT-mCherry$^+$ HPCs, HBs, and AHs were injected into the left liver lobe of NOD/SCID mice (5 mice/group). Metastases were identified using *ex vivo* bioluminescence imaging 16 days after transplantation.

To gain greater insight into the tumorigenicity of H-Ras/SV40LT-transformed hepatic lineage cells, I established and characterized several clonal cell lines (4 per cell type) from tumors generated by direct intrahepatic injection. Irrespective of tumor cell-of-origin, all established primary tumor cell lines expressed hepatic progenitor/biliary cell (CK19, EpCAM, A6) and CSC-associated markers (CD133, CD44, CD29, CD49f, CD90, Sca-1), had comparable size of SP fraction, and possessed high self-renewal capacity through 6 serial passages (**Figures 16** and **17**).[80, 83, 182]

Collectively, these results indicate that any hepatic lineage cell, including terminally differentiated hepatocyte, was susceptible to oncogene-driven transformation. Each H-Ras/SV40LT-transformed cell population acquired similar attributes of liver CSCs producing aggressive liver cancer with a strong potential for intrahepatic and distant organ metastasis. However, primitive HPCs were more susceptible to transformation as compared to more differentiated HBs and AHs.

DOI:10.14753/SE.2019.2291

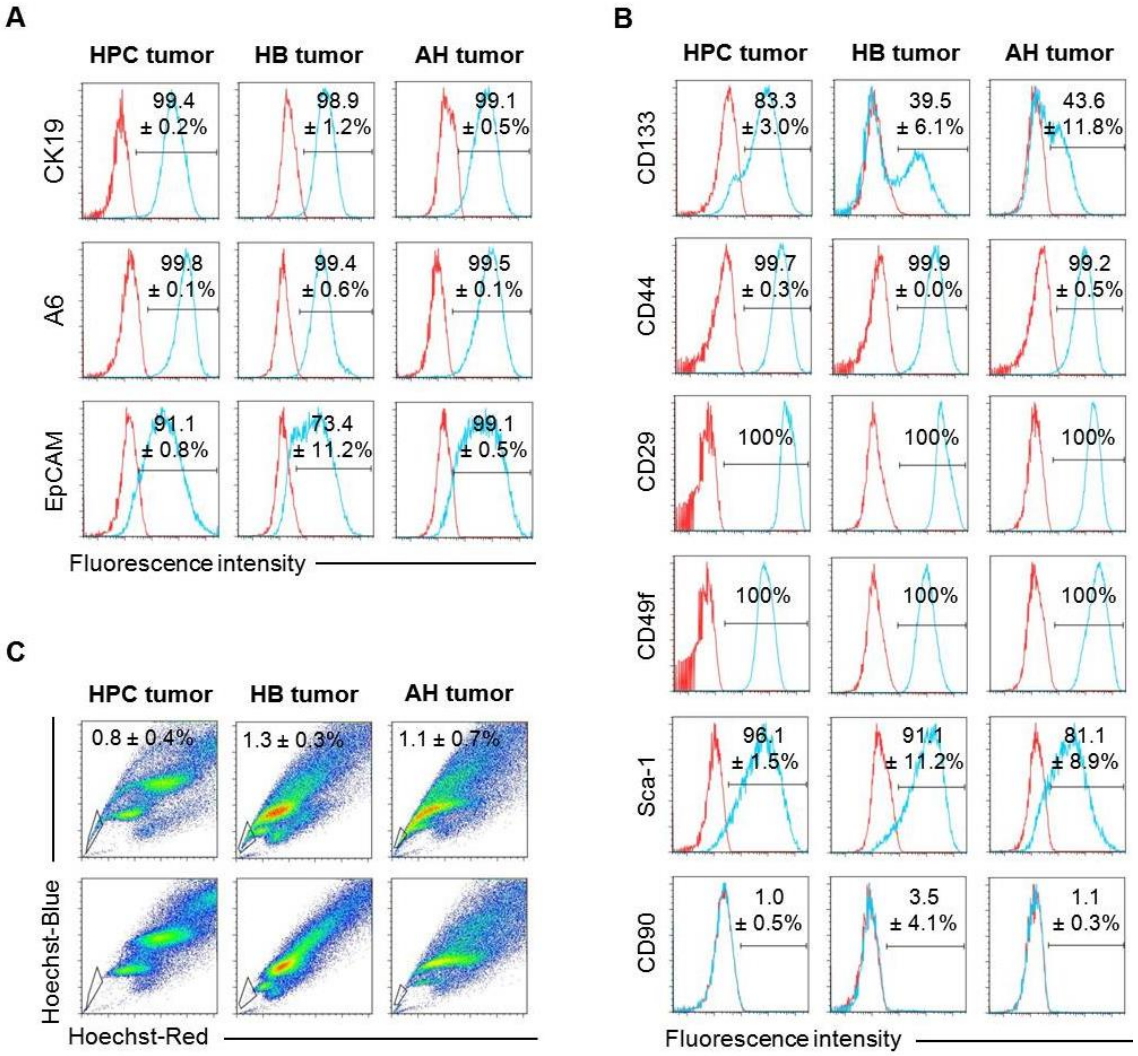

Figure 16. Flow cytometric characterization of mouse hepatic lineage cell-derived tumor cell lines. H-Ras-EGFP^{+}/SV40LT-mCherry^{+} HPCs, HBs, and AHs (1.5×10^5 of each cell type) were grafted into the left liver lobe of NOD/SCID mice. The resulting liver tumors were macrodissected and dissociated to establish tumor cell lines (4/cell type). Tumor cells at passage 2 to 5 were used for flow cytrometric assays. (A and B) Analysis of liver progenitor/biliary cell (A) and CSC-associated (B) markers. Blue lines represent reactivity for the specified antibodies, red lines correspond to the staining obtained with isotype control anti-bodies. Data represent mean ± standard deviation percentages of positive cells in four tumor cell lines. (C) Analysis of side population cells. Side population cells were identified by Hoechst 33342 staining and the use of blue and red filters. Fumitremorgin C was used to set up the SP gate (dot plots shown at the bottom). Data represent mean ± standard deviation of triplicate measurements in four tumor cell lines.

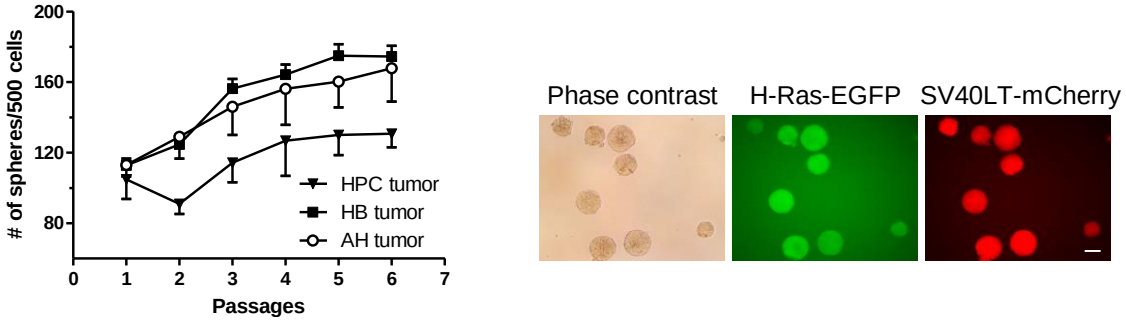

Figure 17. Analysis of spheroid-forming ability of mouse hepatic lineage cell-derived tumor cell lines. H-Ras-EGFP$^+$/SV40LT-mCherry$^+$ HPCs, HBs, and AHs (1.5×10^5 of each cell type) were grafted into the left liver lobe of NOD/SCID mice. The resulting liver tumors were macrodissected and dissociated to establish tumor cell lines (4/cell type). Tumor cells at passage 2 to 5 were used for sphere formation assay. Cells were plated at low density in 1% methylcellulose in 96-well ultra-low attachment plates to generate primary spheroids that were passaged every 7 days for 6 weeks. Data represent mean ± standard error of mean from four tumor cell lines. Phase contrast and fluorescence images of spheroids at passage 6 demonstrate stable expression of transgenes. Scale bar = 100 μm.

4.1.2 Unambiguous oncogenic reprogramming of adult hepatocytes

Hepatic stem cells represent an extremely rare population of cells in adult mouse liver that reside within the terminal bile ductules surrounded by a basal lamina.[183, 184] Although the protocol for isolation and purification was optimized for primary AHs, it could not be ruled out that occasional contaminating HSCs were targeted by H-Ras and SV40LT and selectively amplified during a subsequent 3-week growth in culture. To test this possibility, I used three experimental approaches. First, I injected a low number of H-Ras-/SV40LT-transduced AHs (10^3 cells) into the spleen of NOD/SCID mice, and compared the number of the generated liver tumors with the estimated number of HSCs in normal adult mouse liver. To prevent the possibility of selective overgrowth of HSCs, H-Ras/SV40LT-transduced primary AHs were transplanted via spleen into NOD/SCID mice after a short-term (1-day) culture. Transplanted cells yielded 2-3 liver tumors per mouse by 18 days after injection. Our previous findings and literature reports indicated that the frequency of EpCAM$^+$ non-parenchymal cells in primary AH culture was on average 0.13%, and only 0.16% of this fraction possessed sphere forming potential and ability to differentiate along hepatocytic or biliary epithelial cell lineages.[152, 185] Thus, the estimated frequency of HSCs in primary AH culture did not exceed 2 HSCs per 10^6

hepatocytes. Assuming 100% efficiency of transduction and transformation, the probability of tumor initiation by transduced HSCs is negligible ($\leq 2.1 \times 10^{-6}$; **Figure 18**).

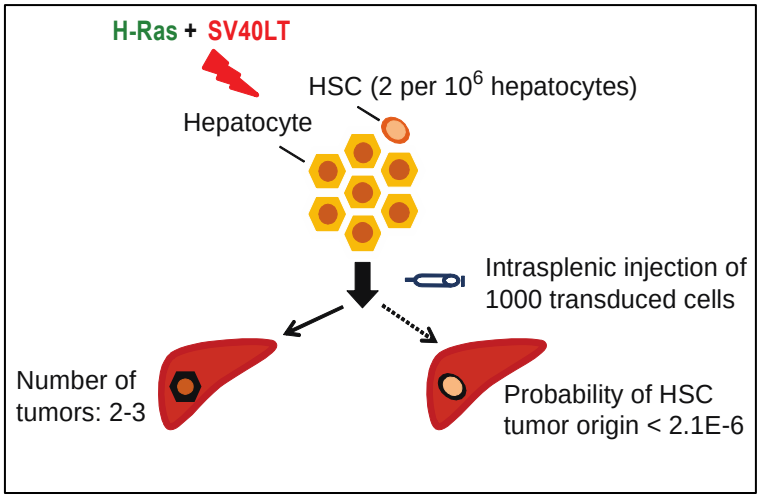

Figure 18. Overview of the approach used to compare the number of resulting tumors with the estimated frequency of hepatic stem cells (HSCs). Primary adult hepatocytes were transduced and then cultured only for 1 day to exclude the possibility of selective overgrowth of HSCs. A total of 1000 transduced cells were injected via the spleen into NOD/SCID mice, and liver tumors were counted after 18 days. Probability of tumor initiation by transduced HSCs was calculated using binomial distribution.

Next, I evaluated the *in vivo* tumorigenicity of genetically labeled, H-Ras/SV40LT-transduced AHs following a short- (1-day) or long- (21-days) term culture. I isolated and transduced primary AHs from homozygous B6.Cg-*Gt(ROSA)26Sor*$^{tm14(CAG-tdTomato)Hze}$/J Cre-reporter mice.[186] These mice harbor a targeted mutation of the *Gt(ROSA)26Sor* locus with a *loxP*-flanked STOP cassette preventing transcription of a downstream red fluorescent protein, tdTomato. Upon adenoviral delivery of Cre recombinase *in vivo*, the STOP cassette is deleted only in hepatocytes, resulting in expression of tdTomato (**Figure 18**, left panel). Regardless whether transduced AHs were maintained *in vitro* for 1 day or 21 days, the number of liver tumors initiated after the transplantation of 10^5 AHs were not significantly different: 7.3 (5-11) and 6 (5-7), respectively. *Ex vivo* imaging of dissected livers confirmed that all tumors displayed overlapping luciferin and tdTomato signals indicating that the tumors originated from AHs (**Figure 19**, right panel).

Lastly, I found a significant increase in nuclear ploidy in cell lines derived from AH tumors, a characteristic of differentiated hepatocytes (**Figure 20**).[187] In contrast, cells

DOI:10.14753/SE.2019.2291

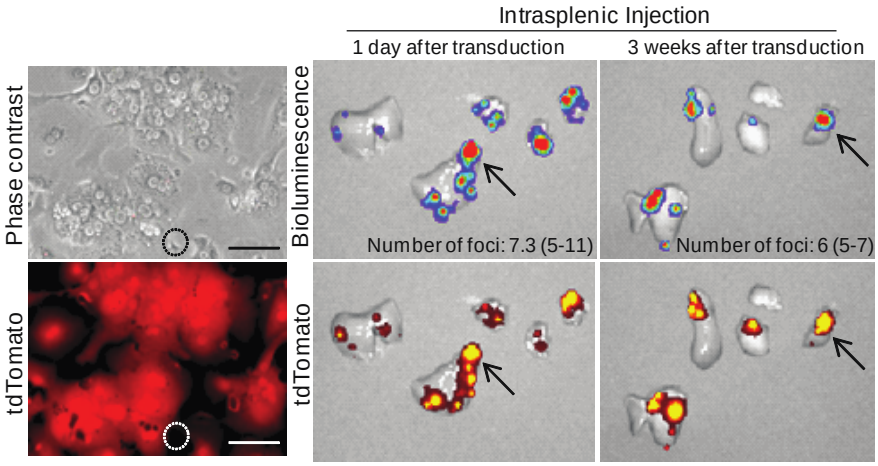

Figure 19. Generation of liver tumors from genetically labeled adult hepatocytes. (Left panel) Phase contrast and fluorescence images of 24-hour primary AH culture established from B6.Cg-Gt(ROSA)26Sor$^{tm14(CAG-tdTomato)Hze}$/J mouse. Isolated AHs showed strong, homogeneous expression of tdTomato 1 week after intravenous injection of adenovirus-Cre. Circle marks tdTomato-negative non-parenchymal cells. Scale bar = 100 µm. (Right panel) *Ex vivo* bioluminescence and fluorescence images of livers 18 days after injection of 10^5 hepatocytes co-transduced with H-Ras-EGFP and SV40LT-mCherry lentiviruses. Transduced AHs were cultured for 1 or 21 days before intrasplenic transplantation.

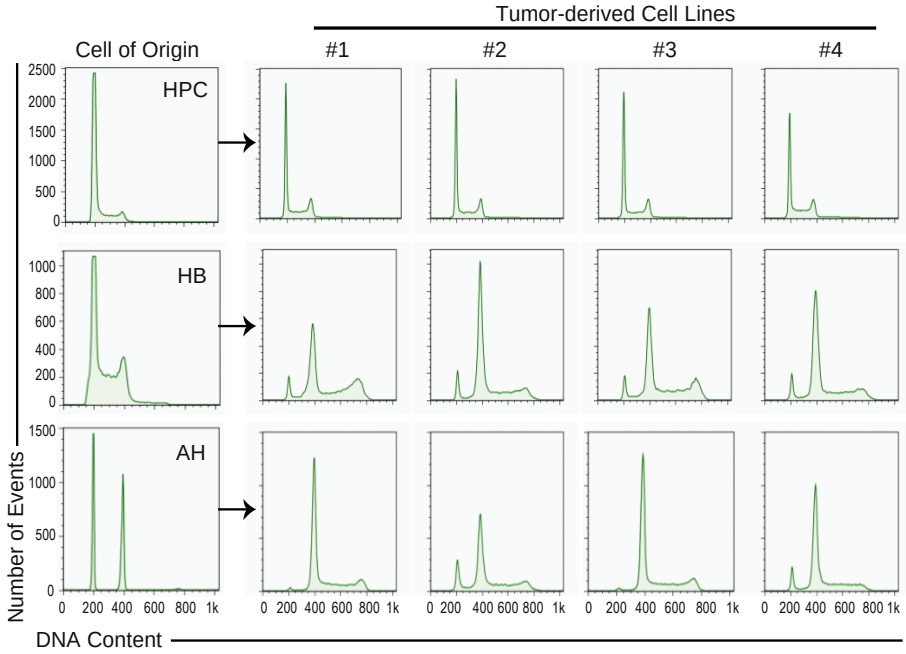

Figure 20. Flow cytometric analysis of DNA content of mouse hepatic lineage cell-derived tumor cell lines. DNA content of clonal cell lines (4/cell type) from tumors generated by direct intrahepatic injection of H-Ras-EGFP$^+$/SV40LT-mCherry$^+$ HPCs, HBs, and AH was compared to that of primary cells.

isolated from HPC tumors were predominantly diploid, similarly to normal HPCs. Taken together, these results demonstrate that terminally differentiated AHs but not contaminating HSCs were the targets of oncogenic transformation.

4.1.3 H-Ras/SV40LT induce liver cancer of multilineage differentiation

To assess the impact of cell-of-origin on tumor histopathology, I injected H-Ras/SV40LT-transduced HPCs, HBs, and AHs into the spleens of NOD/SCID mice to ensure tumor formation from engraftment of a single cell. For comparison, 14 HPC-, 28 HB-, and 28 AH-derived individual tumors were macrodissected and subjected to morphometrical and immunohistochemical analyses. Cancer cells exhibited strong submembranous staining for H-Ras and nuclear staining for SV40LT, confirming that the tumors indeed originated from H-Ras/SV40LT-expressing cells (**Figure 21**).

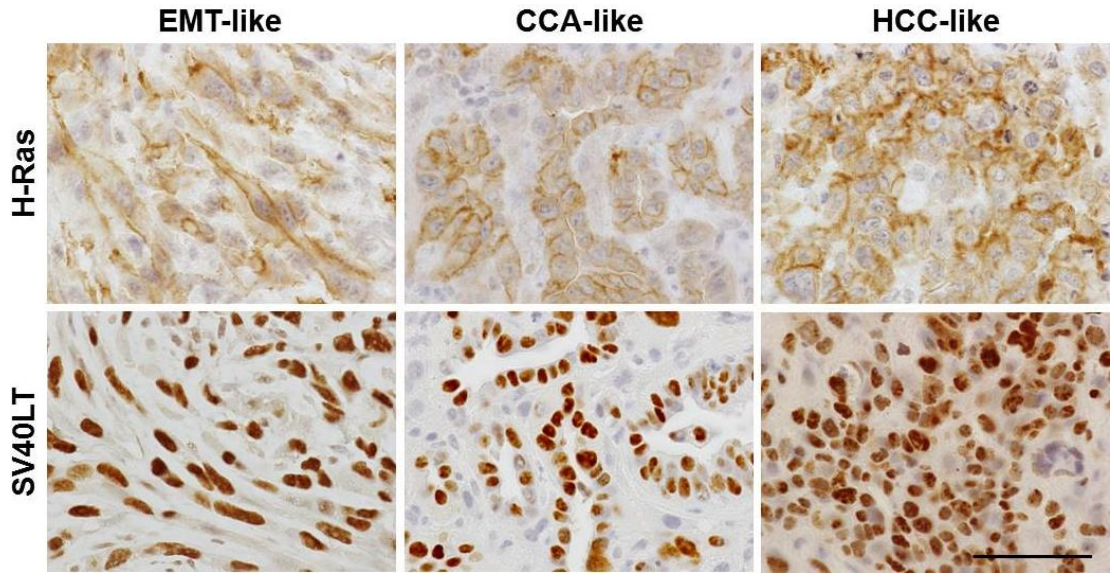

Figure 21. Expression of H-Ras and SV40LT in different tumor phenotypes. Immunohistochemical detection of v-H-Ras and SV40LT was performed on formalin-fixed, paraffin-embedded sections of liver tumors generated by intrasplenic injection of H-Ras-EGFP^{+}/SV40LT-mCherry^{+} HPCs, HBs, and AHs. Reactions were visualized by 3,3'-diaminobenzidine. Mayer's hematoxylin was used as nuclear counterstain. CCA, cholangiocarcinoma; EMT, epithelial-mesenchymal transition; HCC, hepatocellular carcinoma. Scale bar = 50 μm.

Irrespective of cell-of-origin, tumors were moderately to poorly differentiated with varying contribution of EMT-, CCA-, and HCC-like phenotypes supporting the concept of continuous spectrum of human primary liver cancer (PLC; **Figures 22** and **23**).[174] Semiquantitative analysis revealed a dominant EMT-like phenotype (85.0 ± 18.2% of the tumor cross-section areas) in HPC-derived tumors consisting of sheets of spindle-shaped, mesenchymal-like cancer cells. HB-derived tumors showed mostly CCA-like phenotype (52.7 ± 37.8%) composed of heterogeneous, columnar or cuboidal cancer cells arranged in glandular and tubular structures surrounded by abundant fibrous stroma. AH-derived tumors predominantly displayed an HCC-like phenotype (59.7 ± 34.6%) of polygonal, hepatocyte-like tumor cells arranged in solid pattern (**Figure 23**).

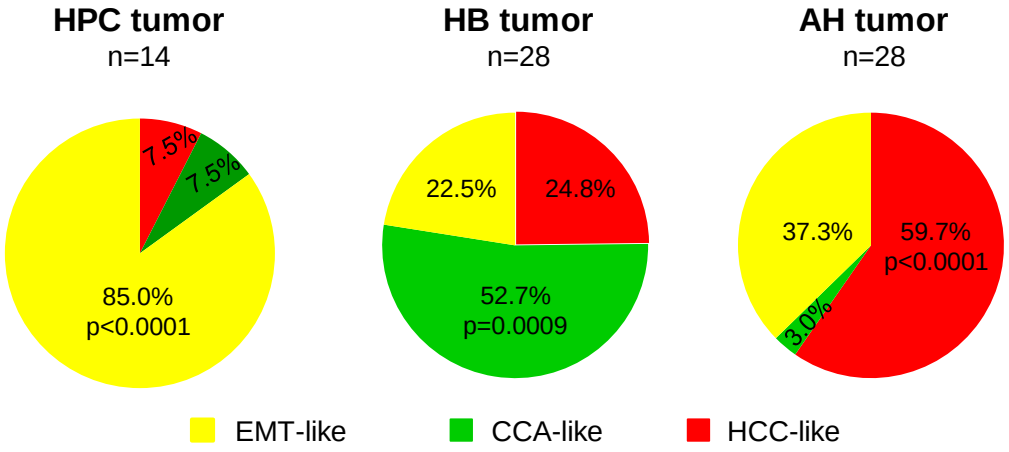

Figure 22. Semiquantitative analysis of EMT-, CCA-, and HCC-like tumor phenotypes. Circle graphs represent the mean percentage of tumor areas occupied by HCC-, CCA-, and EMT-like phenotypes in liver tumors generated by intrasplenic injection of H-Ras-EGFP^{+}/SV40LT-mCherry^{+} HPCs, HBs, and AHs. Significant differences were evaluated by one-way analysis of variance. $P < 0.05$ was considered statistically significant.

The majority of HCC-like tumor cells expressed HNF4A, a central mediator of hepatocyte differentiation.[188] Cholangiocarcinoma- and EMT-like tumor cells were also positive for HNF4A albeit with lower frequency. I observed strong, uniform expression of progenitor/biliary cell markers keratin 19 and A6 regardless of tumor cell-of-origin. Furthermore, EMT- and HCC-like tumor cells showed intense cytoplasmic and extracellular staining for laminin, a component of the hepatic progenitor cell niche in rodent and human livers, and were uniformly positive for mesenchymal marker vimentin (**Figure 23**).[184]

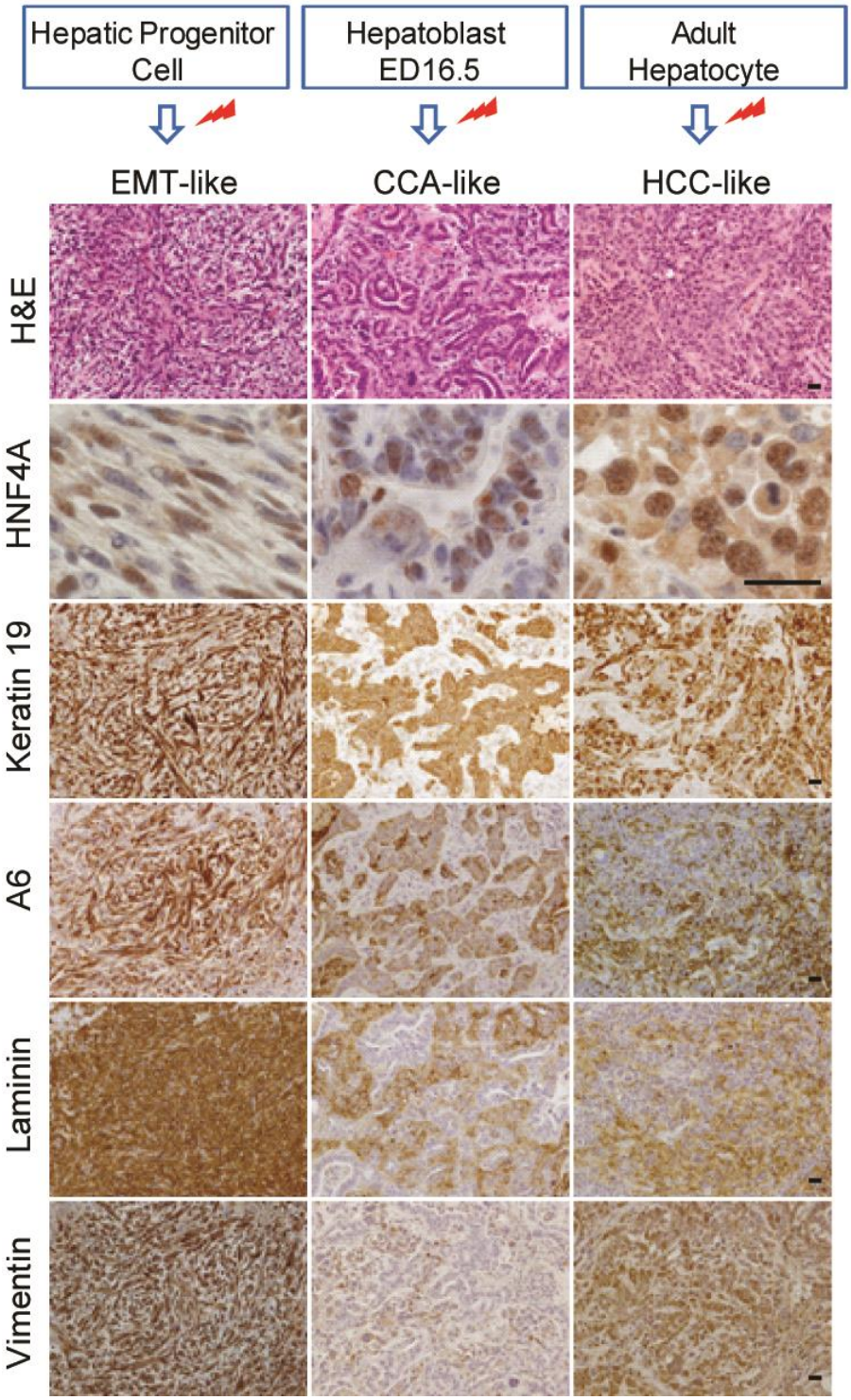

Figure 23. Immunohistochemical characterization of EMT-, CCA-, and HCC-like tumor phenotypes. Liver tumors were generated by intrasplenic injection of H-Ras-EGFP^{+}/SV40LT-mCherry^{+} hepatic progenitor cells, hepatoblasts, and adult hepatocytes. Reactions were visualized by 3,3'-diaminobenzidine. Mayer's hematoxylin was used as nuclear counterstain. Red marks indicate transduction with H-Ras/SV40LT lentiviral vectors. ED, embryonic day; H&E, hematoxylin-eosin. Scale bar = 25 μm.

To confirm that the EMT-, CCA-, and HCC-like tumor phenotypes were initiated by a single cell, I established 15 single cell-derived clonal lines from H-Ras/SV40LT-transduced AHs, and injected them into the spleen of NOD/SCID mice. Fourteen out of 15 clones (93.3%) showed comparable frequency of engraftment and kinetics of tumor growth. More importantly, the 42 examined tumors displayed overlapping EMT-CCA-HCC-like phenotypes indistinguishable from the tumors initiated by a bulk of H-Ras/SV40LT-transduced AHs (**Figure 24**).

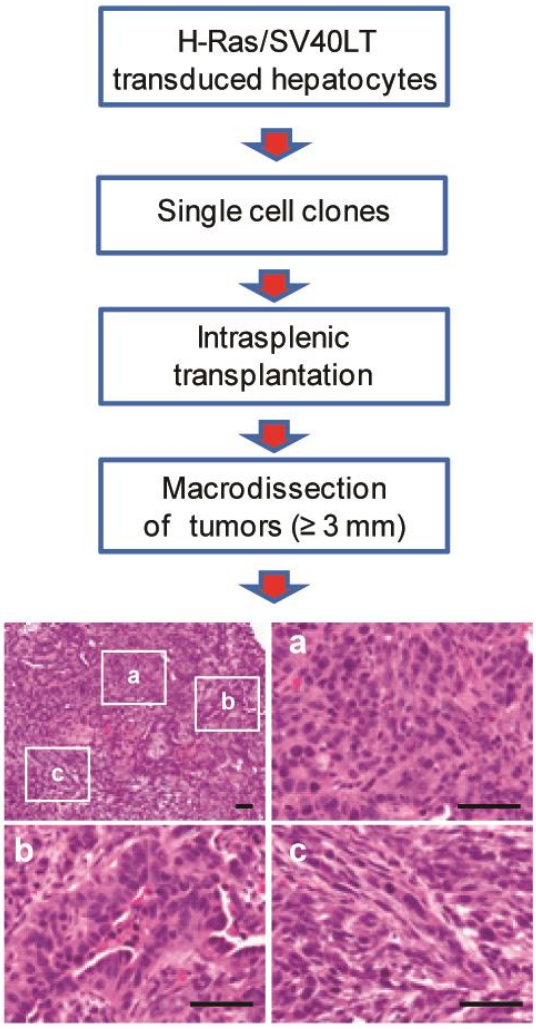

Figure 24. Schematic overview of the strategy and representative hematoxylin-eosin staining of tumors derived from single cell clones of H-Ras/SV40LT-transduced adult hepatocytes. Liver tumors were generated by intrasplenic injection of 15 single cell-derived clonal lines established from H-Ras/SV40LT-transduced adult hepatocytes. a, b, and c denote HCC-, CCA-, and EMT-like areas within the same tumor. Scale bar = 50 μm.

I concluded that upon oncogenic transformation, murine HPCs, HBs, and AHs were capable of propagating liver cancers of multilineage differentiation closely resembling human PLCs, and that the differentiation stage of cell-of-origin had a profound effect on tumor phenotype.

4.1.4 Common activation of epithelial-mesenchymal transition-related pathways during oncogenic reprogramming of hepatic lineage cells

Next, I analyzed the transcriptome of the tumors described above (10 HPC-, 20 HB-, and 20 AH-derived) and freshly isolated mouse HPCs, HBs, and AHs (4 samples each) to define key molecular similarities and differences between tumors and corresponding cell-of-origin. Using bioequivalence test, I found that tumor groups displayed higher degree of similarity to each other than to their cell-of-origin (**Figure 25**). Notably, HPC-derived tumors showed the highest (71%) and AH-derived tumors the lowest (53%) level of similarity to their normal counterparts suggesting that reprogramming of mature hepatocytes into tumor-initiating cells required more substantial genomic changes as compared to HBs or HPCs.

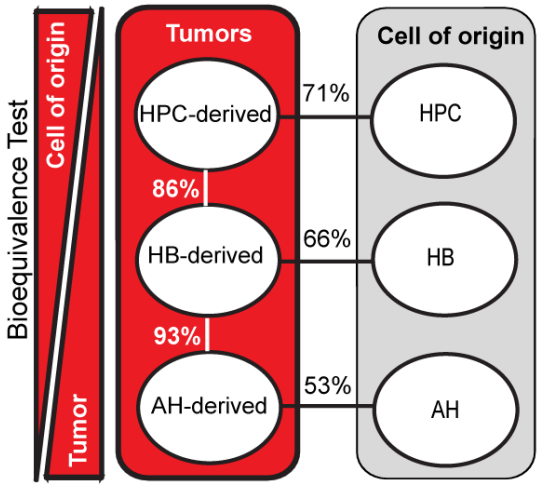

Figure 25. Bioequivalence test of similarities between HPC-, HB-, and AH-derived tumors and their respective cell of origin. Liver tumors were generated by intrasplenic injection of H-Ras-EGFP^{+}/SV40LT-mCherry^{+} HPCs, HBs, and AHs. Molecular similarities between tumors (10 HPC-, 20 HB-, and 20 AH-derived) and freshly isolated mouse HPCs, HBs, and AHs (4 samples each) were identified by bioequivalence test. Data were evaluated at fold change > 1.5 and $P < 0.05$.

I identified 590 genes with significant common dysregulation (409 up- and 181 downregulated genes) among the three tumor groups (**Figure 26**) by bootstrap t-test. Remarkably, hierarchical clustering of common genes separated the tumors according to their cell-of-origin with HPC tumors clustered more closely with HB than AH tumors (**Figure 27**).

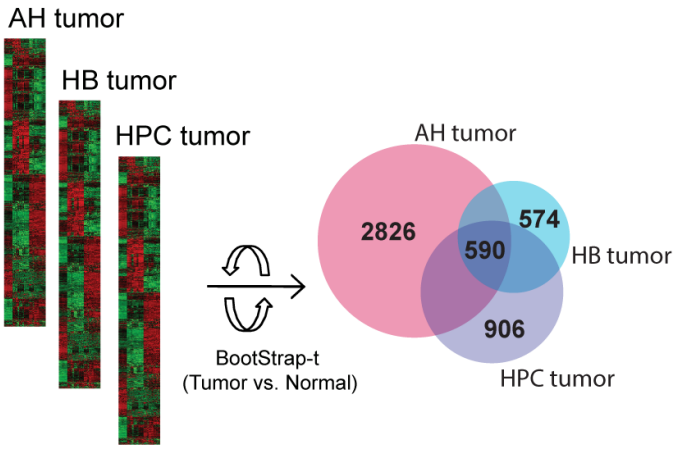

Figure 26. Venn diagram of differentially expressed genes. Genes with significantly different expression in HPC-, HB-, and AH-derived tumors compared to their normal counterparts were identified by bootstrap t-test using 5000 repetitions; $P < 0.001$; fold change > 2.

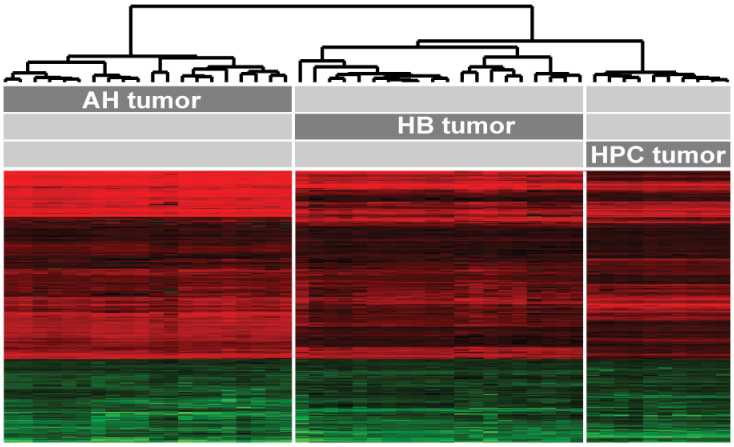

Figure 27. Supervised hierarchical clustering of HPC-, HB-, and AH-derived tumors based on 590 commonly differentially expressed genes. Genes with significant common dysregulation among HPC-, HB-, and AH-derived tumors were identified by bootstrap t-test. Red and green colors represent up-and downregulation of genes, respectively. Note the clear separation of tumors based on their cell-of-origin, suggesting dysregulation of cell-type-specific transcriptional programs.

DOI:10.14753/SE.2019.2291

A significant proportion of common genes were associated with EMT, consistent with the highly metastatic nature of all three tumor groups. In particular, I found a drastic upregulation of *Zeb2*, *Vim*, *Mmp12*, *Mmp13*, *Pdgfra*, *Pdgfrb*, *Ednra*, and *Flt1*, which was also confirmed by qRT-PCR (**Figure 28**).

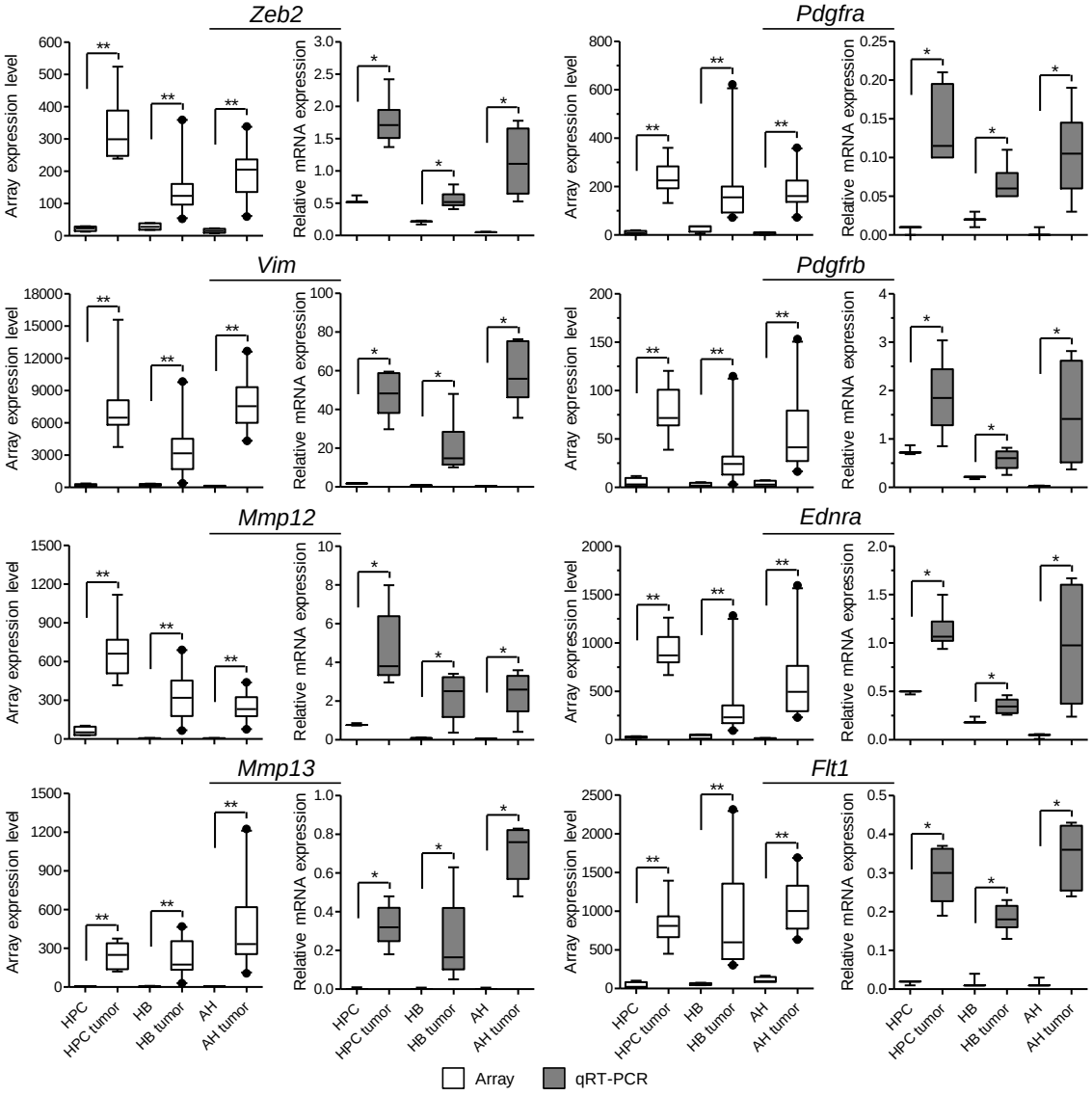

Figure 28. Upregulation of EMT-related genes in HPC-, HB-, and AH-derived tumors. Box-plots represent the expression level of commonly changed EMT genes in HPC-, HB-, and AH-derived tumors and corresponding normal cells based on microarray (white graphs) and quantitative reverse transcription polymerase chain reaction (qRT-PCR) data (grey graphs). Six samples of each tumor group and their normal counterparts (3 samples each) were analyzed in triplicates by qRT-PCR, and mRNA expression of target genes were normalized to *Gapdh*. Significant differences were calculated by Mann-Whitney U test. $P < 0.05$ was considered statistically significant. *$P < 0.05$; **$P < 0.01$.

I further revealed a significant enrichment of a 35-gene EMT-signature in HPC-, HB-, and AH-derived tumors using GSEA (**Figure 29**).[172]

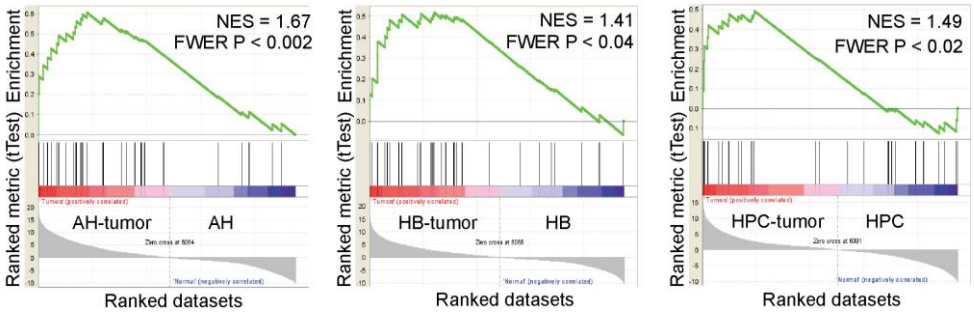

Figure 29. Gene set enrichment analysis using a curated 35-gene EMT signature. Enrichment plots displaying significant enrichment of EMT-related genes in HPC-, HB-, and AH-derived tumors. The EMT gene signature was obtained from the Molecular Signatures Database 3.0.[172] NES, normalized enrichment score; $P < 0.05$ was considered significant.

4.1.5 Hepatic lineage stage determines the transcriptional programs required for oncogenic reprogramming

In total, 12 claudin genes (*Cldn1-7*, *Cldn9*, *Cldn11*, *Cldn12*, *Cldn14*, and *Cldn23*) were significantly dysregulated in HPC-, HB-, and AH-derived tumors, however, none of these claudins were commonly up- or downregulated among the three tumor groups. All of the differentially expressed claudins except *Cldn14* were downregulated in HPC-derived tumors, which might be related to their predominant sarcomatous appearance. Notably, AH-derived tumors showed a drastic upregulation of *Cldn6* (1135.20-fold), a specific marker for mouse pluripotent stem cells (**Table 9**).[189]

Clear separation of mouse liver tumors based on their cell-of-origin by hierarchical clustering suggested that distinct hepatic lineage cells dysregulate cell-type-specific transcriptional programs in response to the same oncogenic stimuli. AH-derived tumors showed the largest number of differentially expressed unique genes compared to their cell-of-origin (2826 versus 574 and 906 genes in HB- and HPC-derived tumors, respectively) by bootstrap t-test (**Figure 26**). In addition, network analysis of significantly changed, tumor-group-specific genes identified a higher number of transcription factors with a predicted activation status in AH-derived tumors (e.g., *E2f1*, *Klf6*, *Myc*) compared to HB- (e.g., *Sp1*, *Foxo1*) and HPC-derived tumors (e.g., *Cebpb*, *Esrrb*).

Table 9. Differentially expressed claudin genes in HPC-, HB-, and AH-derived tumors

Gene symbol	HPC	HB	AH
Cldn1	-	-20.46	-11.61
Cldn2	-7.01	12.90	-
Cldn3	-11.83	7.39	-2.10
Cldn4	-178.42	2.60	36.06
Cldn5	-	5.07	-
Cldn6	-2.42	5.44	1135.20
Cldn7	-4.80	3.72	-
Cldn9	-	-3.63	-3.61
Cldn11	-	-	70.68
Cldn12	-4.58	-	-3.86
Cldn14	5.30	-	-
Cldn23	-42.00	7.47	25.90

Values represent fold change of claudin gene expression between HPC-, HB-, and AH-derived tumors and their their normal counterparts based on microarray.

To evaluate hepatic-lineage-stage-specific transcriptional memory in HPC-, HB-, and AH-derived tumors, I performed GSEA using a hepatocyte-derived iPSC signature of 786 genes.[190, 191] The signature was significantly enriched in AH- ($P < 0.001$) but not in HB- or HPC-derived tumors (**Figure 30**).

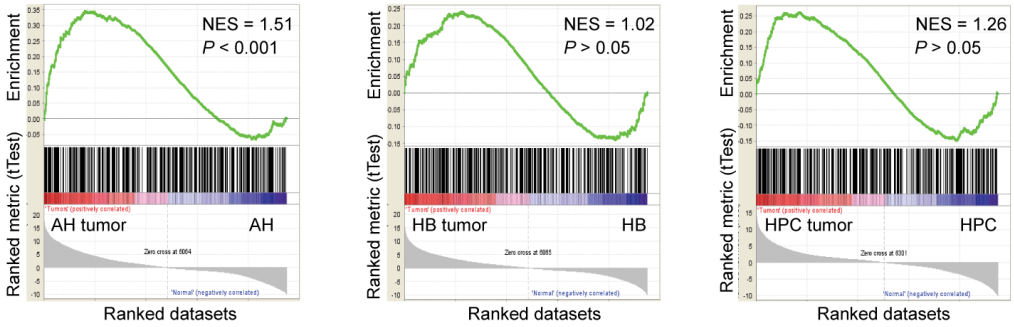

Figure 30. Gene set enrichment analysis using a hepatocyte-derived induced pluripotent stem cell gene signature of 786 genes.[191] Enrichment plots displaying significant enrichment in AH- but not in HB- or HPC-derived tumors. $P < 0.05$ was considered statistically significant.

This provides additional evidence that AHs are indeed the cells of origin of AH-derived tumors and the activation of ESC-related genes is indispensable for oncogenic

reprogramming of mature hepatocytes into CSCs. In support of this notion, AH-derived tumors showed the highest overlap with a 335-gene ESC core module map (42.1% versus 19.7% and 22.7% in HB- and HPC-derived tumors, respectively; **Figure 31**).[170]

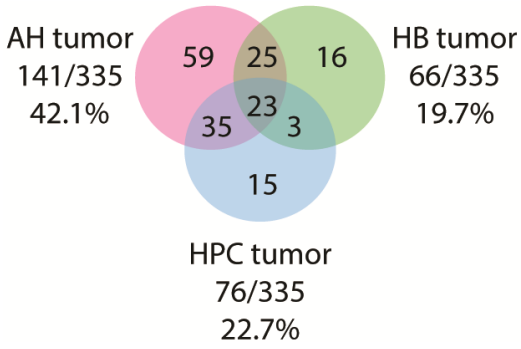

Figure 31. Overlap of differentially expressed genes with a 335-gene embryonic stem cell core module map.[170] Genes with significantly different expression in HPC-, HB-, and AH-derived tumors compared to their normal counterparts were identified by bootstrap t-test using 5000 repetitions; $P < 0.001$; fold change > 2.

Significantly, AH-derived tumors showed a strong upregulation (21.10-fold) of *Myc*, a major link between ESCs and cancer, within the overlapping ESC core genes, while *Myc* expressed at a lower level in HB- and HPC-derived tumors compared to their normal counterparts (**Figure 32**).[192] Gene set enrichment analysis using a list of 229 E-box containing c-Myc target genes confirmed that the target genes were significantly enriched in AH- ($P < 0.0001$) but not in HPC- or HB-derived tumors (**Figure 33**).[173]

From these results, c-Myc signaling emerges as a major AH-specific component of the transcriptional signature induced upon H-Ras/SV40LT-driven transformation in concordance with a previous finding that c-Myc is a driver gene of malignant conversion from dysplastic stage to early HCC in human.[193]

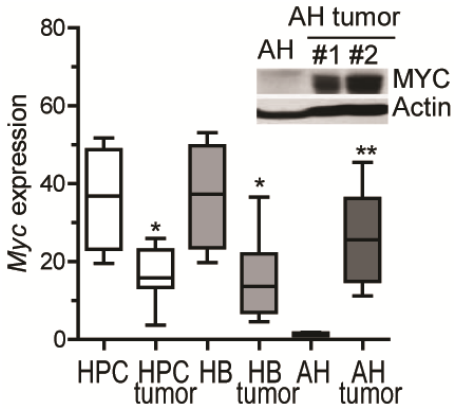

Figure 32. Expression of c-Myc in mouse hepatic lineage cell-derived tumors. Box plots illustrate mRNA expression of Myc in HPC-, HB-, and AH-derived tumors and their normal counterparts based on microarray data. Significant differences were calculated by Mann-Whitney U test. $P < 0.05$ was considered statistically significant. $^{*}P < 0.05$; $^{**}P < 0.01$. (Inset) Western blot analysis of c-Myc protein expression in primary AHs and AH-derived tumors. Actin was used as loading control.

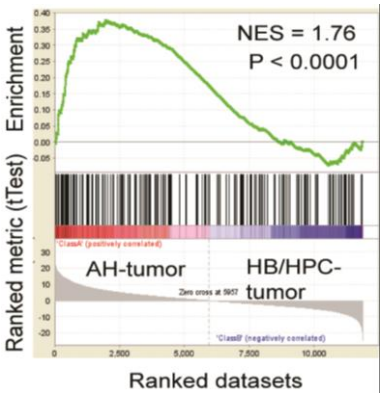

Figure 33. Cell type-dependent activation of Myc-regulated gene networks in tumors initiated by H-Ras/SV40LT-transformed distinct hepatic lineage cells. Gene set enrichment analysis showing significant enrichment of c-Myc Ebox-target genes in AH-derived tumors. The 229-gene list of c-Myc Ebox target genes was obtained from the Molecular Signatures Database 3.0.[173] $P < 0.05$ was considered significant.

4.1.6 Myc is required for H-Ras/SV40LT-mediated oncogenic reprogramming of adult hepatocytes

To substantiate the role of c-Myc in transformation of adult hepatocytes, I carried out c-Myc loss-of-function experiments in AHs transduced with H-Ras/SV40LT. I used a retroviral vector expressing shRNA to achieve stable and effective knockdown of c-Myc.[146] I generated several single cell-derived clones and tested CSC properties of the

cell clone that showed the most efficient (more than 90%) c-Myc protein knockdown (**Figure 34**). Cells stably expressing a scrambled target sequence were used as control.

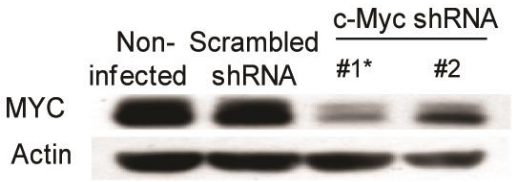

Figure 34. Efficient knockdown of c-Myc expression in H-Ras/SV40LT-transduced AHs. For stable knockdown of c-Myc, H-Ras-EGFP$^+$/SV40LT-mCherry$^+$ AHs were transduced with pRS retroviral vectors expressing c-Myc shRNA or scrambled shRNA. Myc protein level was detected by western blotting, non-infected AHs or AHs transduced with scrambled shRNA were used as negative control. Expression of actin was used as loading control. Asterisk marks the cell clone subjected to cancer stem cell assays.

Knockdown of c-Myc expression significantly reduced the number of CD133$^+$ cells (1.5% compared with 21.4% in control cells transduced with scrambled shRNA) (**Figure 35**), decreased the frequency of SP cells (0.07% compared with 0.46% in control cells) (**Figure 36**), and diminished sphere forming capacity and sphere size (**Figure 37**).

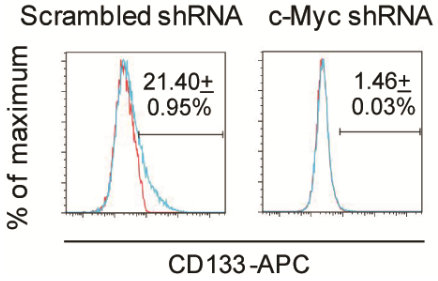

Figure 35. Knockdown of c-Myc expression reduces CD133 expression in H-Ras/SV40LT-transduced AHs. Stable knockdown of c-Myc in H-Ras-EGFP$^+$/SV40LT-mCherry$^+$ AHs was achieved using a retroviral vector expressing c-Myc shRNA. Expression of CD133 was analyzed by flow cytometry, AHs transduced with scrambled shRNA were used as control. Blue line indicates CD133-APC, red line corresponds to staining with isotype control. Data represent mean ± standard deviation of three experiments.

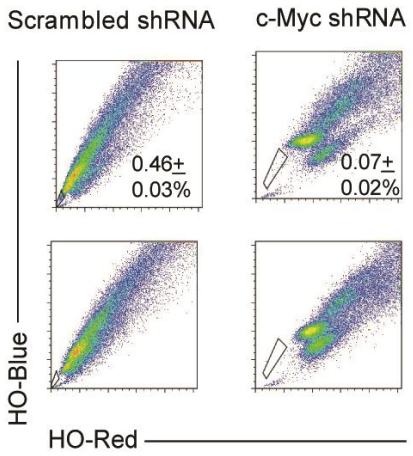

Figure 36. Knockdown of c-Myc reduces the size of side population in H-Ras/SV40LT-transduced AHs. Stable knockdown of c-Myc in H-Ras-EGFP$^+$/SV40LT-mCherry$^+$ AHs was achieved using a retroviral vector expressing c-Myc shRNA. Side population cells were identified by Hoechst 33342 (HO) staining, AHs transduced with scrambled shRNA were used as control. Side population gates were set up by using the fumitremorgin C inhibitor samples (dot plots shown at the bottom). Data represent mean ± standard deviation of triplicate measurements.

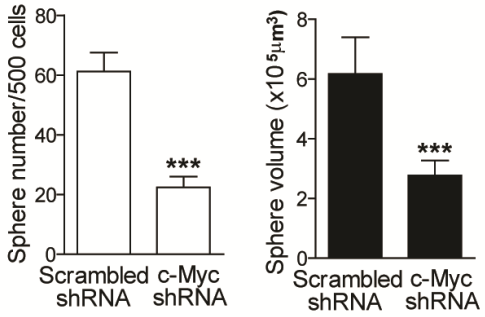

Figure 37. Knockdown of c-Myc expression diminishes sphere forming capacity and sphere size in H-Ras/SV40LT-transduced AHs. H-Ras-EGFP$^+$/SV40LT-mCherry$^+$ AHs expressing c-Myc shRNA or scrambled shRNA were seeded in 1% methylcellulose in ultra-low attachment 96-well plates at low density. Spheroids were counted after 7 days. White bars correspond to sphere number, whereas black bars correspond to sphere volume. Data represent mean ± standard deviation of four experiments. Significant differences were evaluated by Poisson generalized linear model and Student's t-test. $P < 0.05$ was considered statistically significant. $^{***}P < 0.001$.

Furthermore, subcutaneous tumor growth in immunodeficient mice was significantly reduced in c-Myc shRNA-expressing cells compared to control cells transduced with scrambled shRNA (**Figure 38**).

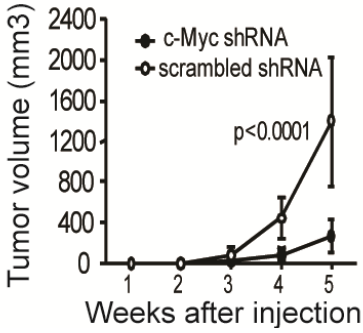

Figure 38. Knockdown of c-myc expression reduces subcutaneous growth of H-Ras/SV40LT-transduced AHs. One hundred cells of H-Ras-EGFP^{+}/SV40LT-mCherry^{+} AHs expressing c-Myc shRNA or scrambled shRNA were injected subcutaneously into both flanks of NOD/SCID mice (5 mice/group). Tumor diameters were measured weekly by an external caliper. Significant differences were evaluated by Student's t-test. $P < 0.05$ was considered significant.

4.2 Distinct claudin expression profiles of human HCC and metastatic colorectal and pancreatic carcinomas

4.2.1 Immunohistochemical and morphometric analysis

I analyzed the expressions of CLDN-1, -2, -3, -4, and -7 in 20 cases of HCCs, and liver metastases of 20 colorectal adenocarcinomas and 15 pancreatic adenocarcinomas with paired surrounding non-tumorous liver tissues, as well as 5 normal liver samples by immunohistochemistry. The results of the morphometric analysis of CLDN immunostainings are presented in **Table 10**.

Hepatocellular carcinoma cells arranged in trabecular, glandular or acinar patterns revealed moderate apical membrane reactivity for CLDN-1 (**Figure 39A**). In contrast, the membranous staining appeared on the entire circumference of tumor cells in CRLM and PLM (**Figure 39B**, **C**). In normal and non-tumorous livers, intense apical staining appeared in bile duct cells, whereas hepatocytes exhibited a weak apical positivity (**Figure 39D**). Morphometric analysis revealed the highest expression level of CLDN-1 in CRLMs (**Table 10**, **Figure 40A**). However, the difference in CLDN-1 expression among CRLMs, HCCs, and PLMs was statistically significant only when surrounding non-tumorous and normal livers were excluded from the Kruskal-Wallis test (**Figure 40F**; CRLM versus HCC, $P = 0.032$; CRLM versus PLM, $P = 0.008$).

Claudin-2 immunostaining showed cytoplasmic, granular positivity in both tumorous (**Figure 39E-G**) and normal cells (**Figure 39H**). By morphometry, significantly lower expression was observed in all three tumor groups compared to surrounding non-tumorous liver tissue (**Figure 40B**), where both hepatocytes and bile duct cells exhibited intense cytoplasmic staining.

Significantly increased CLDN-3 membrane staining was detected in CRLMs (**Figure 39J**) compared to HCCs and PLMs (**Figure 39I**, **K**; **Figure 40C**). Ten (66.7%) out of 15 PLM samples showed weak, focal positivity (**Figure 39K**). HCCs and non-tumorous hepatocytes displayed weak, scattered membrane staining (**Figure 39I**, **L**), while bile duct cells were strongly positive for CLDN-3 (**Figure 39L**).

Tumor cells of all CRLM and PLM samples exhibited a strong membranous staining pattern for CLDN-4 (**Figure 39N**, **O**). Morphometric analysis revealed no significant difference in CLDN-4 expression between CRLM and PLM tumor groups (**Figure 40D**). Hepatocellular carcinoma cells (**Figure 39M**), non-tumorous and normal hepatocytes did not express CLDN-4, while we detected weak to moderate membranous expression in the bile duct cells of non-tumorous and normal liver (**Figure 39P**).

Claudin-7 immunostaining was significantly increased in CRLMs (**Figure 39R**) in comparison with the other groups (**Table 10**, **Figure 40E**). In all, 9/15 (60.0%) PLMs showed focal, faint reactivity (**Figure 39S**), and weak membrane staining was present on HCC cells and normal hepatocytes (**Figure 39Q**, **T**). All normal bile ducts were uniformly CLDN-7 positive (**Figure 39T**).

In summary, we demonstrated that HCCs are characterized by moderate CLDN-1 and weak CLDN-2, -3, and -7 expression, whereas do not express CLDN-4. Liver metastases of colorectal adenocarcinomas displayed strong CLDN-1, -3, -4, -7, and weak CLDN-2 immunostaining. Liver metastases of pancreatic adenocarcinomas showed strong CLDN-4 and moderate or weak CLDN-1, -2, -3, and -7 positivity.

DOI:10.14753/SE.2019.2291

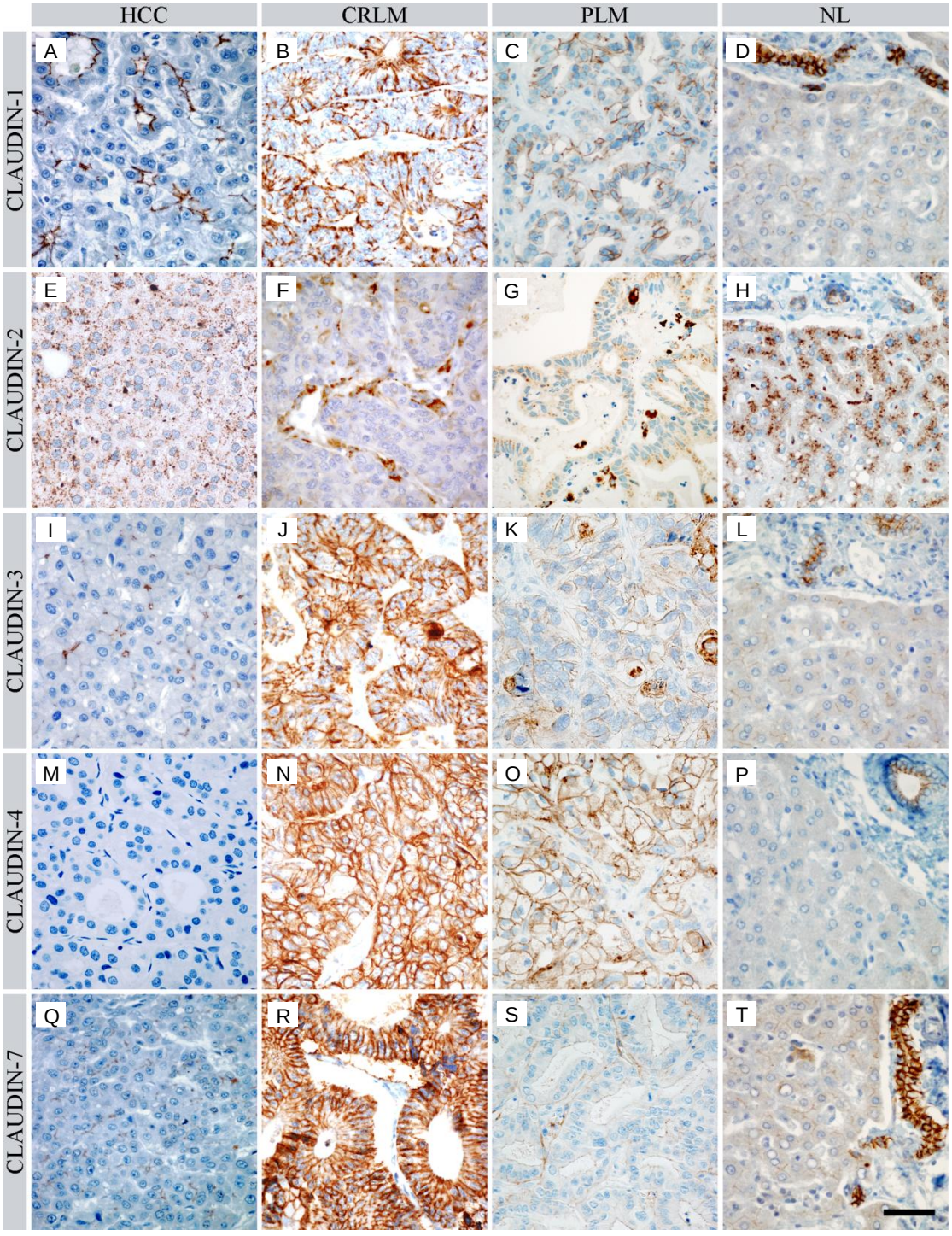

Figure 39. Immunohistochemical detection of claudins in HCC, liver metastases of colorectal adenocarcinomas (CRLM) and pancreatic adenocarcinomas (PLM), and normal liver (NL). (A-D) Claudin-1 in HCC, CRLM, PLM, and NL. (E-H) Claudin-2 in HCC, CRLM, PLM, and NL. (I-L) Claudin-3 in HCC, CRLM, PLM, and NL. (M-P) Claudin-4 in HCC, CRLM, PLM, and NL. (Q-T) Claudin-7 in HCC, CRLM, PLM, and NL. Scale bar = 50 µm**.**

Table 10. Morphometric analysis of claudin expression

	Group	Area positivity (%)	*P* (K-W)	*P* (pairwise comparison)			
				vs CRLM	vs PLM	vs SL	vs NL
CLDN-1	HCC	1.83 ± 0.41	< 0.001	NS	NS	NS	NS
	CRLM	5.29 ± 0.88			NS	< 0.001	NS
	PLM	1.45 ± 0.49				NS	NS
	SL	0.67 ± 0.11					NS
	NL	0.42 ± 0.18					
CLDN-2	HCC	1.35 ± 0.23	< 0.001	NS	NS	< 0.001	NS
	CRLM	0.98 ± 0.27			NS	< 0.001	NS
	PLM	1.82 ± 0.39				NS	NS
	SL	4.29 ± 0.18					NS
	NL	3.33 ± 0.61					
CLDN-3	HCC	0.31 ± 0.07	< 0.001	< 0.001	NS	NS	NS
	CRLM	7.61 ± 1.09			< 0.001	< 0.001	0.026
	PLM	0.79 ± 0.25				NS	NS
	SL	0.45 ± 0.09					NS
	NL	0.28 ± 0.08					
CLDN-4	HCC	0.00 ± 0.00	< 0.001	< 0.001	< 0.001	0.046	NS
	CRLM	10.82 ± 0.63			NS	< 0.001	0.029
	PLM	7.16 ± 0.98				< 0.001	NS
	SL	0.01 ± 0.00					NS
	NL	0.01 ± 0.00					
CLDN-7	HCC	0.38 ± 0.09	< 0.001	< 0.001	NS	NS	NS
	CRLM	9.32 ± 0.93			< 0.001	< 0.001	0.001
	PLM	0.57 ± 0.20				NS	NS
	SL	0.22 ± 0.05					NS
	NL	0.10 ± 0.06					

Claudin expression was measured as percentage of immunopositive area by morphometry. Data represent mean ± standard error of mean. Expression levels among the groups were compared by Kruskal-Wallis and post hoc tests; the surrounding non-tumorous livers were treated as one group. $P < 0.05$ was considered statistically significant. K-W, Kruskal-Wallis test; NS, not significant; *P*, significance; SL, surrounding non-tumorous liver.

DOI:10.14753/SE.2019.2291

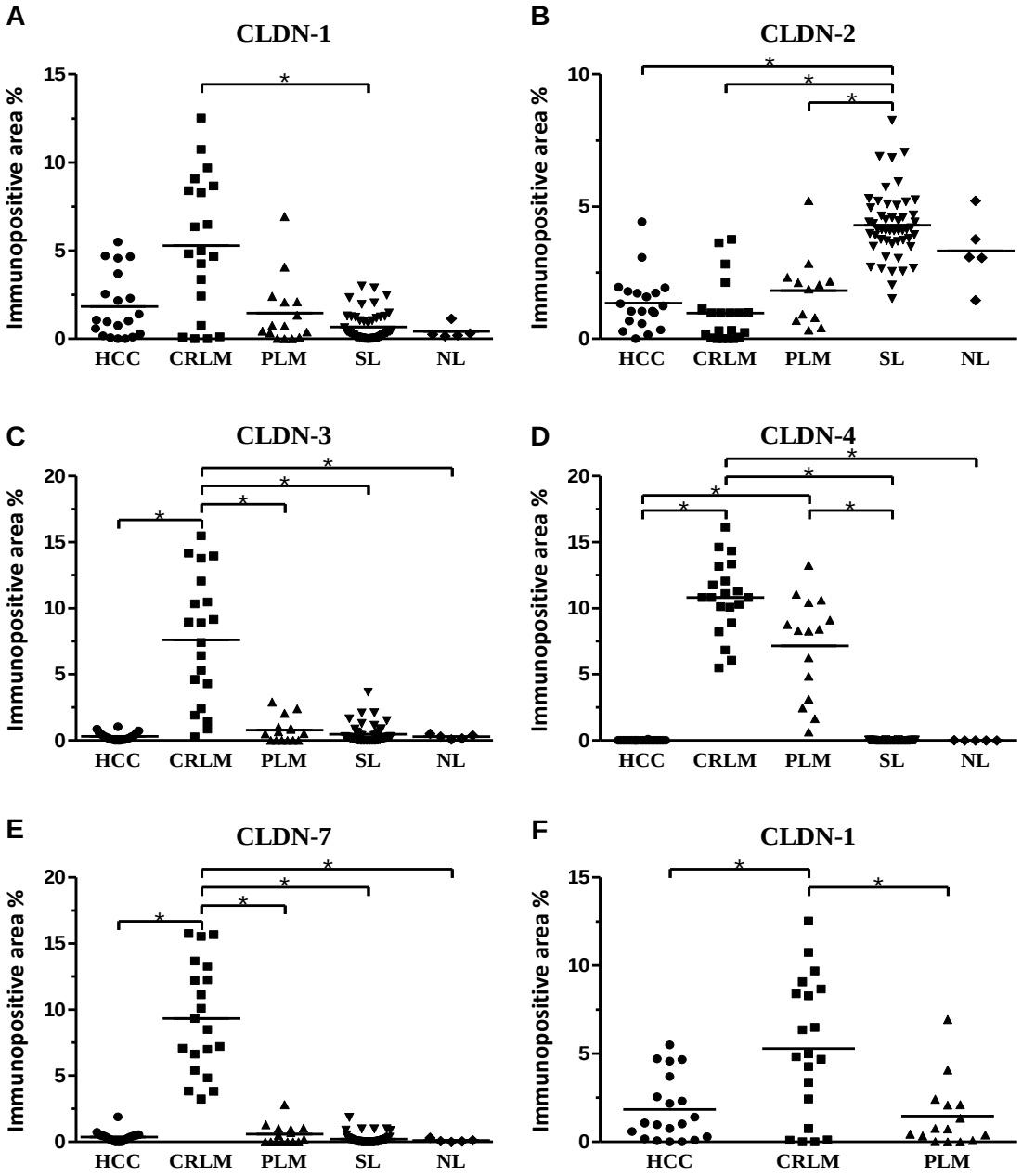

Figure 40. Scatter dot plots illustrating the differences in claudin expression evaluated by morphometric analysis. Claudin expression was measured as percentage of immunopositive area. Dots represent individual samples; horizontal lines represent mean values for each group. Expression levels among the groups were compared by Kruskal-Wallis and post hoc tests; the surrounding non-tumorous livers were treated as one group. Claudin-1 expression was compared including (A) or excluding (F) surrounding non-tumorous and normal livers. Asterisk indicates significant difference ($P < 0.05$).

4.2.2 Quantitative RT-PCR analysis

Claudin-1, -2, -3, -4, and -7 mRNA expressions were analyzed in 20 HCCs, 20 CRLMs, and 20 PLMs with paired SL samples and 5 normal livers. The results of qRT-PCR analysis are presented in **Table 11** and **Figure 41**.

Table 11. Quantitative RT-PCR analysis of claudin mRNA expression

	Group	Relative mRNA level	*P* (K-W)	*P* (pairwise comparison)			
				vs CRLM	vs PLM	vs SL	vs NL
CLDN-1	HCC	0.35 ± 0.07	< 0.001	0.012	NS	NS	NS
	CRLM	0.11 ± 0.03			NS	< 0.001	0.004
	PLM	0.15 ± 0.02				0.006	NS
	SL	0.49 ± 0.05					NS
	NL	0.86 ± 0.25					
CLDN-2	HCC	0.02 ± 0.01	< 0.001	NS	< 0.001	< 0.001	NS
	CRLM	0.03 ± 0.01			0.001	NS	NS
	PLM	0.15 ± 0.03				NS	NS
	SL	0.09 ± 0.02					NS
	NL	0.09 ± 0.05					
CLDN-3	HCC	0.05 ± 0.01	< 0.001	< 0.001	NS	NS	NS
	CRLM	0.27 ± 0.05			0.001	< 0.001	NS
	PLM	0.05 ± 0.02				NS	NS
	SL	0.07 ± 0.02					NS
	NL	0.09 ± 0.02					
CLDN-4	HCC	0.01 ± 0.00	< 0.001	< 0.001	0.003	NS	NS
	CRLM	0.08 ± 0.02			NS	< 0.001	NS
	PLM	0.03 ± 0.01				0.024	NS
	SL	0.01 ± 0.00					NS
	NL	0.02 ± 0.01					
CLDN-7	HCC	0.02 ± 0.00	< 0.001	NS	0.011	NS	NS
	CRLM	0.03 ± 0.01			< 0.001	< 0.001	NS
	PLM	0.00 ± 0.00				NS	NS
	SL	0.01 ± 0.00					NS
	NL	0.01 ± 0.01					

Samples were analyzed in duplicates by qRT-PCR, and mRNA expression of claudins was normalized to β-actin**.** Data represent mean ± standard error of mean. Claudin expression levels were compared by Kruskal-Wallis and post hoc tests; the surrounding non-tumorous livers were treated as one group. $P < 0.05$ was considered statistically significant.

Claudin-2, -3, -4, and -7 showed overall good concordance between their mRNA and protein expression patterns indicating that they are regulated largely at the level of transcription. However, a striking difference was observed between CLDN-1 mRNA and protein expression. Claudin-1 expression was significantly downregulated in CRLM when compared with HCC, SL, and normal liver; mRNA expression in PLM was also lower than in SL. I detected lower CLDN-2 expression in HCC and CRLM than in SL, however, the difference was statistically significant only between HCC and SL. Claudin-3 and -4 mRNA levels were significantly higher in CRLM than in HCC and SL, expression of CLDN-3 was also increased in CRLM compared to PLM. Furthermore, I found that CLDN-7 mRNA expression was significantly higher in CRLM than in PLM and SL.

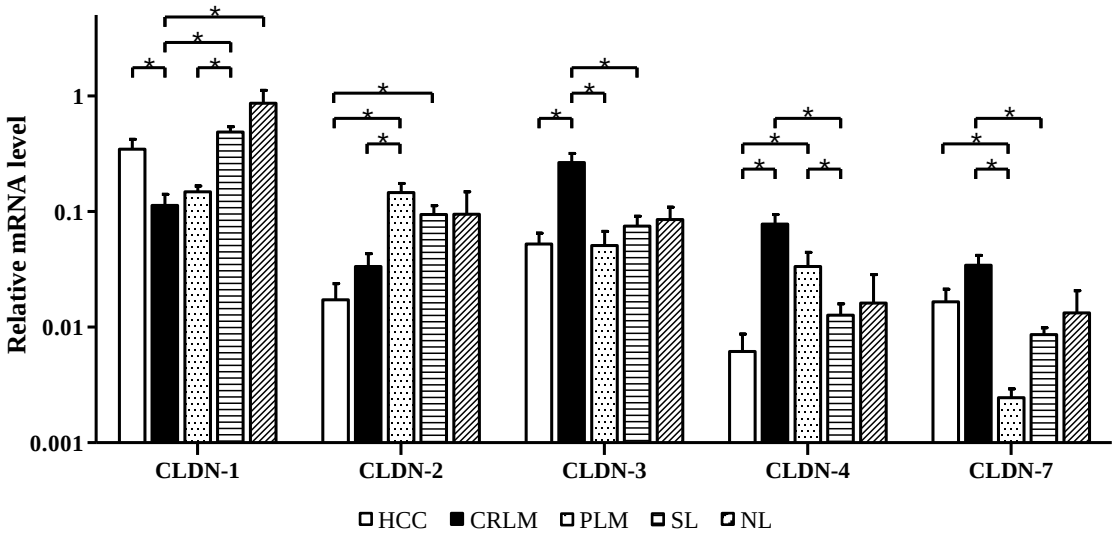

Figure 41. Differences in claudin mRNA expression. Bar graphs illustrate the relative mRNA expression levels of claudin-1, -2, -3, -4, and -7 in HCC, CRLM, PLM, SL, and NL by qRT-PCR after normalization to β-actin**.** Data represent mean ± standard error of mean. Claudin expression levels were compared by Kruskal-Wallis and post hoc tests; the surrounding non-tumorous livers were treated as one group. Asterisk indicates significant difference ($P < 0.05$).

DOI:10.14753/SE.2019.2291

5. DISCUSSION

5.1 Contribution of distinct mouse hepatic lineage cells to the evolution of liver cancer stem cells and heterogeneity of HCC

In the present study, I aimed to explore the contribution of distinct hepatic lineage cells to the evolution of liver CSCs and genetic and phenotypic heterogeneity of HCC using a mouse model of genetically defined liver cancer.[194] I provide for the first time direct evidence that diverse hepatic lineage cells from fetal and adult progenitor cells to terminally differentiated hepatocytes can be targets for neoplastic transformation and acquire a high degree of genetic similarity through activation of diverse donor-cell-specific signaling pathways.

The origin of CSCs has recently become the focus of intensive research. Multiple hypotheses have emerged implicating adult stem cells, adult progenitor cells, differentiated cells, and non-stem cancer cells as the origin of CSCs. Many tissues and organs contain a small, dedicated population of undifferentiated adult stem cells (also known as tissue stem cells or somatic stem cells) throughout the majority of postnatal life.[195] Adult stem cells reside in a specialized microenvironment, denoted as 'niche', that provides extracellular cues to maintain and regulate stem cells.[196] The primary roles of adult stem cells are to maintain and repair the tissues where they reside.[197] They usually remain in a quiescent state until being activated by external stimuli. Adult stem cells, like all stem cells, have two hallmark capabilities: the ability to self-renew, and the ability to differentiate and generate multiple cell lineages over long periods of time. Typically, adult stem cells give rise to an intermediate cell type or types before achieving a fully differentiated state. This intermediate cell type is referred to as a progenitor or precursor cell. Progenitor or precursor cells are partly differentiated cells that are committed to differentiating along a particular cellular development pathway.[87, 195] Notably, some adult stem cells from one tissue possess the ability to generate the differentiated cell types of another tissue; this phenomenon is referred to as 'plasticity' or 'transdifferentiation'.[198, 199] Adult stem cells in tissues with high turnover rate are compelling targets of malignant transformation because of their frequent cell divisions and

long lifespan. This creates ideal circumstances for DNA damage to accumulate, which is the primary driving force behind cancer initiation.[200]

In HCC, CSCs have been identified using several markers, including CD133, CD90, CD44, CD24, CD13, oval cell marker OV6, EpCAM, and Hoechst dye efflux or aldehyde dehydrogenase activities.[80, 83, 201-206] Many of these markers are also expressed in normal hepatic stem/progenitor cells. However, despite extensive efforts, the origin of CSCs in HCC is not fully elucidated. Several candidates in the hepatocyte lineage including adult hepatic stem cells, hepatic progenitor cells, and terminally differentiated hepatocytes have been implicated as cellular targets for oncogenic transformation. Adult hepatic stem cells reside in the small terminal bile ductules that form the canals of Hering and get activated following hepatocyte injury.[207] The early descendants of hepatic stem cells are called hepatic progenitor cells or oval cells in rodents.[183] These cells have the capacity to differentiate into both hepatocytes and cholangiocytes. Frequent expression of hepatic stem/progenitor cell markers in experimental and human HCCs favors the hypothesis of stem/progenitor cell origin at least for some HCCs.[178] Human combined hepatocellular cholangiocarcinoma (CHC), a rare form of primary liver cancer that displays morphological features of both HCC and cholangiocarcinoma, is considered the best example of a hepatic stem/progenitor cell-derived tumor.[178, 209, 210] On the other hand, expression of stem/progenitor cell markers may reflect dedifferentiation of mature hepatocytes or phenotypic plasticity of cancer cells. Long life span and remarkable regenerative potential of mature hepatocytes strongly support their susceptibility to malignant transformation under selective pressure induced by chronic inflammatory cell death.[211] This concept is supported by various mouse models of hepatocarcinogenesis, especially by those established using hydrodynamic gene delivery that predominantly induces genetic alterations in mature hepatocytes.[212, 213] Sequential phenotypic changes in diseased liver, such as emergence of dysplastic foci, nodules, and HCC further supports oncogenic transformation of mature hepatocytes.[214]

My novel data show that forced expression of oncogenic H-Ras/SV40LT reprograms diverse hepatic lineage cells into CSCs as judged by an increase or acquisition of (1) CSC/progenitor cell markers (CK19, A6, EpCAM, CD133) and (2) side population, (3) activation of EMT- and ESC-like transcriptional programs, (4) long-term self-renewal capacity *in vitro*, (5) high tumorigenicity and (6) metastatic capacity, and (7) multilineage

differentiation in various *in vivo* tumorigenicity assays. My results indicating that committed progenitor cells and mature hepatocytes can be converted into CSCs and the generated tumors contain a high proportion of CSCs are in accordance with several recent studies, thus prompting a revision of the canonical stem cell/CSC concept. The classical stem cell and CSC models suggest that rare, relatively quiescent stem cells/CSCs reside at the apices of hierarchies and differentiate into nonstem progeny in a unidirectional manner. However, several lines of evidence indicate that stem cells/CSCs are not necessarily rare or quiescent and are regulated by niche signals following neutral competition dynamics.[215] In intestinal crypts, up to 10 percent of crypt cells are intestinal stem cells expressing Lgr5.[216] Adult stem cells can actively divide throughout life in many tissues, such as intestinal crypts and stomach pylorus.[216, 217] Stem cell hierarchies can display a cellular plasticity more widespread than previously thought, meaning that progenitor cells and differentiated cells are able to re-enter the niche and undergo reprogramming to replace lost stem cells.[215] For example, $Dll1^+$ secretory progenitor cells and $Alpi^+$ enterocyte-lineage progenitors in the mouse intestine acquire stem cell functions and replace lost $Lgr5^+$ stem cells in response to tissue damage.[218, 219] In mouse trachea, luminal secretory cells can revert into functional stem cells upon the ablation of airway stem cells. Notably, the tendency to dedifferentiate is inversely correlated to the maturity of the secretory cell.[220] Furthermore, terminally differentiated hepatocytes can enter the cell cycle to replace lost tissue during liver regeneration without reverting back to a stem cell-like state.[221]

In concordance with recent findings that associate EMT, stem cell traits, and cancer, my genome-wide expression analysis revealed a significant upregulation of EMT- and ESC-related genes in HPC, HB, and AH tumors compared to their respective cell of origin.[173, 174, 222] EMT is a biologic process that allows epithelial cells to acquire a mesenchymal cell phenotype with an enhanced migratory capacity, invasiveness, and increased resistance to apoptosis.[223] Several studies have demonstrated a direct link between EMT and the gain of epithelial stem cell properties. Mani et al. reported that overexpression of the transcription factors Snail or Twist in human mammary epithelial cells not only induced EMT, but also led to the acquisition of stem cell properties.[92] Moreover, stem-like cells isolated either from mouse or human mammary glands or mammary carcinomas expressed markers associated with EMT. The same study further showed that induction

of EMT in transformed human mammary epithelial cells promoted the generation of CSCs. Notably, CSCs may exist in an intermediate state of EMT and can transition between epithelial and mesenchymal states.[224, 225] Using epithelial lineage tracing, Rhim et al. demonstrated that a small population of PDAC cells displayed features of an intermediate stage of EMT, co-expressing the EMT marker Zeb1 or Fsp1, and the epithelial marker E-cadherin, whereas 42% of cancer cells completed an EMT. Furthermore, they found that a large fraction of circulating pancreatic cancer cells maintained a mesenchymal phenotype in the circulation and stained positive for putative pancreatic CSC markers CD24 and CD44. When PDAC cells were separated according to their EMT status (i.e., partial or complete EMT) and transplanted into the pancreas, the generated tumors were similar with respect to their mesenchymal and epithelial composition. Collectively, these studies indicate that cancer cells passing through EMT acquire stem cell properties.

Similar to my findings, recent work has shown generation of CSCs by oncogenic reprogramming of human fibroblasts.[226] Plasticity of both normal and neoplastic non-stem cells was neatly demonstrated by Chaffer et al.[227] They identified a subset of basal-like human mammary epithelial cells that spontaneously dedifferentiated into stem-like cells, and generated cancer stem-like cells upon transformation by SV40 early region and H-Ras. Moreover, they described that non-stem cancer cells also underwent spontaneous conversion and gave rise to CSC-like cells *in vitro* and *in vivo*. Gupta et al. provided further evidence that both CSCs and non-stem cancer cells exhibit plasticity and are capable of undergoing phenotypic transitions in response to certain stimuli.[228] Cellular subpopulations displaying luminal, basal or stem-like phenotypes were purified from two human breast cancer cell lines. Over time, each isolated subpopulation of cells returned towards equilibrium proportions of the parental cell lines by generating cells of the other two phenotypes. Notably, CSC-like cells arose from non-stem luminal or basal cells *de novo*. The interconversion between cell states occurred in a stochastic manner, irrespective of the phenotype of the isolated subpopulation. The luminal and basal subpopulations also regenerated functional stem-like cells *in vivo* when certain environmental stimuli were modified, and the proportions of luminal, basal, and stem-like cells in the tumors were comparable. Thus, convergence toward equilibrium proportions could be occurring because of cell-state interconversion within tumors.

Together these studies suggest that stemness should be regarded as a property

that can be acquired at any stage of cellular differentiation, rather than as an intrinsic property acquired only on a cell's formation. The bidirectional interconversion between neoplastic stem and non-stem cell populations holds important implications for therapeutic strategies to eradicate cancer. If non-CSCs can spontaneously convert into CSCs, then anticancer therapies that target exclusively CSCs are not likely to be effective because non-CSCs would replace the eradicated CSCs after cessation of therapy, leading to renewed tumor growth. Therefore, anti-CSC agents should be combined with therapeutic agents that target the non-CSCs population within the tumors. Alternatively, combination of anti-CSC agents with agents that block conversion of non-CSCs into CSCs is required for durable clinical benefit. These clinical implications have been highlighted in a recent study by de Sousa e Melo et al.[229] They demonstrated that depletion of $Lgr5^+$ CSCs restricted primary tumor growth in a mouse model of colorectal cancer, but did not led to tumor regression. Instead, tumors were maintained by proliferating $Lgr5^-$ cells that continuously attempted to replace $Lgr5^+$ CSCs in a way reminiscent of the plasticity observed in normal intestine upon $Lgr5^+$ stem cell depletion.[218, 219] Notably, depletion of $Lgr5^+$ CSCs in primary tumors or in established liver metastases resulted in substantial decrease in liver metastatic burden, suggesting that the functional contribution of CSCs during colorectal carcinogenesis was influenced by tissue location and tumor microenvironment.[229]

I demonstrate that irrespective of the hepatic lineage hierarchy, H-Ras/SV40LT-transduced cells are capable of multilineage differentiation and give rise to tumors with varying contribution of EMT-, CCA-, and HCC-like phenotypes. My novel findings suggest that hepatic lineage cells at distinct differentiation stages can be the cell of origin of not only HCC but also of other types of PLC, such as CCA and CHC. Human PLCs are pheno- and genotypically highly heterogeneous.[177] Cholangiocarcinoma is the second most common type of PLC with increasing incidence worldwide.[230] Cholangiocarcinoma is classified according to its anatomical location along the biliary tree into three subtypes: intrahepatic, perihilar, and distal CCA. Tumors of different locations display pronounced heterogeneity, implicating potential diverse cellular origins in each CCA subtype. In accordance with my results, $CD34^+$ CSCs isolated from a human HCC cell line generated HCC, CCA, and CHC in immunodeficient mice, supporting the concept that primary liver tumors comprise a continuous spectrum.[231] Moreover, subpopulations of $CD34^+$ CSCs

with distinct antigenic profiles determined the types of PLC that would be generated in the xenograft assay, indicating the contribution of liver CSC heterogeneity to the heterogeneity of PLC. However, this study did not directly address the origin of $CD34^+$ liver CSCs but assumed that these CSCs originated from $CD34^+$ hepatic stem cells.

One of the most intriguing findings of my study is that mature hepatocytes can give rise to CCA. This is supported by several studies that suggest that hepatocytes can convert into biliary epithelial cells in response to acute and chronic biliary injury.[232-236] Michalopoulos et al. have demonstrated that chronic biliary injury in rats with chimeric livers carrying the hepatocyte marker dipeptidyl peptidase IV (DPPIV) leads to an increased number of DPPIV-positive biliary ductules. The frequency of biliary ductules derived from DPPIV-positive hepatocytes was dramatically enhanced by pretreatment with the biliary toxin methylene diamiline, indicating a large-scale conversion of hepatocytes into biliary ductules when the proliferative capacity of the biliary epithelium was compromised by toxic injury.[232] Using a dynamic lineage tracing approach, Yanger et al. have recently reported that activation of Notch, a signaling pathway that regulates biliary differentiation during liver development and in adult liver, is sufficient to reprogram hepatocytes into biliary epithelial cells in injured liver. Furthermore, lack of functional Notch signaling inhibited the generation of hepatocyte-derived biliary epithelial cells after injury.[234] Importantly, lineage tracing analyses have confirmed that thioacetamide-induced intrahepatic CCA is derived from hepatocytes through Notch-mediated conversion of hepatocytes into biliary lineage cells.[237] Forced expression of the Notch1 intracellular domain in mouse hepatocytes as well as forced co-activation of Notch and Akt signaling pathways using hydrodynamic gene delivery not only induced biliary lineage cells but also resulted in the development of intrahepatic CCA, supporting the concept that reprogramming of hepatocytes into biliary epithelial cells could lead to CCA development.[238, 239] In contrast to my findings, adult hepatocytes gave rise to only CCAs in these mouse models, whereas H-Ras and SV40LT induce the development of tumors with EMT-, CCA-, and HCC- like phenotypes. Since Notch is a major regulator of biliary differentiation, this difference could be related to the nature of the transforming agent, suggesting that different transforming stimuli may define directions of differentiation in the same target cell. In my mouse model, I used oncogenic H-Ras and SV40LT as transforming agents. Oncogenic H-Ras is a potent inducer of EMT, while SV40LT inhibits the

function of both p53 and Rb.[240] The major tumor suppressor p53 has been extensively studied since its discovery in 1979.[241] Notably, conditional deletion of p53 in murine liver induces tumors with a mixed HCC/CCA histology.[242] A recent study by Tschaharganeh et al. provided compelling evidence that p53 restricts cellular plasticity and tumorigenesis in liver cancer through transcriptional repression of Nestin.[243] Expression of nestin, an intermediate filament protein that is expressed in a variety of stem and progenitor cells, was restricted by p53 in an Sp1- or Sp3-dependent manner. Moreover, loss of p53 facilitated dedifferentiation of mature hepatocytes into hepatic progenitor-like cells, which generated HCCs or intrahepatic CCAs in response to additional oncogenic hits that target Wnt and Notch signaling pathways, respectively. These results again confirm the importance of cellular reprogramming of mature hepatocytes into a stem/progenitor cell state during the generation of PLCs. Although it remains unclear whether human CCA also originates from adult hepatocytes, these intriguing findings may explain why patients with viral hepatitis often develop intrahepatic CCA.[244]

Nonetheless, the nature of target cells may have a profound effect on susceptibility to oncogenic transformation, tumor histopathology, and global gene expression profiles. Thus, the same oncogenic alterations yielded a significantly higher frequency of tumor-initiating cells among transduced HPCs compared to HBs and AHs. Similarly, Cozzio et al. reported that the leukemogenic MLL-ENL fusion gene introduced by retrovirus transformed both hematopoietic stem cells and committed myeloid progenitor cells with highest efficiency in the hematopoietic stem cell population.[245] In a study of target cells and oncogene dosage, a higher dosage of MLL-AF9 was necessary for transformation of committed myeloid progenitors as compared to hematopoietic stem cells.[246] A more striking difference was described in the study by Heuser et al., in which only common myeloid but not committed progenitors could be transformed by meningioma 1 gene.[247] The findings of these experiments strongly suggest that the cell of origin affects the efficiency of oncogenic transformation, and susceptibility to transformation is decreasing as cells differentiate. In my study, the relatively small differences in the frequency of tumor-initiating cells among transduced HPCs, HBs, and AHs may be attributed to the strong transforming potential of oncogenic H-Ras and SV40LT that diminishes the differences in the susceptibility to transformation among diverse hepatic lineage cells.

Likewise, the differentiation state of the cell of origin influenced the histopathology of the resulting tumors. Even though all transformed hepatic lineage cells initiated liver cancer with EMT-, CCA-, and HCC-like phenotypes, the frequency of each phenotype was very variable in tumors with different cell of origin. Tumors initiated by mature AHs displayed a predominant HCC-like phenotype, suggesting that tumorigenic cells retained at least part of the differentiation program characteristic of the original cells. Moreover, a hepatocyte-derived iPSC signature was enriched only in AH but not in HPC or HB tumors, indicating the existence of a hepatic-lineage-stage-specific transcriptional memory in AH tumors.[190, 191] Hepatoblast-derived tumors exhibited a prominent presence of CCA-like phenotype, whereas HPC-derived tumors adopted a more primitive mesenchymal-like state. This is consistent with recent findings that histological diversity in human CCA may reflect the differences in cholangiocyte phenotypes that initiate the corresponding tumors.[248] Thus, the phenotypic features of primary liver tumors may have roots in the origins of the cells that underwent oncogenic transformation.

Consistent with this, global gene expression analysis clearly distinguished tumors of different cells of origin, indicating that distinct genetic alterations are involved in the process of malignant transformation of diverse hepatic lineage cells. Similarly, a comprehensive integrative molecular analysis of tumors in The Cancer Genome Atlas has recently revealed that cell-of-origin patterns dominate the molecular classification of approximately 10,000 specimens representing 33 types of cancer.[249] Notably, comparison of gene expression profiles among HPC, HB, and AH tumors and their freshly isolated normal counterparts revealed drastically more differentially expressed genes in AH tumors than in HB or HPC tumors. Furthermore, the highest number of activated ESC-related genes was found in AH tumors. Within this group of genes, *Myc* stood out with a remarkable 21-fold upregulation that was associated with coordinated activation of *Myc*-centered interaction networks. *MYC* is one of the most commonly activated oncogenes involved in human carcinogenesis. The *MYC* gene encodes the transcription factor c-Myc that is involved in the regulation of 15% of genes in the human genome associated with diverse biological processes, such as cell growth, apoptosis, and metabolism.[250, 251] The transcription factor c-Myc is also reported to be an essential regulator of self-renewal and pluripotency in ESCs and iPSCs.[252, 253] Although the central role of c-Myc in hepatocarcinogenesis is widely described in rodents and humans, I am the first to identify *Myc* as a

key player in the oncogenic reprogramming of AHs linked to activation of an ESC-like transcriptional program.[193, 254, 255] I validated these findings by stable knockdown of c-Myc in H-Ras/SV40LT-expressing AHs, which significantly reduced the frequency of CSCs and delayed tumor growth in immunocompromised mice. In accordance with my results, low level of forced c-Myc expression caused upregulation of pluripotency and stemness genes NANOG, OCT4, BMI1, SOX2, and EpCAM, and also markedly increased the frequency of SP cells and promoted tumorigenicity in human liver cancer cell lines. Notably, c-Myc induced CSC phenotype in a p53-dependent manner.[256]

In conclusion, my study provides the first comprehensive and systematic comparison of genetically defined liver carcinomas initiatiated by mouse hepatic lineage cells at different stages of differentiation. Mature hepatocytes, committed hepatoblasts, and adult hepatic progenitor cells were isolated at high purity and efficiently transduced *ex vivo* with lentiviral vectors expressing oncogenic H-Ras and SV40LT. This allowed a unique and direct side-by-side comparison of cellular and molecular characteristics of transformed cells both *in vitro* and *in vivo*. I formally demonstrated that any hepatic lineage cell can be reprogrammed into CSC by activating diverse cell-type-specific pathways. I identified common and cell-of-origin-specific phenotypic and genetic changes that differentiated murine tumors according to their origin. Identification of normal cells that can transform into CSCs and relevant molecular pathways is essential for a deeper understanding of the biology of PLC and development of novel therapeutic approaches for targeting CSCs. It may also allow earlier detection of PLCs and may lead to preventive therapies for high-risk individuals.

5.2 Distinct claudin expression profiles of human HCC and metastatic colorectal and pancreatic carcinomas

In the present study, I sought to analyze the protein and mRNA expression of CLDN-1, -2, -3, -4, and -7 in human HCC, CRLM, and PLM. For the first time, I demonstrate that the examined primary and metastatic neoplasms of the liver display distinct claudin expression profiles. HCC is characterized by moderate CLDN-1 and weak CLDN-2, -3, and -7 expression, however, does not express CLDN-4. CRLM shows strong CLDN-1, -3, -4, -7 and moderate CLDN-2 positivities, whereas PLM exhibits strong

CLDN-4, moderate CLDN-2, and weak CLDN-1, -3, and -7 stainings.

Claudins, the major components of epithelial cell tight junctions, exhibit highly tissue- and cell-specific expression patterns. They play a critical role in cell adhesion, polarity and paracellular permeability. Claudin-1-deficient mice die within one day of birth accompanied by excessive water loss from the skin, whereas overexpression of certain claudins *in vitro* alters Na^+ permeability.[257-259] Claudins have recently been recognized as signaling proteins that are functionally associated with various signal transduction pathways including proto-oncogene c-Yes, protein kinase A, protein kinase C, Rho, PI3K, and MAPK signaling.[108, 124, 260] Claudins are tightly regulated by multiple molecular mechanisms, and deregulated CLDN expression directly results in several distinct abnormalities in cellular physiology.[100, 261]

Claudins are often dysregulated in epithelial malignancies, coinciding with tumor initiation and progression.[262] It has been shown that CLDN dysregulation can occur at both transcriptional and post-transcriptional levels.[263-265] Tumor development and metastatic dissemination are frequently associated with a continuous decrease of CLDN expression and consequent disruption of cell-cell adhesion and cell polarity.[266-272] In contrast, upregulated CLDN expression has also been reported in various cancer types, albeit the functional significance of CLDN overexpression in carcinogenesis is not well established. Several lines of evidence have demonstrated that CLDNs play a role in the process of EMT. Overexpression of Snail in cultured mouse epithelial cells induced EMT with concomitant repression of CLDN-3, -4, and -7 mRNA and protein expression.[273] Interestingly, some CLDNs induce EMT and promote cancer cell invasion and metastatic progression, whereas others function to sustain an epithelial phenotype.[274-276] In the first part of the thesis, I demonstrated that, in accordance with other studies, activation of the EMT program is involved in the generation of CSCs. The recently identified claudin-low molecular subtype of breast cancer is characterized by low expression of adherens and tight junction proteins, such as E-cadherin, CLDN-3, -4, and -7. Notably, this subtype is associated with poor prognosis and chemoresistance, expresses stem cell and EMT markers, and is enriched in $CD44^+/CD24^{-/low}$ breast CSCs. Similarly, downregulation of CLDN-3, -4, and -7 genes was observed in breast CSCs generated through TGF-β/TNF-α-mediated EMT in mouse mammary carcinoma cells, suggesting a strong association between mammary CSCs and low CLDN expression.[277-280] Potential involvement of

CLDNs in the regulation of CSCs has also been demonstrated in other cancer types.[261] Gene expression profiling has revealed that CLDN-1 is significantly upregulated in $CD133^+/CD117^+$ ovarian CSCs compared to non-stem cancer cells.[281] The same group described that microRNA (miRNA)-155 negatively regulates CLDN-1 in ovarian CSCs both *in vitro* and *in vivo*.[282] However, overexpression of miRNA-155 enhanced the migration and invasive ability of colorectal cancer cells through upregulation of CLDN-1 expression.[283] Short hairpin RNA-mediated knockdown of CLDN-4 in ovarian cancer cells delayed spheroid formation, a key feature of CSCs.[284] Others have reported that miRNA-1275 inhibits the expression of CLDN-11 in glioblastoma CSCs, which represses the proliferation of CSCs.[285] In colorectal cancer, CLDN-2 promotes self-renewal of CSCs and regulates the expression of 9 miRNAs known to control stem cell signaling. Among these miRNAs, decrease of miRNA-222-3p expression is essential for the promotion of self-renewal by CLDN-2.[286]

Several CLDNs have been associated with the activation of matrix metalloproteinases, promoting the migration of cancer cells cell by degradation of the extracellular matrix.[287-289] Significant disorganization of TJ strands and increased paracellular permeability were observed in colorectal tumors despite upregulation of CLDN-1, -3, and -4, indicating that CLDN overexpression compromises TJ barrier function and thus may have other effects on cellular homeostasis.[290] Increased paracellular permeability may also facilitate the access of cancer cells to nutrients and growth factors critical for tumor growth and survival. Furthermore, unique CLDN expression profiles of various cancers are recognized to carry differential diagnostic, prognostic, and therapeutic potential. Claudin immunostaining can aid in the differential diagnosis between mesothelioma and metastatic adenocarcinoma of the pleura as malignant mesotheliomas have lower expression of CLDN-1, -3, -4, -5, and -7, than adenocarcinomas.[291] Among the different histologic subtypes of lung cancer, adenocarcinomas express higher levels of CLDN-3, -4, and -7 compared to squamous cell carcinomas, whereas they differ only in CLDN-2 expression as compared to small cell lung cancers.[128] Claudin-1 overexpression confers a good prognosis in squamous cell carcinoma of the lung and in papillary urothelial neoplasms of low malignant potential.[166, 292] On the other hand, high CLDN-4 protein levels in low-grade urothelial cell carcinomas are associated with significantly shorter recurrence-free survival.[166] In HCC, patients with high CLDN-10 mRNA expression were found to have

shorter disease-free survival.[293]

Claudin-1 is one of the most frequently dysregulated CLDNs in human cancer, and its role in carcinogenesis has been thoroughly investigated. I report definite CLDN-1 positivity in both primary HCC and metastatic tumors, implicating the involvement of this protein in hepatocarcinogenesis and metastasis formation. Liver metastases of colorectal adenocarcinomas expressed the highest levels of CLDN-1 protein, whereas HCCs and PLMs displayed moderate and weak expression, respectively. Depending on the type of cancer, CLDN-1 can act as a tumor suppressor or cancer promoting factor. In human CRC, a role for CLDN-1 as a promoter of cellular transformation, tumor growth and metastasis has been established by overexpression and knockdown experiments. Claudin-1 overexpression in CRC cells increased the activity of MMP-2 and MMP-9, whereas inhibition of CLDN-1 expression decreased the expression of mesenchymal markers and robustly increased E-cadherin expression.[294] Singh et al. reported that overexpression of CLDN-1 reduced expression of E-cadherin through upregulation of Zeb1 resulting in EMT and increased invasion.[295] Similarly, CLDN-1 was found to promote TNF-α-induced EMT and migration in CRC cells.[296] In line with this, increased mRNA and protein levels of CLDN-1 in CRC tissues have been observed in several studies.[290, 294, 297-302] Immunohistochemical analysis of matched normal colonic mucosa, primary CRC tumors, and CRC lymph node or liver metastatic lesions revealed a significant linear association between CLDN-1 nuclear, cytoplasmic, or membranous staining and tumor progression.[294] Similarly, Kinugasa et al. demonstrated upregulated CLDN-1 protein expression in matched CRC and liver metastatic lesions as compared to normal colon samples.[302] On the contrary, Matsuoka et al. reported decreased CLDN-1 protein expression in both the central parts and invasive fronts of colorectal tumors compared to normal colon mucosa, with more prominent loss of expression at the invasive fronts than in the central parts. Reduced expression of CLDN-1 was associated with poor tumor differentiation, advanced stage, and poor prognosis.[303] In another study, loss of claudin-1 expression was found to be a strong predictor of disease recurrence and poor patient survival in stage II colon cancer.[269] Similarly, Nakagawa et al. demonstrated that the overall survival rate was significantly higher in CRC patients with high CLDN-1 high expression than in patients with low expression.[304] Interestingly, similarly conflicting results have been reported on CLDN-1 expression in HCC. Preserved expression of CLDN-1 protein was observed in

well-differentiated HCCs compared to surrounding liver tissues, whereas CLDN-1 immunostaining was lost in poorly differentiated HCCs. Attenuated CLDN-1 expression was associated with increased incidence of portal invasion, and a lower overall survival rate after hepatectomy.[305] In contrast, significantly elevated CLDN-1 expression was found in cirrhosis and HCC developed in cirrhotic liver.[306] Bouchagier et al. observed increased CLDN-1 expression in HCC and tumor surrounding liver, suggesting that upregulaton of CLDN-1 expression is an early event during hepatocarcinogenesis. Increased levels of CLDN-1 were associated with early stage, presence of a single tumor nodule, small tumor size, and better prognosis.[307] Several lines of evidence support a role for CLDN-1 as a potent inducer of cancer cell invasion in HCC. Overexpression of CLDN-1 promoted the acquisition of invasive capacity by activating c-Abl-PKC signaling pathway in normal liver cells, while knockdown of CLDN-1 expression inhibited cellular invasion in CLDN-1-overexpressing, invasive HCC cells.[308] Furthermore, Suh et al. demonstrated that CLDN-1 promoted an invasive phenotype in human liver cells by inducing EMT through activation of the c-Abl-Ras-Raf-1/ERK1/2 signaling pathway.[275] In PDAC, reduced CLDN-1 expression levels were observed in poorly differentiated compared to well-differentiated tumors. Furthermore, upregulation of Snail and downregulation of CLDN-1 were detected in human pancreatic cancer cells after treatment with TGF-β1.[309]

Claudin-2 expression is typical of leaky epithelia characterized by high paracellular permeability.[310] Recent evidence suggests the involvement of CLDN-2 in neoplastic transformation and tumor progression. Elevation of CLDN-2 expression has been reported in several cancer types, including lung adenocarcinoma, CRC, and gastric cancer.[299, 311, 312] In stage II/III colorectal tumors, elevated CLDN-2 expression was associated with poor recurrence-free survival following chemotherapy, underlining the importance of CLDN-2 in the regulation of CSCs.[286] Similarly, Dhawan et al. have reported that overexpression of CLDN-2 in human colon cancer cells enhances colony formation, cell proliferation, and chemoresistance *in vitro*, and increases tumor growth in xenografted mice.[313] However, my results demonstrate strong CLDN-2 positivity in non-tumorous liver tissue, whereas significantly weaker positivity was observed in HCCs, CRLMs, and PLMs. Decreased CLDN-2 expression has also been shown in breast cancer compared to adjacent non-neoplastic breast tissue, and downregulation of CLDN-2 expression was particularly associated with advanced clinical stage.[314] Interestingly,

Tabaries et al. found that CLDN-2 levels were elevated exclusively in liver metastases of breast cancer compared to matched primary tumors. Moreover, CLDN-2 promoted breast cancer metastasis to the liver through CLDN-2-mediated interactions between metastatic breast cancer cells and primary hepatocytes.[315, 316] This suggests that CLDN-2 not only participates in the carcinogenesis of these tumors but may also contribute to a metastatic phenotype.

Claudin-3 and claudin-4 are located in close proximity on chromosome 7. Whether this genomic arrangement leads to coordinate regulation is unknown, but coordinate expression of these genes has been reported in several normal and neoplastic tissues, and they are often simultaneously overexpressed in various human malignancies, including colorectal, gastric, breast, ovarian, uterine, prostate, and gastric cancers.[317-319] In ovarian cancer, CLDN-3 and CLDN-4 have been shown to promote tumorigenesis and metastasis.[288] However, Shang et al. demonstrated that knockdown of CLDN-3 and CLDN-4 enhanced primary tumor growth and metastasis with concomitant downregulation of E-cadherin and activation of β-catenin pathway signaling, suggesting a tumor suppressor role for CLDN-3 and CLDN-4 in ovarian cancer.[320] In line with this, loss of CLDN-3 and CLDN-4 have been reported to promote EMT in ovarian cancer cells, reflected by upregulation of Twist, downregulation of E-cadherin, and activation of the PI3K-AKT pathway.[274] Importantly, CLDN-3 and CLDN-4 proteins have been identified as natural receptors for CPE.[113] Binding of CPE to tumor cells expressing CLDN-3 or CLDN-4 leads to an acute dose-dependent cytotoxic response.[321, 322] Thus, CPE may be exploited for therapeutic use for CLDN-3 and -4 expressing tumors.[323] In my sample set, HCC, PLM, and non-tumorous liver cells exhibited weak CLDN-3 positivity. Expression of CLDN-3 in PLM is especially intriguing, because no CLDN-3 staining was detected in primary PDAC.[133] Furthermore, intrahepatic bile duct cancers were also characterized by absence or scarcity of CLDN-3.[132] Claudin-3 expression might therefore contribute to the metastatic phenotype in pancreatic cancer and could also be used to differentiate between intrahepatic bile duct cancer and PLM. In contrast, I observed strong CLDN-3 positivity in CRLM samples, and upregulation of CLDN-3 mRNA and protein have already been described in primary CRC.[290, 319, 324] The functional significance of elevated CLDN-3 level in CRC has not yet been fully elucidated. Supporting a role in cancer promotion,

EGF-mediated increased expression of CLDN-3 increased cell migration and colony formation in CRC cells.[325] On the contrary, Ahmad et al. demonstrated a tumor suppressive role of CLDN-3 in CRC. Claudin-3 protein was expressed abundantly in normal colonic mucosa, but decreased levels were detected in primary CRC and lymph node metastasis. Furthermore, loss of CLDN-3 was associated with CRC progression and poor patient survival. Claudin-3-null mice exhibited increased susceptibility to colon carcinogenesis in response to azoxymethane/dextran sodium.[326] A similar decrease in CLDN-3 expression was observed to promote HCC. Moreover, epigenetic regulation of CLDN-3 involving promoter hypermeythylation was reported in both CRC and HCC.[327]

I found that both CRLMs and PLMs were strongly positive for CLDN-4 with no significant difference between these two groups, underlining its role in the pathogenesis of these lesions. In accordance with previous findings, bile duct cells of non-tumorous and normal liver were also positive, whereas I did not detect CLDN-4 expression in HCCs and non-tumorous hepatocytes.[328] My results indicate that the expression of CLDN-4 differentiates between adenocarcinoma liver metastases and HCCs. However, CLDN-4 does not distinguish between CRLMs and PLMs. Overexpression of CLDN-4 has also been observed both in primary colorectal and pancreatic cancers, as well as in pancreatic intraepithelial neoplasia, the precursor lesion of pancreatic cancer.[319, 321, 329] Interestingly, liver metastases of pancreatic cancer exhibited similarly elevated CLDN-4 expression as compared to primary tumors.[329] To add another layer of complexity, CLDN-4 was associated with less differentiated and invasive phenotypes in primary colorectal and pancreatic cancers, suggesting its inhibitory effect on invasion and metastasis. Ueda et al. demonstrated that decreased expression of CLDN-4 at the invasive front was correlated with infiltrating growth pattern, lymphovascular invasion, and metastasis in colorectal cancer.[271] Similarly, Matsuoka et al. reported loss of CLDN-4 expression at the invasive front of CRCs, which was associated with poor tumor differentiation and advanced TNM stage.[303] Overexpression of CLDN-4 in pancreatic cancer cells reduced invasive potential *in vitro* and reduced lung metastasis burden *in vivo*.[330] By contrast, CLDN-4 expression in ovarian epithelial cells was reported to enhance cell invasion by an increase of MMP-2 activity.[288]

Claudin-7 is one of the highly expressed claudins in normal colon and plays an important role in colonic physiology. Unlike other members of the claudin family, the

majority of CLDN-7 protein is localized at the basolateral membrane in normal intestinal epithelial cells. Its knockdown in mice leads to disruption of intestinal architecture, barrier dysfunction, inflammation, and neonatal death.[331] Claudin-7 is dysregulated in various malignancies, including lung, liver, colorectal, esophageal, pancreatic, prostate, breast, and ovarian cancers.[124, 128] Increased CLDN-7 levels were detected in primary CRC samples, and overexpression of CLDN-7 in CRC cells disrupted cell polarity and increased proliferation, and tumorigenicity.[332] Interestingly, Kuhn et al. proposed that tumorigenic roles of CLDN-7 are exerted in complex with EpCAM, CD44 variant isoforms, and tetraspanins.[333] Furthermore, CLDN-7 promoted EMT and tumor cell motility, and enhanced metastasis formation.[276] In concordance with these results, I also observed strong immunostaining for CLDN-7 in CRLM samples. However, other authors described CLDN-7 as a cancer suppressor. Reduction of CLDN-7 mRNA levels correlates with venous invasion and liver metastasis but not with lymph node metastasis in CRC.[319] Interestingly, downregulation of CLDN-7 mRNA expression was described as an early event during colorectal carcinogenesis, whereas its re-expression was frequently detected in lymph node metastases; this may also explain CLDN-7 positivity in my CRLM samples.[334, 335] Reduced CLDN-7 expression is associated with metastasis formation in breast cancer and squamous cell carcinoma of the esophagus.[270, 336] Kominsky et al. have described that loss of claudin-7 correlates with histological grade in both ductal carcinoma *in situ* and invasive ductal carcinoma of the breast.[266] I detected weak CLDN-7 positivity in HCC samples with no significant difference in comparison to non-tumorous and normal livers, whereas bile duct cells exhibited very strong membranous staining. Interestingly, our research group has previously found elevated CLDN-7 levels in cirrhosis and HCCs developed in cirrhotic livers, indicating that certain structural changes in TJs may begin before malignant transformation occurs.[306] Liver metastases of pancreatic adenocarcinomas were negative or exhibited faint, focal positivity for CLDN-7. In normal pancreas, CLDN-7 positivity was reported in both ductal and acinar epithelial cells. In accordance with my results, CLDN-7 protein appeared to be underexpressed in PDACs as compared to normal glands with a gradual decline in parallel with the degree of tumor differentiation. No association was found between CLDN-7 expression and tumor size, the presence of metastatic lymph nodes or patient survival, indicating that CLDN-7 does not play a role in the progression of PDAC.[337] In my study, I observed a good correlation

between claudin protein and mRNA expression with two intriguing exceptions. CLDN-1 and -7 protein levels were lower in HCCs compared to CRLMs, whereas mRNA levels were higher or comparable. This raises the possibility of post-transcriptional regulation of these claudins that might be mediated by miRNAs.[338] Rapid protein turnover may also be responsible for this discrepancy.

Taken together, my results support the role of altered claudin expression in both hepatocarcinogenesis and metastasis formation of colorectal and pancreatic cancers. I demonstrate here that HCC, CRLM, and PLM display distinct claudin expression profiles that may carry great differential diagnostic value. Liver metastasis of colorectal adenocarcinoma is characterized by strong positivity for CLDN-1, -3, -4, and -7, HCC is associated with CLDN-1 immunostaining and a lack of CLDN-4, and PLM exhibits strong CLDN-4 and weak CLDN-1 positivity. My findings suggest a complex and well-regulated system of claudin expression that is distinct in primary and metastatic liver tumors. However, the exact role and functional importance of claudin overexpression and claudin downregulation in the development of HCC, CRLM, and PLM remain unclear. One plausible mechanism is that altered claudin expression may modify the structure and function of tight junction, which could contribute to the malignant potential of affected cells. Furthermore, these claudins might be involved in signaling pathways that play important role in cellular transformation. Downregulation of certain claudins has been demonstrated in advanced CRCs, but I detected strong claudin expression in CRLMs. Several factors may attribute to this difference, including biological selection of cancer cells during tumor progression and microenvironmental influence.[339] Dedifferentiated primary CRCs have been shown to undergo redifferentiation at liver metastases with concomitant re-expression of the tight junction protein ZO-1, which may also be associated with recovery of the claudin phenotype.[340] In conclusion, primary hepatocellular carcinoma and metastatic colorectal and pancreatic carcinomas exhibit distinct claudin expression profiles. This provides further insight into their pathobiology and may aid in differentiating focal liver lesions. The observed expression changes indicate that these claudins play a pivotal role in the process of carcinogenesis and metastasis formation. Claudins may therefore be good candidates for targeted therapy not only in primary liver tumors but also in colorectal and pancreatic cancer patients with hepatic metastasis.

DOI:10.14753/SE.2019.2291

6. CONCLUSIONS

In the present study, I demonstrated several novel findings that support the substantial role of cancer stem cells and their cellular origin in the emergence of heterogeneity in hepatocellular carcinoma, and the diagnostic utility of claudin proteins in primary and secondary liver cancers. The following conclusions can be drawn from my results:

1. Any cell within the mouse hepatic lineage can be a target of oncogenic reprogramming and acquire cancer stem cell traits; however, hepatic progenitor cells are more susceptible to oncogenic reprogramming than more differentiated cells.

2. Oncogenic transformation of distinct mouse hepatic lineage cells may give rise to liver cancer of multilineage differentiation resembling human primary liver cancers; nevertheless, tumors display distinct phenotypes according to their cell-of-origin; hepatic progenitor cell-derived tumors show epithelial-mesenchymal transition-like phenotype, hepatoblast-derived tumors predominantly exhibit cholangiocarcinoma-like features, and adult hepatocyte-derived tumors display an HCC-like phenotype.

3. Common activation of epithelial-mesenchymal transition-related pathways and activation of diverse, hepatic-lineage-stage-specific transcriptional programs contribute to oncogenic transformation of distinct mouse hepatic lineage cells.

4. Upregulation of c-Myc in adult mouse hepatocytes is required for acquisition of cancer stem cell phenotype.

5. Human hepatocellular carcinoma and liver metastases of colorectal adenocarcinoma and pancreatic adenocarcinoma display distinct claudin expression profiles: HCCs exhibit moderate claudin-1 and weak or no claudin-2, -3, -4, and -7 expression, liver metastases of colorectal adenocarcinoma display strong claudin-1, -3, -4, -7 and moderate claudin-2 positivity, and liver metastases of pancreatic adenocarcinoma show strong claudin-4, moderate claudin-2, and weak claudin-1, -3, and -7 staining.

DOI:10.14753/SE.2019.2291

7. SUMMARY

Human hepatocellular carcinoma (HCC) and liver metastases of colorectal cancer (CRLM) and pancreatic cancer (PLM) are major health problems globally. Although cancer stem cells, a small subset of tumor cells with stem cell features, and claudins, the major components of tight junctions have recently been implicated in their development, their complex pathogenesis is still not fully elucidated. The aim of the thesis was to explore the role of cancer stem cells and claudins in the development of HCC, CRLM, and PLM. In the first part of the work, I investigated the contribution of hepatic lineage cells at different stages of differentiation to the evolution of liver cancer stem cells and genetic and phenotypic heterogeneity of HCC. I showed that all mouse hepatic lineage cells (i.e., bipotential hepatic progenitor cells, lineage-committed hepatoblasts, and differentiated adult hepatocytes) can be target of oncogenic transformation and give rise to primary liver cancer; however, hepatic progenitor cells are more susceptible to oncogenic transformation than more differentiated cells. I demonstrated that all hepatic lineage cells can be reprogrammed into cancer stem cells by activation of epithelial-mesenchymal transition (EMT)-related and hepatic-lineage-stage-specific pathways. Notably, c-Myc acts as the driver of reprogramming in adult hepatocytes. Furthermore, I showed that tumors originated from these three independent stages of hepatic lineage cells exhibit the phenotypic diversity of HCC and cholangiocarcinoma. Hepatic progenitor cell-derived tumors displayed EMT-like phenotype, hepatoblasts were predominantly reprogrammed into cholangiocarcinoma-like tumors, whereas adult hepatocyte-derived tumors exhibited a prominent presence of HCC-like phenotype. In the second part of the thesis, I aimed to characterize the claudin expression profiles in human HCC, CRLM, and PLM. I demonstrated that HCC, CRLM, and PLM display distinct claudin expression profiles. HCC was characterized by moderate claudin-1 and weak claudin-2, -3, and -7 expression, whereas did not express claudin-4. CRLM displayed strong claudin-1, -3, -4, -7 and moderate claudin-2 positivity, and PLM showed strong claudin-4, moderate claudin-2, and weak claudin-1, -3, and -7 staining. In summary, my study yielded multiple novel findings supporting the contribution of distinct hepatic lineage cells to the evolution of cancer stem cells and genetic and phenotypic heterogeneity of HCC and the diagnostic utility of claudin expression in primary and secondary liver cancers.

DOI:10.14753/SE.2019.2291

8. ÖSSZEFOGLALÁS

A humán hepatocellularis carcinoma (HCC), valamint a colorectalis carcinoma (CRLM) és a pancreas carcinoma (PLM) májáttétei világszinten jelentős egészségügyi problémát jelentenek. Bár kialakulásukban számos vizsgálat felvetette a daganatőssejtek, a daganatokban csekély számban jelen lévő őssejtek, és a tight junction típusú sejtkapcsoló struktúrák gerincét alkotó claudin fehérjék szerepét, rendkívül összetett patogenezisük még nem tisztázott. Kutatásaim célkitűzése a daganatőssejtek és claudinok szerepének vizsgálata volt a HCC, CRLM és PLM kialakulásában. Kutatásaim első részében azt vizsgáltam, hogy a hepatocyta irányú differenciáció különböző stádiumaiban lévő sejtalakok mennyiben járulnak hozzá a HCC-ben előforduló daganatőssejtek és a HCC-re jellemző genetikai és fenotípusos heterogenitás kialakulásához. Eredményeim szerint egerekben a bipotens hepatikus progenitor sejtekben, hepatocyta irányba elkötelezett hepatoblastokban és érett hepatocytákban egyaránt végbemehet malignus transzformáció és ennek következtében kialakulhat primer májrák, de a hepatikus progenitor sejtek fogékonyabbak a malignus transzformációra, mint a differenciáltabb fenotípusú sejtek. Kimutattam, hogy az összes vizsgált sejtalak átprogramozható daganatőssejtté az epithelialis-mesenchymalis átmenetet szabályozó és különböző sejtspecifikus jelátviteli utak aktivációja révén. Kiemelendő, hogy az érett hepatocyták átprogramozásában vezető szerepe van a c-Myc proto-onkogénnek. Kimutattam továbbá, hogy a hepatikus progenitor sejtekből származó tumorok elsősorban sarcomatoid típusúak, míg a hepatoblastokból kiinduló tumorok cholangiocarcinomára, az érett hepatocytákból származó tumorok HCC-re jellemző szövettani képet mutatnak. Kutatásaim második felében a HCC, CRLM és PLM claudin expresszióját tanulmányoztam. Eredményeim arra utalnak, hogy a HCC, CRLM és PLM jelentősen eltér egymástól a claudinok expressziós mintázatában. A HCC mérsékelt claudin-1 és gyenge claudin-2, -3 és -7 expressziót mutatott, míg a claudin-4 negatívnak bizonyult. A CRLM erős claudin-1, -3, -4, -7 és mérsékelt claudin-2 pozitivitást, míg a PLM erős claudin-4, mérsékelt claudin-2 és gyenge claudin-1, -3 és -7 pozitivitást mutatott. Összefoglalva elmondható, hogy kutatásaim számos új eredménnyel támasztják alá a hepatocyta irányú sejtvonal különböző sejtjeinek fontos szerepét a daganatőssejtek és a HCC-re jellemző feno- és genotípus heterogenitás kialakulásában és a claudinok jelentőségét a primer és áttéti májrákok elkülönítésében.

DOI:10.14753/SE.2019.2291

9. BIBLIOGRAPHY

[1] Torre LA, Bray F, Siegel RL, Ferlay J, Lortet-Tieulent J, Jemal A. (2015) Global cancer statistics, 2012. CA Cancer J Clin, 65: 87-108.

[2] Castelli G, Pelosi E, Testa U. (2017) Liver Cancer: Molecular Characterization, Clonal Evolution and Cancer Stem Cells. Cancers (Basel), 9.

[3] El-Serag HB. (2011) Hepatocellular carcinoma. N Engl J Med, 365: 1118-1127.

[4] Mittal S, El-Serag HB. (2013) Epidemiology of hepatocellular carcinoma: consider the population. J Clin Gastroenterol, 47 Suppl: S2-6.

[5] Llovet JM, Zucman-Rossi J, Pikarsky E, Sangro B, Schwartz M, Sherman M, Gores G. (2016) Hepatocellular carcinoma. Nat Rev Dis Primers, 2: 16018.

[6] Gomaa AI, Khan SA, Toledano MB, Waked I, Taylor-Robinson SD. (2008) Hepatocellular carcinoma: epidemiology, risk factors and pathogenesis. World J Gastroenterol, 14: 4300-4308.

[7] Bralet MP, Regimbeau JM, Pineau P, Dubois S, Loas G, Degos F, Valla D, Belghiti J, Degott C, Terris B. (2000) Hepatocellular carcinoma occurring in nonfibrotic liver: epidemiologic and histopathologic analysis of 80 French cases. Hepatology, 32: 200-204.

[8] Schaff Z, Kovalszky I, Lotz G, Kiss A. (2010) [Hepatocellular carcinoma--from macroscopy to molecular pathology]. Orv Hetil, 151: 982-989.

[9] Gurtsevitch VE. (2008) Human oncogenic viruses: hepatitis B and hepatitis C viruses and their role in hepatocarcinogenesis. Biochemistry (Mosc), 73: 504-513.

[10] Schaff Z, Gogl A, Dora R, Halasz T. (2015) [The pathology of hepatitis C]. Orv Hetil, 156: 836-839.

[11] Moll R. (1994) Cytokeratins in the histological diagnosis of malignant tumors. Int J Biol Markers, 9: 63-69.

[12] Siegel AB, Zhu AX. (2009) Metabolic syndrome and hepatocellular carcinoma: two growing epidemics with a potential link. Cancer, 115: 5651-5661.

[13] Park YN. (2011) Update on precursor and early lesions of hepatocellular carcinomas. Arch Pathol Lab Med, 135: 704-715.

[14] Schlageter M, Terracciano LM, D'Angelo S, Sorrentino P. (2014) Histopathology of hepatocellular carcinoma. World J Gastroenterol, 20: 15955-15964.

[15] Goodman ZD. (2007) Neoplasms of the liver. Mod Pathol, 20 Suppl 1: S49-60.

[16] Verslype C, Rosmorduc O, Rougier P, Group EGW. (2012) Hepatocellular carcinoma: ESMO-ESDO Clinical Practice Guidelines for diagnosis, treatment and follow-up. Ann Oncol, 23 Suppl 7: vii41-48.

[17] Dank M, Padányi, P. (2018) Systemic treatment options of primary hepatocellular carcinoma. Magy Onkol: 53-61.

[18] Bruix J, Sherman M, American Association for the Study of Liver D. (2011) Management of hepatocellular carcinoma: an update. Hepatology, 53: 1020-1022.

[19] European Association For The Study Of The L, European Organisation For R, Treatment Of C. (2012) EASL-EORTC clinical practice guidelines: management of hepatocellular carcinoma. J Hepatol, 56: 908-943.

[20] Bruix J, Reig M, Sherman M. (2016) Evidence-Based Diagnosis, Staging, and Treatment of Patients With Hepatocellular Carcinoma. Gastroenterology, 150: 835-853.

[21] International Consensus Group for Hepatocellular NeoplasiaThe International Consensus Group for Hepatocellular N. (2009) Pathologic diagnosis of early hepatocellular carcinoma: a report of the international consensus group for hepatocellular neoplasia. Hepatology, 49: 658-664.

[22] Thorgeirsson SS, Grisham JW. (2002) Molecular pathogenesis of human hepatocellular carcinoma. Nat Genet, 31: 339-346.

[23] Llovet JM, Bruix J. (2008) Molecular targeted therapies in hepatocellular carcinoma. Hepatology, 48: 1312-1327.

[24] Alizadeh AA, Aranda V, Bardelli A, Blanpain C, Bock C, Borowski C, Caldas C, Califano A, Doherty M, Elsner M, Esteller M, Fitzgerald R, Korbel JO, Lichter P, Mason CE, Navin N, Pe'er D, Polyak K, Roberts CW, Siu L, Snyder A, Stower H, Swanton C, Verhaak RG, Zenklusen JC, Zuber J, Zucman-Rossi J. (2015) Toward understanding and exploiting tumor heterogeneity. Nat Med, 21: 846-853.

[25] Youn A, Simon R. (2011) Identifying cancer driver genes in tumor genome sequencing studies. Bioinformatics, 27: 175-181.

[26] Schulze K, Imbeaud S, Letouze E, Alexandrov LB, Calderaro J, Rebouissou S, Couchy G, Meiller C, Shinde J, Soysouvanh F, Calatayud AL, Pinyol R, Pelletier L, Balabaud C, Laurent A, Blanc JF, Mazzaferro V, Calvo F, Villanueva A, Nault JC, Bioulac-Sage P, Stratton MR, Llovet JM, Zucman-Rossi J. (2015) Exome sequencing of

hepatocellular carcinomas identifies new mutational signatures and potential therapeutic targets. Nat Genet, 47: 505-511.

[27] Cancer Genome Atlas Research Network. Electronic address wbe, Cancer Genome Atlas Research N. (2017) Comprehensive and Integrative Genomic Characterization of Hepatocellular Carcinoma. Cell, 169: 1327-1341 e1323.

[28] Lee S, Lee HJ, Kim JH, Lee HS, Jang JJ, Kang GH. (2003) Aberrant CpG island hypermethylation along multistep hepatocarcinogenesis. Am J Pathol, 163: 1371-1378.

[29] Farazi PA, DePinho RA. (2006) Hepatocellular carcinoma pathogenesis: from genes to environment. Nat Rev Cancer, 6: 674-687.

[30] Lachenmayer A, Alsinet C, Chang CY, Llovet JM. (2010) Molecular approaches to treatment of hepatocellular carcinoma. Dig Liver Dis, 42 Suppl 3: S264-272.

[31] Villanueva A, Portela A, Sayols S, Battiston C, Hoshida Y, Mendez-Gonzalez J, Imbeaud S, Letouze E, Hernandez-Gea V, Cornella H, Pinyol R, Sole M, Fuster J, Zucman-Rossi J, Mazzaferro V, Esteller M, Llovet JM, Consortium H. (2015) DNA methylation-based prognosis and epidrivers in hepatocellular carcinoma. Hepatology, 61: 1945-1956.

[32] Wang J, Chenivesse X, Henglein B, Brechot C. (1990) Hepatitis B virus integration in a cyclin A gene in a hepatocellular carcinoma. Nature, 343: 555-557.

[33] Sung WK, Zheng H, Li S, Chen R, Liu X, Li Y, Lee NP, Lee WH, Ariyaratne PN, Tennakoon C, Mulawadi FH, Wong KF, Liu AM, Poon RT, Fan ST, Chan KL, Gong Z, Hu Y, Lin Z, Wang G, Zhang Q, Barber TD, Chou WC, Aggarwal A, Hao K, Zhou W, Zhang C, Hardwick J, Buser C, Xu J, Kan Z, Dai H, Mao M, Reinhard C, Wang J, Luk JM. (2012) Genome-wide survey of recurrent HBV integration in hepatocellular carcinoma. Nat Genet, 44: 765-769.

[34] Marquardt JU, Seo D, Andersen JB, Gillen MC, Kim MS, Conner EA, Galle PR, Factor VM, Park YN, Thorgeirsson SS. (2014) Sequential transcriptome analysis of human liver cancer indicates late stage acquisition of malignant traits. J Hepatol, 60: 346-353.

[35] Lee JS, Chu IS, Heo J, Calvisi DF, Sun Z, Roskams T, Durnez A, Demetris AJ, Thorgeirsson SS. (2004) Classification and prediction of survival in hepatocellular carcinoma by gene expression profiling. Hepatology, 40: 667-676.

[36] Lee JS, Heo J, Libbrecht L, Chu IS, Kaposi-Novak P, Calvisi DF, Mikaelyan A, Roberts LR, Demetris AJ, Sun Z, Nevens F, Roskams T, Thorgeirsson SS. (2006) A novel prognostic subtype of human hepatocellular carcinoma derived from hepatic progenitor cells. Nat Med, 12: 410-416.

[37] Hoshida Y, Nijman SM, Kobayashi M, Chan JA, Brunet JP, Chiang DY, Villanueva A, Newell P, Ikeda K, Hashimoto M, Watanabe G, Gabriel S, Friedman SL, Kumada H, Llovet JM, Golub TR. (2009) Integrative transcriptome analysis reveals common molecular subclasses of human hepatocellular carcinoma. Cancer Res, 69: 7385-7392.

[38] Zucman-Rossi J, Villanueva A, Nault JC, Llovet JM. (2015) Genetic Landscape and Biomarkers of Hepatocellular Carcinoma. Gastroenterology, 149: 1226-1239 e1224.

[39] Houten L, Reilley AA. (1980) An investigation of the cause of death from cancer. J Surg Oncol, 13: 111-116.

[40] Kadry Z, Malekkiani N, Clavien PA. (2001) Treatment of primary and secondary liver malignancy. Swiss Med Wkly, 131: 338-345.

[41] Ananthakrishnan A, Gogineni V, Saeian K. (2006) Epidemiology of primary and secondary liver cancers. Semin Intervent Radiol, 23: 47-63.

[42] Disibio G, French SW. (2008) Metastatic patterns of cancers: results from a large autopsy study. Arch Pathol Lab Med, 132: 931-939.

[43] Dennis JL, Hvidsten TR, Wit EC, Komorowski J, Bell AK, Downie I, Mooney J, Verbeke C, Bellamy C, Keith WN, Oien KA. (2005) Markers of adenocarcinoma characteristic of the site of origin: development of a diagnostic algorithm. Clin Cancer Res, 11: 3766-3772.

[44] Centeno BA. (2006) Pathology of liver metastases. Cancer Control, 13: 13-26.

[45] Hanahan D, Weinberg RA. (2000) The hallmarks of cancer. Cell, 100: 57-70.

[46] Chambers AF, Groom AC, MacDonald IC. (2002) Dissemination and growth of cancer cells in metastatic sites. Nat Rev Cancer, 2: 563-572.

[47] Nguyen DX, Bos PD, Massague J. (2009) Metastasis: from dissemination to organ-specific colonization. Nat Rev Cancer, 9: 274-284.

[48] Braet F, Nagatsuma K, Saito M, Soon L, Wisse E, Matsuura T. (2007) The hepatic sinusoidal endothelial lining and colorectal liver metastases. World J Gastroenterol, 13: 821-825.

[49] Kan Z, Ivancev K, Lunderquist A, McCuskey PA, McCuskey RS, Wallace S. (1995) In vivo microscopy of hepatic metastases: dynamic observation of tumor cell invasion and interaction with Kupffer cells. Hepatology, 21: 487-494.

[50] Wisse E, van't Noordende JM, van der Meulen J, Daems WT. (1976) The pit cell: description of a new type of cell occurring in rat liver sinusoids and peripheral blood. Cell Tissue Res, 173: 423-435.

[51] Peng H, Wisse E, Tian Z. (2016) Liver natural killer cells: subsets and roles in liver immunity. Cell Mol Immunol, 13: 328-336.

[52] Van den Eynden GG, Majeed AW, Illemann M, Vermeulen PB, Bird NC, Hoyer-Hansen G, Eefsen RL, Reynolds AR, Brodt P. (2013) The multifaceted role of the microenvironment in liver metastasis: biology and clinical implications. Cancer Res, 73: 2031-2043.

[53] Lunevicius R, Nakanishi H, Ito S, Kozaki K, Kato T, Tatematsu M, Yasui K. (2001) Clinicopathological significance of fibrotic capsule formation around liver metastasis from colorectal cancer. J Cancer Res Clin Oncol, 127: 193-199.

[54] Arnold M, Sierra MS, Laversanne M, Soerjomataram I, Jemal A, Bray F. (2017) Global patterns and trends in colorectal cancer incidence and mortality. Gut, 66: 683-691.

[55] Kasler M, Otto S, Kenessey I. (2017) [The current situation of cancer morbidity and mortality in the light of the National Cancer Registry]. Orv Hetil, 158: 84-89.

[56] Manfredi S, Lepage C, Hatem C, Coatmeur O, Faivre J, Bouvier AM. (2006) Epidemiology and management of liver metastases from colorectal cancer. Ann Surg, 244: 254-259.

[57] Adam R, de Gramont A, Figueras J, Kokudo N, Kunstlinger F, Loyer E, Poston G, Rougier P, Rubbia-Brandt L, Sobrero A, Teh C, Tejpar S, Van Cutsem E, Vauthey JN, Pahlman L, of the Eg. (2015) Managing synchronous liver metastases from colorectal cancer: a multidisciplinary international consensus. Cancer Treat Rev, 41: 729-741.

[58] Garden OJ, Rees M, Poston GJ, Mirza D, Saunders M, Ledermann J, Primrose JN, Parks RW. (2006) Guidelines for resection of colorectal cancer liver metastases. Gut, 55 Suppl 3: iii1-8.

[59] Taylor I. (1996) Liver metastases from colorectal cancer: lessons from past and present clinical studies. Br J Surg, 83: 456-460.

[60] Fleming M, Ravula S, Tatishchev SF, Wang HL. (2012) Colorectal carcinoma: Pathologic aspects. J Gastrointest Oncol, 3: 153-173.

[61] Hugen N, van de Velde CJ, de Wilt JH, Nagtegaal ID. (2014) Metastatic pattern in colorectal cancer is strongly influenced by histological subtype. Ann Oncol, 25: 651-657.

[62] Razenberg LG, van Gestel YR, Lemmens VE, de Wilt JH, Creemers GJ, de Hingh IH. (2015) The Prognostic Relevance of Histological Subtype in Patients With Peritoneal Metastases From Colorectal Cancer: A Nationwide Population-Based Study. Clin Colorectal Cancer, 14: e13-19.

[63] Ducreux M, Cuhna AS, Caramella C, Hollebecque A, Burtin P, Goere D, Seufferlein T, Haustermans K, Van Laethem JL, Conroy T, Arnold D, Committee EG. (2015) Cancer of the pancreas: ESMO Clinical Practice Guidelines for diagnosis, treatment and follow-up. Ann Oncol, 26 Suppl 5: v56-68.

[64] Becker AE, Hernandez YG, Frucht H, Lucas AL. (2014) Pancreatic ductal adenocarcinoma: risk factors, screening, and early detection. World J Gastroenterol, 20: 11182-11198.

[65] Mao C, Domenico DR, Kim K, Hanson DJ, Howard JM. (1995) Observations on the developmental patterns and the consequences of pancreatic exocrine adenocarcinoma. Findings of 154 autopsies. Arch Surg, 130: 125-134.

[66] Whatcott CJ, Diep CH, Jiang P, Watanabe A, LoBello J, Sima C, Hostetter G, Shepard HM, Von Hoff DD, Han H. (2015) Desmoplasia in Primary Tumors and Metastatic Lesions of Pancreatic Cancer. Clin Cancer Res, 21: 3561-3568.

[67] Varadhachary GR, Abbruzzese JL, Lenzi R. (2004) Diagnostic strategies for unknown primary cancer. Cancer, 100: 1776-1785.

[68] Wennerberg AE, Nalesnik MA, Coleman WB. (1993) Hepatocyte paraffin 1: a monoclonal antibody that reacts with hepatocytes and can be used for differential diagnosis of hepatic tumors. Am J Pathol, 143: 1050-1054.

[69] Lau SK, Prakash S, Geller SA, Alsabeh R. (2002) Comparative immunohistochemical profile of hepatocellular carcinoma, cholangiocarcinoma, and metastatic adenocarcinoma. Hum Pathol, 33: 1175-1181.

[70] Karabork A, Kaygusuz G, Ekinci C. (2010) The best immunohistochemical panel for differentiating hepatocellular carcinoma from metastatic adenocarcinoma. Pathol Res Pract, 206: 572-577.

[71] Baumhoer D, Tornillo L, Stadlmann S, Roncalli M, Diamantis EK, Terracciano LM. (2008) Glypican 3 expression in human nonneoplastic, preneoplastic, and neoplastic tissues: a tissue microarray analysis of 4,387 tissue samples. Am J Clin Pathol, 129: 899-906.

[72] Gokden M, Shinde A. (2005) Recent immunohistochemical markers in the differential diagnosis of primary and metastatic carcinomas of the liver. Diagn Cytopathol, 33: 166-172.

[73] Porcell AI, De Young BR, Proca DM, Frankel WL. (2000) Immunohistochemical analysis of hepatocellular and adenocarcinoma in the liver: MOC31 compares favorably with other putative markers. Mod Pathol, 13: 773-778.

[74] Borscheri N, Roessner A, Rocken C. (2001) Canalicular immunostaining of neprilysin (CD10) as a diagnostic marker for hepatocellular carcinomas. Am J Surg Pathol, 25: 1297-1303.

[75] Wang L, Vuolo M, Suhrland MJ, Schlesinger K. (2006) HepPar1, MOC-31, pCEA, mCEA and CD10 for distinguishing hepatocellular carcinoma vs. metastatic adenocarcinoma in liver fine needle aspirates. Acta Cytol, 50: 257-262.

[76] Lapidot T, Sirard C, Vormoor J, Murdoch B, Hoang T, Caceres-Cortes J, Minden M, Paterson B, Caligiuri MA, Dick JE. (1994) A cell initiating human acute myeloid leukaemia after transplantation into SCID mice. Nature, 367: 645-648.

[77] Bonnet D, Dick JE. (1997) Human acute myeloid leukemia is organized as a hierarchy that originates from a primitive hematopoietic cell. Nat Med, 3: 730-737.

[78] Al-Hajj M, Wicha MS, Benito-Hernandez A, Morrison SJ, Clarke MF. (2003) Prospective identification of tumorigenic breast cancer cells. Proc Natl Acad Sci U S A, 100: 3983-3988.

[79] Singh SK, Clarke ID, Terasaki M, Bonn VE, Hawkins C, Squire J, Dirks PB. (2003) Identification of a cancer stem cell in human brain tumors. Cancer Res, 63: 5821-5828.

[80] Chiba T, Kita K, Zheng YW, Yokosuka O, Saisho H, Iwama A, Nakauchi H, Taniguchi H. (2006) Side population purified from hepatocellular carcinoma cells harbors cancer stem cell-like properties. Hepatology, 44: 240-251.

[81] Li C, Heidt DG, Dalerba P, Burant CF, Zhang L, Adsay V, Wicha M, Clarke MF, Simeone DM. (2007) Identification of pancreatic cancer stem cells. Cancer Res, 67: 1030-1037.

[82] Hermann PC, Huber SL, Herrler T, Aicher A, Ellwart JW, Guba M, Bruns CJ, Heeschen C. (2007) Distinct populations of cancer stem cells determine tumor growth and metastatic activity in human pancreatic cancer. Cell Stem Cell, 1: 313-323.

[83] Ma S, Chan KW, Hu L, Lee TK, Wo JY, Ng IO, Zheng BJ, Guan XY. (2007) Identification and characterization of tumorigenic liver cancer stem/progenitor cells. Gastroenterology, 132: 2542-2556.

[84] O'Brien CA, Pollett A, Gallinger S, Dick JE. (2007) A human colon cancer cell capable of initiating tumour growth in immunodeficient mice. Nature, 445: 106-110.

[85] Zhang S, Balch C, Chan MW, Lai HC, Matei D, Schilder JM, Yan PS, Huang TH, Nephew KP. (2008) Identification and characterization of ovarian cancer-initiating cells from primary human tumors. Cancer Res, 68: 4311-4320.

[86] Sugihara E, Saya H. (2013) Complexity of cancer stem cells. Int J Cancer, 132: 1249-1259.

[87] Reya T, Morrison SJ, Clarke MF, Weissman IL. (2001) Stem cells, cancer, and cancer stem cells. Nature, 414: 105-111.

[88] Clarke MF, Dick JE, Dirks PB, Eaves CJ, Jamieson CH, Jones DL, Visvader J, Weissman IL, Wahl GM. (2006) Cancer stem cells--perspectives on current status and future directions: AACR Workshop on cancer stem cells. Cancer Res, 66: 9339-9344.

[89] Gupta PB, Chaffer CL, Weinberg RA. (2009) Cancer stem cells: mirage or reality? Nat Med, 15: 1010-1012.

[90] Shackleton M, Quintana E, Fearon ER, Morrison SJ. (2009) Heterogeneity in cancer: cancer stem cells versus clonal evolution. Cell, 138: 822-829.

[91] Kang Y, Massague J. (2004) Epithelial-mesenchymal transitions: twist in development and metastasis. Cell, 118: 277-279.

[92] Mani SA, Guo W, Liao MJ, Eaton EN, Ayyanan A, Zhou AY, Brooks M, Reinhard F, Zhang CC, Shipitsin M, Campbell LL, Polyak K, Brisken C, Yang J,

Weinberg RA. (2008) The epithelial-mesenchymal transition generates cells with properties of stem cells. Cell, 133: 704-715.

[93] Diehn M, Cho RW, Lobo NA, Kalisky T, Dorie MJ, Kulp AN, Qian D, Lam JS, Ailles LE, Wong M, Joshua B, Kaplan MJ, Wapnir I, Dirbas FM, Somlo G, Garberoglio C, Paz B, Shen J, Lau SK, Quake SR, Brown JM, Weissman IL, Clarke MF. (2009) Association of reactive oxygen species levels and radioresistance in cancer stem cells. Nature, 458: 780-783.

[94] Seguin L, Kato S, Franovic A, Camargo MF, Lesperance J, Elliott KC, Yebra M, Mielgo A, Lowy AM, Husain H, Cascone T, Diao L, Wang J, Wistuba, II, Heymach JV, Lippman SM, Desgrosellier JS, Anand S, Weis SM, Cheresh DA. (2014) An integrin beta(3)-KRAS-RalB complex drives tumour stemness and resistance to EGFR inhibition. Nat Cell Biol, 16: 457-468.

[95] Kim WT, Ryu CJ. (2017) Cancer stem cell surface markers on normal stem cells. BMB Rep, 50: 285-298.

[96] Grosse-Gehling P, Fargeas CA, Dittfeld C, Garbe Y, Alison MR, Corbeil D, Kunz-Schughart LA. (2013) CD133 as a biomarker for putative cancer stem cells in solid tumours: limitations, problems and challenges. J Pathol, 229: 355-378.

[97] Giepmans BN, van Ijzendoorn SC. (2009) Epithelial cell-cell junctions and plasma membrane domains. Biochim Biophys Acta, 1788: 820-831.

[98] Gonzalez-Mariscal L, Betanzos A, Nava P, Jaramillo BE. (2003) Tight junction proteins. Prog Biophys Mol Biol, 81: 1-44.

[99] Zihni C, Mills C, Matter K, Balda MS. (2016) Tight junctions: from simple barriers to multifunctional molecular gates. Nat Rev Mol Cell Biol, 17: 564-580.

[100] Chiba H, Osanai M, Murata M, Kojima T, Sawada N. (2008) Transmembrane proteins of tight junctions. Biochim Biophys Acta, 1778: 588-600.

[101] Furuse M, Hirase T, Itoh M, Nagafuchi A, Yonemura S, Tsukita S, Tsukita S. (1993) Occludin: a novel integral membrane protein localizing at tight junctions. J Cell Biol, 123: 1777-1788.

[102] Furuse M, Fujita K, Hiiragi T, Fujimoto K, Tsukita S. (1998) Claudin-1 and -2: novel integral membrane proteins localizing at tight junctions with no sequence similarity to occludin. J Cell Biol, 141: 1539-1550.

[103] Steed E, Balda MS, Matter K. (2010) Dynamics and functions of tight junctions. Trends Cell Biol, 20: 142-149.

[104] Forster C. (2008) Tight junctions and the modulation of barrier function in disease. Histochem Cell Biol, 130: 55-70.

[105] Guttman JA, Finlay BB. (2009) Tight junctions as targets of infectious agents. Biochim Biophys Acta, 1788: 832-841.

[106] Saitou M, Furuse M, Sasaki H, Schulzke JD, Fromm M, Takano H, Noda T, Tsukita S. (2000) Complex phenotype of mice lacking occludin, a component of tight junction strands. Mol Biol Cell, 11: 4131-4142.

[107] Lal-Nag M, Morin PJ. (2009) The claudins. Genome Biol, 10: 235.

[108] Krause G, Winkler L, Mueller SL, Haseloff RF, Piontek J, Blasig IE. (2008) Structure and function of claudins. Biochim Biophys Acta, 1778: 631-645.

[109] Colegio OR, Van Itallie CM, McCrea HJ, Rahner C, Anderson JM. (2002) Claudins create charge-selective channels in the paracellular pathway between epithelial cells. Am J Physiol Cell Physiol, 283: C142-147.

[110] Wen H, Watry DD, Marcondes MC, Fox HS. (2004) Selective decrease in paracellular conductance of tight junctions: role of the first extracellular domain of claudin-5. Mol Cell Biol, 24: 8408-8417.

[111] Suzuki H, Nishizawa T, Tani K, Yamazaki Y, Tamura A, Ishitani R, Dohmae N, Tsukita S, Nureki O, Fujiyoshi Y. (2014) Crystal structure of a claudin provides insight into the architecture of tight junctions. Science, 344: 304-307.

[112] Piontek J, Winkler L, Wolburg H, Muller SL, Zuleger N, Piehl C, Wiesner B, Krause G, Blasig IE. (2008) Formation of tight junction: determinants of homophilic interaction between classic claudins. FASEB J, 22: 146-158.

[113] Katahira J, Inoue N, Horiguchi Y, Matsuda M, Sugimoto N. (1997) Molecular cloning and functional characterization of the receptor for Clostridium perfringens enterotoxin. J Cell Biol, 136: 1239-1247.

[114] Itoh M, Furuse M, Morita K, Kubota K, Saitou M, Tsukita S. (1999) Direct binding of three tight junction-associated MAGUKs, ZO-1, ZO-2, and ZO-3, with the COOH termini of claudins. J Cell Biol, 147: 1351-1363.

[115] Hamazaki Y, Itoh M, Sasaki H, Furuse M, Tsukita S. (2002) Multi-PDZ domain protein 1 (MUPP1) is concentrated at tight junctions through its possible interaction with claudin-1 and junctional adhesion molecule. J Biol Chem, 277: 455-461.

[116] Gonzalez-Mariscal L, Tapia R, Chamorro D. (2008) Crosstalk of tight junction components with signaling pathways. Biochim Biophys Acta, 1778: 729-756.

[117] D'Souza T, Agarwal R, Morin PJ. (2005) Phosphorylation of claudin-3 at threonine 192 by cAMP-dependent protein kinase regulates tight junction barrier function in ovarian cancer cells. J Biol Chem, 280: 26233-26240.

[118] D'Souza T, Indig FE, Morin PJ. (2007) Phosphorylation of claudin-4 by PKCepsilon regulates tight junction barrier function in ovarian cancer cells. Exp Cell Res, 313: 3364-3375.

[119] Tsukita S, Furuse M, Itoh M. (2001) Multifunctional strands in tight junctions. Nat Rev Mol Cell Biol, 2: 285-293.

[120] Daugherty BL, Ward C, Smith T, Ritzenthaler JD, Koval M. (2007) Regulation of heterotypic claudin compatibility. J Biol Chem, 282: 30005-30013.

[121] Gunzel D, Yu AS. (2013) Claudins and the modulation of tight junction permeability. Physiol Rev, 93: 525-569.

[122] Van Itallie CM, Anderson JM. (2006) Claudins and epithelial paracellular transport. Annu Rev Physiol, 68: 403-429.

[123] Piontek A, Rossa J, Protze J, Wolburg H, Hempel C, Gunzel D, Krause G, Piontek J. (2017) Polar and charged extracellular residues conserved among barrier-forming claudins contribute to tight junction strand formation. Ann N Y Acad Sci, 1397: 143-156.

[124] Osanai M, Takasawa A, Murata M, Sawada N. (2017) Claudins in cancer: bench to bedside. Pflugers Arch, 469: 55-67.

[125] Hintsala HR, Siponen M, Haapasaari KM, Karihtala P, Soini Y. (2013) Claudins 1, 2, 3, 4, 5 and 7 in solar keratosis and squamocellular carcinoma of the skin. Int J Clin Exp Pathol, 6: 2855-2863.

[126] Leotlela PD, Wade MS, Duray PH, Rhode MJ, Brown HF, Rosenthal DT, Dissanayake SK, Earley R, Indig FE, Nickoloff BJ, Taub DD, Kallioniemi OP, Meltzer P, Morin PJ, Weeraratna AT. (2007) Claudin-1 overexpression in melanoma is regulated by PKC and contributes to melanoma cell motility. Oncogene, 26: 3846-3856.

[127] Nemeth J, Nemeth Z, Tatrai P, Peter I, Somoracz A, Szasz AM, Kiss A, Schaff Z. (2010) High expression of claudin-1 protein in papillary thyroid tumor and its regional lymph node metastasis. Pathol Oncol Res, 16: 19-27.

[128] Moldvay J, Jackel M, Paska C, Soltesz I, Schaff Z, Kiss A. (2007) Distinct claudin expression profile in histologic subtypes of lung cancer. Lung Cancer, 57: 159-167.

[129] Sung CO, Han SY, Kim SH. (2011) Low expression of claudin-4 is associated with poor prognosis in esophageal squamous cell carcinoma. Ann Surg Oncol, 18: 273-281.

[130] Gyorffy H, Holczbauer A, Nagy P, Szabo Z, Kupcsulik P, Paska C, Papp J, Schaff Z, Kiss A. (2005) Claudin expression in Barrett's esophagus and adenocarcinoma. Virchows Arch, 447: 961-968.

[131] Patonai A, Erdelyi-Belle B, Korompay A, Somoracz A, Straub BK, Schirmacher P, Kovalszky I, Lotz G, Kiss A, Schaff Z. (2011) Claudins and tricellulin in fibrolamellar hepatocellular carcinoma. Virchows Arch, 458: 679-688.

[132] Nemeth Z, Szasz AM, Tatrai P, Nemeth J, Gyorffy H, Somoracz A, Szijarto A, Kupcsulik P, Kiss A, Schaff Z. (2009) Claudin-1, -2, -3, -4, -7, -8, and -10 protein expression in biliary tract cancers. J Histochem Cytochem, 57: 113-121.

[133] Borka K, Kaliszky P, Szabo E, Lotz G, Kupcsulik P, Schaff Z, Kiss A. (2007) Claudin expression in pancreatic endocrine tumors as compared with ductal adenocarcinomas. Virchows Arch, 450: 549-557.

[134] Naldini L, Blomer U, Gallay P, Ory D, Mulligan R, Gage FH, Verma IM, Trono D. (1996) In vivo gene delivery and stable transduction of nondividing cells by a lentiviral vector. Science, 272: 263-267.

[135] Willumsen BM, Vass WC, Velu TJ, Papageorge AG, Schiller JT, Lowy DR. (1991) The bovine papillomavirus E5 oncogene can cooperate with ras: identification of p21 amino acids critical for transformation by c-rasH but not v-rasH. Mol Cell Biol, 11: 6026-6033.

[136] Pelletier J, Sonenberg N. (1988) Internal initiation of translation of eukaryotic mRNA directed by a sequence derived from poliovirus RNA. Nature, 334: 320-325.

[137] Day CP, Carter J, Bonomi C, Esposito D, Crise B, Ortiz-Conde B, Hollingshead M, Merlino G. (2009) Lentivirus-mediated bifunctional cell labeling for in vivo melanoma study. Pigment Cell Melanoma Res, 22: 283-295.

[138] Ventura A, Meissner A, Dillon CP, McManus M, Sharp PA, Van Parijs L, Jaenisch R, Jacks T. (2004) Cre-lox-regulated conditional RNA interference from transgenes. Proc Natl Acad Sci U S A, 101: 10380-10385.

[139] Oren M, Maltzman W, Levine AJ. (1981) Post-translational regulation of the 54K cellular tumor antigen in normal and transformed cells. Mol Cell Biol, 1: 101-110.

[140] DeCaprio JA, Ludlow JW, Figge J, Shew JY, Huang CM, Lee WH, Marsilio E, Paucha E, Livingston DM. (1988) SV40 large tumor antigen forms a specific complex with the product of the retinoblastoma susceptibility gene. Cell, 54: 275-283.

[141] Ahuja D, Saenz-Robles MT, Pipas JM. (2005) SV40 large T antigen targets multiple cellular pathways to elicit cellular transformation. Oncogene, 24: 7729-7745.

[142] Dull T, Zufferey R, Kelly M, Mandel RJ, Nguyen M, Trono D, Naldini L. (1998) A third-generation lentivirus vector with a conditional packaging system. J Virol, 72: 8463-8471.

[143] Zufferey R, Dull T, Mandel RJ, Bukovsky A, Quiroz D, Naldini L, Trono D. (1998) Self-inactivating lentivirus vector for safe and efficient in vivo gene delivery. J Virol, 72: 9873-9880.

[144] Zennou V, Petit C, Guetard D, Nerhbass U, Montagnier L, Charneau P. (2000) HIV-1 genome nuclear import is mediated by a central DNA flap. Cell, 101: 173-185.

[145] Zhao JJ, Gjoerup OV, Subramanian RR, Cheng Y, Chen W, Roberts TM, Hahn WC. (2003) Human mammary epithelial cell transformation through the activation of phosphatidylinositol 3-kinase. Cancer Cell, 3: 483-495.

[146] David CJ, Chen M, Assanah M, Canoll P, Manley JL. (2010) HnRNP proteins controlled by c-Myc deregulate pyruvate kinase mRNA splicing in cancer. Nature, 463: 364-368.

[147] Stewart SA, Dykxhoorn DM, Palliser D, Mizuno H, Yu EY, An DS, Sabatini DM, Chen IS, Hahn WC, Sharp PA, Weinberg RA, Novina CD. (2003) Lentivirus-delivered stable gene silencing by RNAi in primary cells. RNA, 9: 493-501.

[148] Shaw A, Cornetta K. (2014) Design and potential of non-integrating lentiviral vectors. Biomedicines, 2: 14-35.

[149] Salmon P, Trono D. (2007) Production and titration of lentiviral vectors. Curr Protoc Hum Genet, Chapter 12: Unit 12 10.

[150] Preisegger KH, Factor VM, Fuchsbichler A, Stumptner C, Denk H, Thorgeirsson SS. (1999) Atypical ductular proliferation and its inhibition by transforming growth factor beta1 in the 3,5-diethoxycarbonyl-1,4-dihydrocollidine mouse model for chronic alcoholic liver disease. Lab Invest, 79: 103-109.

[151] Seglen PO. (1976) Preparation of isolated rat liver cells. Methods Cell Biol, 13: 29-83.

[152] Okabe M, Tsukahara Y, Tanaka M, Suzuki K, Saito S, Kamiya Y, Tsujimura T, Nakamura K, Miyajima A. (2009) Potential hepatic stem cells reside in EpCAM+ cells of normal and injured mouse liver. Development, 136: 1951-1960.

[153] Ishikawa T, Factor VM, Marquardt JU, Raggi C, Seo D, Kitade M, Conner EA, Thorgeirsson SS. (2012) Hepatocyte growth factor/c-met signaling is required for stem-cell-mediated liver regeneration in mice. Hepatology, 55: 1215-1226.

[154] Engelhardt NV, Factor VM, Yasova AK, Poltoranina VS, Baranov VN, Lasareva MN. (1990) Common antigens of mouse oval and biliary epithelial cells. Expression on newly formed hepatocytes. Differentiation, 45: 29-37.

[155] Nitou M, Sugiyama Y, Ishikawa K, Shiojiri N. (2002) Purification of fetal mouse hepatoblasts by magnetic beads coated with monoclonal anti-e-cadherin antibodies and their in vitro culture. Exp Cell Res, 279: 330-343.

[156] Lee SB, Seo D, Choi D, Park KY, Holczbauer A, Marquardt JU, Conner EA, Factor VM, Thorgeirsson SS. (2012) Contribution of hepatic lineage stage-specific donor memory to the differential potential of induced mouse pluripotent stem cells. Stem Cells, 30: 997-1007.

[157] Kaufman MH: The Atlas of Mouse Development: Academic Press, 1992.

[158] Kao CY, Factor VM, Thorgeirsson SS. (1996) Reduced growth capacity of hepatocytes from c-myc and c-myc/TGF-alpha transgenic mice in primary culture. Biochem Biophys Res Commun, 222: 64-70.

[159] Akagi K, Sandig V, Vooijs M, Van der Valk M, Giovannini M, Strauss M, Berns A. (1997) Cre-mediated somatic site-specific recombination in mice. Nucleic Acids Res, 25: 1766-1773.

[160] Block GD, Locker J, Bowen WC, Petersen BE, Katyal S, Strom SC, Riley T, Howard TA, Michalopoulos GK. (1996) Population expansion, clonal growth, and specific differentiation patterns in primary cultures of hepatocytes induced by HGF/SF, EGF and TGF alpha in a chemically defined (HGM) medium. J Cell Biol, 132: 1133-1149.

[161] Golebiewska A, Brons NH, Bjerkvig R, Niclou SP. (2011) Critical appraisal of the side population assay in stem cell and cancer stem cell research. Cell Stem Cell, 8: 136-147.

[162] Marquardt JU, Raggi C, Andersen JB, Seo D, Avital I, Geller D, Lee YH, Kitade M, Holczbauer A, Gillen MC, Conner EA, Factor VM, Thorgeirsson SS. (2011) Human hepatic cancer stem cells are characterized by common stemness traits and diverse oncogenic pathways. Hepatology, 54: 1031-1042.

[163] Soini Y. (2005) Expression of claudins 1, 2, 3, 4, 5 and 7 in various types of tumours. Histopathology, 46: 551-560.

[164] Laurila JJ, Karttunen T, Koivukangas V, Laurila PA, Syrjala H, Saarnio J, Soini Y, Ala-Kokko TI. (2007) Tight junction proteins in gallbladder epithelium: different expression in acute acalculous and calculous cholecystitis. J Histochem Cytochem, 55: 567-573.

[165] Torzsok P, Riesz P, Kenessey I, Szekely E, Somoracz A, Nyirady P, Romics I, Schaff Z, Lotz G, Kiss A. (2011) Claudins and ki-67: potential markers to differentiate low- and high-grade transitional cell carcinomas of the urinary bladder. J Histochem Cytochem, 59: 1022-1030.

[166] Szekely E, Torzsok P, Riesz P, Korompay A, Fintha A, Szekely T, Lotz G, Nyirady P, Romics I, Timar J, Schaff Z, Kiss A. (2011) Expression of claudins and their prognostic significance in noninvasive urothelial neoplasms of the human urinary bladder. J Histochem Cytochem, 59: 932-941.

[167] Koressaar T, Remm M. (2007) Enhancements and modifications of primer design program Primer3. Bioinformatics, 23: 1289-1291.

[168] Wellek S: Testing Stastistical Hypothesis of Equivalence. Boca Raton, FL: Chapman & Hall/crc Press LLC, 2003.

[169] Neuhauser M, Jockel KH. (2006) A bootstrap test for the analysis of microarray experiments with a very small number of replications. Appl Bioinformatics, 5: 173-179.

[170] Wong DJ, Liu H, Ridky TW, Cassarino D, Segal E, Chang HY. (2008) Module map of stem cell genes guides creation of epithelial cancer stem cells. Cell Stem Cell, 2: 333-344.

[171] Subramanian A, Tamayo P, Mootha VK, Mukherjee S, Ebert BL, Gillette MA, Paulovich A, Pomeroy SL, Golub TR, Lander ES, Mesirov JP. (2005) Gene set enrichment analysis: a knowledge-based approach for interpreting genome-wide expression profiles. Proc Natl Acad Sci U S A, 102: 15545-15550.

[172] Alonso SR, Tracey L, Ortiz P, Perez-Gomez B, Palacios J, Pollan M, Linares J, Serrano S, Saez-Castillo AI, Sanchez L, Pajares R, Sanchez-Aguilera A, Artiga MJ, Piris MA, Rodriguez-Peralto JL. (2007) A high-throughput study in melanoma identifies epithelial-mesenchymal transition as a major determinant of metastasis. Cancer Res, 67: 3450-3460.

[173] Ben-Porath I, Thomson MW, Carey VJ, Ge R, Bell GW, Regev A, Weinberg RA. (2008) An embryonic stem cell-like gene expression signature in poorly differentiated aggressive human tumors. Nat Genet, 40: 499-507.

[174] Seok JY, Na DC, Woo HG, Roncalli M, Kwon SM, Yoo JE, Ahn EY, Kim GI, Choi JS, Kim YB, Park YN. (2012) A fibrous stromal component in hepatocellular carcinoma reveals a cholangiocarcinoma-like gene expression trait and epithelial-mesenchymal transition. Hepatology, 55: 1776-1786.

[175] Yaswen P, Goyette M, Shank PR, Fausto N. (1985) Expression of c-Ki-ras, c-Ha-ras, and c-myc in specific cell types during hepatocarcinogenesis. Mol Cell Biol, 5: 780-786.

[176] Calvisi DF, Ladu S, Gorden A, Farina M, Conner EA, Lee JS, Factor VM, Thorgeirsson SS. (2006) Ubiquitous activation of Ras and Jak/Stat pathways in human HCC. Gastroenterology, 130: 1117-1128.

[177] Nault JC, Zucman-Rossi J. (2011) Genetics of hepatobiliary carcinogenesis. Semin Liver Dis, 31: 173-187.

[178] Roskams T. (2006) Liver stem cells and their implication in hepatocellular and cholangiocarcinoma. Oncogene, 25: 3818-3822.

[179] Zaret KS. (2000) Liver specification and early morphogenesis. Mech Dev, 92: 83-88.

[180] Zorn AM: Liver development. StemBook. Cambridge (MA), 2008.

[181] Jones EA, Clement-Jones M, James OF, Wilson DI. (2001) Differences between human and mouse alpha-fetoprotein expression during early development. J Anat, 198: 555-559.

[182] Xin L, Lawson DA, Witte ON. (2005) The Sca-1 cell surface marker enriches for a prostate-regenerating cell subpopulation that can initiate prostate tumorigenesis. Proc Natl Acad Sci U S A, 102: 6942-6947.

[183] Paku S, Schnur J, Nagy P, Thorgeirsson SS. (2001) Origin and structural evolution of the early proliferating oval cells in rat liver. Am J Pathol, 158: 1313-1323.

[184] Lorenzini S, Bird TG, Boulter L, Bellamy C, Samuel K, Aucott R, Clayton E, Andreone P, Bernardi M, Golding M, Alison MR, Iredale JP, Forbes SJ. (2010) Characterisation of a stereotypical cellular and extracellular adult liver progenitor cell niche in rodents and diseased human liver. Gut, 59: 645-654.

[185] Kitade M, Factor VM, Andersen JB, Tomokuni A, Kaji K, Akita H, Holczbauer A, Seo D, Marquardt JU, Conner EA, Lee SB, Lee YH, Thorgeirsson SS. (2013) Specific fate decisions in adult hepatic progenitor cells driven by MET and EGFR signaling. Genes Dev, 27: 1706-1717.

[186] Madisen L, Zwingman TA, Sunkin SM, Oh SW, Zariwala HA, Gu H, Ng LL, Palmiter RD, Hawrylycz MJ, Jones AR, Lein ES, Zeng H. (2010) A robust and high-throughput Cre reporting and characterization system for the whole mouse brain. Nat Neurosci, 13: 133-140.

[187] Gupta S. (2000) Hepatic polyploidy and liver growth control. Semin Cancer Biol, 10: 161-171.

[188] Li J, Ning G, Duncan SA. (2000) Mammalian hepatocyte differentiation requires the transcription factor HNF-4alpha. Genes Dev, 14: 464-474.

[189] Wang L, Xue Y, Shen Y, Li W, Cheng Y, Yan X, Shi W, Wang J, Gong Z, Yang G, Guo C, Zhou Y, Wang X, Zhou Q, Zeng F. (2012) Claudin 6: a novel surface marker for characterizing mouse pluripotent stem cells. Cell Res, 22: 1082-1085.

[190] Kim K, Doi A, Wen B, Ng K, Zhao R, Cahan P, Kim J, Aryee MJ, Ji H, Ehrlich LI, Yabuuchi A, Takeuchi A, Cunniff KC, Hongguang H, McKinney-Freeman S, Naveiras O, Yoon TJ, Irizarry RA, Jung N, Seita J, Hanna J, Murakami P, Jaenisch R, Weissleder R, Orkin SH, Weissman IL, Feinberg AP, Daley GQ. (2010) Epigenetic memory in induced pluripotent stem cells. Nature, 467: 285-290.

[191] Ohi Y, Qin H, Hong C, Blouin L, Polo JM, Guo T, Qi Z, Downey SL, Manos PD, Rossi DJ, Yu J, Hebrok M, Hochedlinger K, Costello JF, Song JS, Ramalho-Santos M. (2011) Incomplete DNA methylation underlies a transcriptional memory of somatic cells in human iPS cells. Nat Cell Biol, 13: 541-549.

[192] Kim J, Woo AJ, Chu J, Snow JW, Fujiwara Y, Kim CG, Cantor AB, Orkin SH. (2010) A Myc network accounts for similarities between embryonic stem and cancer cell transcription programs. Cell, 143: 313-324.

[193] Kaposi-Novak P, Libbrecht L, Woo HG, Lee YH, Sears NC, Coulouarn C, Conner EA, Factor VM, Roskams T, Thorgeirsson SS. (2009) Central role of c-Myc during malignant conversion in human hepatocarcinogenesis. Cancer Res, 69: 2775-2782.

[194] Zender L, Xue W, Cordon-Cardo C, Hannon GJ, Lucito R, Powers S, Flemming P, Spector MS, Lowe SW. (2005) Generation and analysis of genetically defined liver carcinomas derived from bipotential liver progenitors. Cold Spring Harb Symp Quant Biol, 70: 251-261.

[195] Goodell MA, Nguyen H, Shroyer N. (2015) Somatic stem cell heterogeneity: diversity in the blood, skin and intestinal stem cell compartments. Nat Rev Mol Cell Biol, 16: 299-309.

[196] Morrison SJ, Spradling AC. (2008) Stem cells and niches: mechanisms that promote stem cell maintenance throughout life. Cell, 132: 598-611.

[197] Bu Y, Cao D. (2012) The origin of cancer stem cells. Front Biosci (Schol Ed), 4: 819-830.

[198] Lagasse E, Connors H, Al-Dhalimy M, Reitsma M, Dohse M, Osborne L, Wang X, Finegold M, Weissman IL, Grompe M. (2000) Purified hematopoietic stem cells can differentiate into hepatocytes in vivo. Nat Med, 6: 1229-1234.

[199] Krause DS, Theise ND, Collector MI, Henegariu O, Hwang S, Gardner R, Neutzel S, Sharkis SJ. (2001) Multi-organ, multi-lineage engraftment by a single bone marrow-derived stem cell. Cell, 105: 369-377.

[200] Lopez-Lazaro M. (2018) The stem cell division theory of cancer. Crit Rev Oncol Hematol, 123: 95-113.

[201] Yang ZF, Ngai P, Ho DW, Yu WC, Ng MN, Lau CK, Li ML, Tam KH, Lam CT, Poon RT, Fan ST. (2008) Identification of local and circulating cancer stem cells in human liver cancer. Hepatology, 47: 919-928.

[202] Ma S, Chan KW, Lee TK, Tang KH, Wo JY, Zheng BJ, Guan XY. (2008) Aldehyde dehydrogenase discriminates the CD133 liver cancer stem cell populations. Mol Cancer Res, 6: 1146-1153.

[203] Yamashita T, Ji J, Budhu A, Forgues M, Yang W, Wang HY, Jia H, Ye Q, Qin LX, Wauthier E, Reid LM, Minato H, Honda M, Kaneko S, Tang ZY, Wang XW. (2009) EpCAM-positive hepatocellular carcinoma cells are tumor-initiating cells with stem/progenitor cell features. Gastroenterology, 136: 1012-1024.

[204] Haraguchi N, Ishii H, Mimori K, Tanaka F, Ohkuma M, Kim HM, Akita H, Takiuchi D, Hatano H, Nagano H, Barnard GF, Doki Y, Mori M. (2010) CD13 is a therapeutic target in human liver cancer stem cells. J Clin Invest, 120: 3326-3339.

[205] Lee TK, Castilho A, Cheung VC, Tang KH, Ma S, Ng IO. (2011) CD24(+) liver tumor-initiating cells drive self-renewal and tumor initiation through STAT3-mediated NANOG regulation. Cell Stem Cell, 9: 50-63.

[206] Yang W, Wang C, Lin Y, Liu Q, Yu LX, Tang L, Yan HX, Fu J, Chen Y, Zhang HL, Tang L, Zheng LY, He YQ, Li YQ, Wu FQ, Zou SS, Li Z, Wu MC, Feng GS, Wang HY. (2012) OV6(+) tumor-initiating cells contribute to tumor progression and invasion in human hepatocellular carcinoma. J Hepatol, 57: 613-620.

[207] Kordes C, Haussinger D. (2013) Hepatic stem cell niches. J Clin Invest, 123: 1874-1880.

[208] Maximin S, Ganeshan DM, Shanbhogue AK, Dighe MK, Yeh MM, Kolokythas O, Bhargava P, Lalwani N. (2014) Current update on combined hepatocellular-cholangiocarcinoma. Eur J Radiol Open, 1: 40-48.

[209] Yeh MM. (2010) Pathology of combined hepatocellular-cholangiocarcinoma. J Gastroenterol Hepatol, 25: 1485-1492.

[210] Woo HG, Lee JH, Yoon JH, Kim CY, Lee HS, Jang JJ, Yi NJ, Suh KS, Lee KU, Park ES, Thorgeirsson SS, Kim YJ. (2010) Identification of a cholangiocarcinoma-like gene expression trait in hepatocellular carcinoma. Cancer Res, 70: 3034-3041.

[211] Marquardt JU, Andersen JB, Thorgeirsson SS. (2015) Functional and genetic deconstruction of the cellular origin in liver cancer. Nat Rev Cancer, 15: 653-667.

[212] Fausto N, Campbell JS. (2010) Mouse models of hepatocellular carcinoma. Semin Liver Dis, 30: 87-98.

[213] Chen X, Calvisi DF. (2014) Hydrodynamic transfection for generation of novel mouse models for liver cancer research. Am J Pathol, 184: 912-923.

[214] Hytiroglou P. (2004) Morphological changes of early human hepatocarcinogenesis. Semin Liver Dis, 24: 65-75.

[215] Batlle E, Clevers H. (2017) Cancer stem cells revisited. Nat Med, 23: 1124-1134.

[216] Barker N, van Es JH, Kuipers J, Kujala P, van den Born M, Cozijnsen M, Haegebarth A, Korving J, Begthel H, Peters PJ, Clevers H. (2007) Identification of stem cells in small intestine and colon by marker gene Lgr5. Nature, 449: 1003-1007.

[217] Barker N, Huch M, Kujala P, van de Wetering M, Snippert HJ, van Es JH, Sato T, Stange DE, Begthel H, van den Born M, Danenberg E, van den Brink S, Korving J, Abo A, Peters PJ, Wright N, Poulsom R, Clevers H. (2010) Lgr5(+ve) stem cells drive self-renewal in the stomach and build long-lived gastric units in vitro. Cell Stem Cell, 6: 25-36.

[218] van Es JH, Sato T, van de Wetering M, Lyubimova A, Yee Nee AN, Gregorieff A, Sasaki N, Zeinstra L, van den Born M, Korving J, Martens ACM, Barker N, van Oudenaarden A, Clevers H. (2012) Dll1+ secretory progenitor cells revert to stem cells upon crypt damage. Nat Cell Biol, 14: 1099-1104.

[219] Tetteh PW, Basak O, Farin HF, Wiebrands K, Kretzschmar K, Begthel H, van den Born M, Korving J, de Sauvage F, van Es JH, van Oudenaarden A, Clevers H. (2016) Replacement of Lost Lgr5-Positive Stem Cells through Plasticity of Their Enterocyte-Lineage Daughters. Cell Stem Cell, 18: 203-213.

[220] Tata PR, Mou H, Pardo-Saganta A, Zhao R, Prabhu M, Law BM, Vinarsky V, Cho JL, Breton S, Sahay A, Medoff BD, Rajagopal J. (2013) Dedifferentiation of committed epithelial cells into stem cells in vivo. Nature, 503: 218-223.

[221] Stanger BZ. (2015) Cellular homeostasis and repair in the mammalian liver. Annu Rev Physiol, 77: 179-200.

[222] Polyak K, Weinberg RA. (2009) Transitions between epithelial and mesenchymal states: acquisition of malignant and stem cell traits. Nat Rev Cancer, 9: 265-273.

[223] Kalluri R, Weinberg RA. (2009) The basics of epithelial-mesenchymal transition. J Clin Invest, 119: 1420-1428.

[224] Rhim AD, Mirek ET, Aiello NM, Maitra A, Bailey JM, McAllister F, Reichert M, Beatty GL, Rustgi AK, Vonderheide RH, Leach SD, Stanger BZ. (2012) EMT and dissemination precede pancreatic tumor formation. Cell, 148: 349-361.

[225] Liu S, Cong Y, Wang D, Sun Y, Deng L, Liu Y, Martin-Trevino R, Shang L, McDermott SP, Landis MD, Hong S, Adams A, D'Angelo R, Ginestier C, Charafe-Jauffret E, Clouthier SG, Birnbaum D, Wong ST, Zhan M, Chang JC, Wicha MS. (2014) Breast cancer stem cells transition between epithelial and mesenchymal states reflective of their normal counterparts. Stem Cell Reports, 2: 78-91.

[226] Scaffidi P, Misteli T. (2011) In vitro generation of human cells with cancer stem cell properties. Nat Cell Biol, 13: 1051-1061.

[227] Chaffer CL, Brueckmann I, Scheel C, Kaestli AJ, Wiggins PA, Rodrigues LO, Brooks M, Reinhardt F, Su Y, Polyak K, Arendt LM, Kuperwasser C, Bierie B, Weinberg RA. (2011) Normal and neoplastic nonstem cells can spontaneously convert to a stem-like state. Proc Natl Acad Sci U S A, 108: 7950-7955.

[228] Gupta PB, Fillmore CM, Jiang G, Shapira SD, Tao K, Kuperwasser C, Lander ES. (2011) Stochastic state transitions give rise to phenotypic equilibrium in populations of cancer cells. Cell, 146: 633-644.

[229] de Sousa e Melo F, Kurtova AV, Harnoss JM, Kljavin N, Hoeck JD, Hung J, Anderson JE, Storm EE, Modrusan Z, Koeppen H, Dijkgraaf GJ, Piskol R, de Sauvage FJ. (2017) A distinct role for Lgr5(+) stem cells in primary and metastatic colon cancer. Nature, 543: 676-680.

[230] Banales JM, Cardinale V, Carpino G, Marzioni M, Andersen JB, Invernizzi P, Lind GE, Folseraas T, Forbes SJ, Fouassier L, Geier A, Calvisi DF, Mertens JC, Trauner M, Benedetti A, Maroni L, Vaquero J, Macias RI, Raggi C, Perugorria MJ, Gaudio E, Boberg KM, Marin JJ, Alvaro D. (2016) Expert consensus document: Cholangiocarcinoma: current knowledge and future perspectives consensus statement from the European Network for the Study of Cholangiocarcinoma (ENS-CCA). Nat Rev Gastroenterol Hepatol, 13: 261-280.

[231] Park SC, Nguyen NT, Eun JR, Zhang Y, Jung YJ, Tschudy-Seney B, Trotsyuk A, Lam A, Ramsamooj R, Zhang Y, Theise ND, Zern MA, Duan Y. (2015) Identification of cancer stem cell subpopulations of CD34(+) PLC/PRF/5 that result in three types of human liver carcinomas. Stem Cells Dev, 24: 1008-1021.

[232] Michalopoulos GK, Barua L, Bowen WC. (2005) Transdifferentiation of rat hepatocytes into biliary cells after bile duct ligation and toxic biliary injury. Hepatology, 41: 535-544.

[233] Malato Y, Naqvi S, Schurmann N, Ng R, Wang B, Zape J, Kay MA, Grimm D, Willenbring H. (2011) Fate tracing of mature hepatocytes in mouse liver homeostasis and regeneration. J Clin Invest, 121: 4850-4860.

[234] Yanger K, Zong Y, Maggs LR, Shapira SN, Maddipati R, Aiello NM, Thung SN, Wells RG, Greenbaum LE, Stanger BZ. (2013) Robust cellular reprogramming occurs spontaneously during liver regeneration. Genes Dev, 27: 719-724.

[235] Lemaigre FP. (2014) Hepatocytes as a source of cholangiocytes in injured liver. Hepatology, 59: 726-728.

[236] Sekiya S, Suzuki A. (2014) Hepatocytes, rather than cholangiocytes, can be the major source of primitive ductules in the chronically injured mouse liver. Am J Pathol, 184: 1468-1478.

[237] Sekiya S, Suzuki A. (2012) Intrahepatic cholangiocarcinoma can arise from Notch-mediated conversion of hepatocytes. J Clin Invest, 122: 3914-3918.

[238] Fan B, Malato Y, Calvisi DF, Naqvi S, Razumilava N, Ribback S, Gores GJ, Dombrowski F, Evert M, Chen X, Willenbring H. (2012) Cholangiocarcinomas can originate from hepatocytes in mice. J Clin Invest, 122: 2911-2915.

[239] Zender S, Nickeleit I, Wuestefeld T, Sorensen I, Dauch D, Bozko P, El-Khatib M, Geffers R, Bektas H, Manns MP, Gossler A, Wilkens L, Plentz R, Zender L, Malek NP. (2013) A critical role for notch signaling in the formation of cholangiocellular carcinomas. Cancer Cell, 23: 784-795.

[240] Edme N, Downward J, Thiery JP, Boyer B. (2002) Ras induces NBT-II epithelial cell scattering through the coordinate activities of Rac and MAPK pathways. J Cell Sci, 115: 2591-2601.

[241] Kastenhuber ER, Lowe SW. (2017) Putting p53 in Context. Cell, 170: 1062-1078.

[242] Katz SF, Lechel A, Obenauf AC, Begus-Nahrmann Y, Kraus JM, Hoffmann EM, Duda J, Eshraghi P, Hartmann D, Liss B, Schirmacher P, Kestler HA, Speicher MR, Rudolph KL. (2012) Disruption of Trp53 in livers of mice induces formation of carcinomas with bilineal differentiation. Gastroenterology, 142: 1229-1239 e1223.

[243] Tschaharganeh DF, Xue W, Calvisi DF, Evert M, Michurina TV, Dow LE, Banito A, Katz SF, Kastenhuber ER, Weissmueller S, Huang CH, Lechel A, Andersen JB, Capper D, Zender L, Longerich T, Enikolopov G, Lowe SW. (2014) p53-dependent Nestin regulation links tumor suppression to cellular plasticity in liver cancer. Cell, 158: 579-592.

[244] Lee CH, Chang CJ, Lin YJ, Yeh CN, Chen MF, Hsieh SY. (2009) Viral hepatitis-associated intrahepatic cholangiocarcinoma shares common disease processes with hepatocellular carcinoma. Br J Cancer, 100: 1765-1770.

[245] Cozzio A, Passegue E, Ayton PM, Karsunky H, Cleary ML, Weissman IL. (2003) Similar MLL-associated leukemias arising from self-renewing stem cells and short-lived myeloid progenitors. Genes Dev, 17: 3029-3035.

[246] Chen W, Kumar AR, Hudson WA, Li Q, Wu B, Staggs RA, Lund EA, Sam TN, Kersey JH. (2008) Malignant transformation initiated by Mll-AF9: gene dosage and critical target cells. Cancer Cell, 13: 432-440.

[247] Heuser M, Yun H, Berg T, Yung E, Argiropoulos B, Kuchenbauer F, Park G, Hamwi I, Palmqvist L, Lai CK, Leung M, Lin G, Chaturvedi A, Thakur BK, Iwasaki M, Bilenky M, Thiessen N, Robertson G, Hirst M, Kent D, Wilson NK, Gottgens B, Eaves C, Cleary ML, Marra M, Ganser A, Humphries RK. (2011) Cell of origin in AML: susceptibility to MN1-induced transformation is regulated by the MEIS1/AbdB-like HOX protein complex. Cancer Cell, 20: 39-52.

[248] Komuta M, Govaere O, Vandecaveye V, Akiba J, Van Steenbergen W, Verslype C, Laleman W, Pirenne J, Aerts R, Yano H, Nevens F, Topal B, Roskams T. (2012) Histological diversity in cholangiocellular carcinoma reflects the different cholangiocyte phenotypes. Hepatology, 55: 1876-1888.

[249] Hoadley KA, Yau C, Hinoue T, Wolf DM, Lazar AJ, Drill E, Shen R, Taylor AM, Cherniack AD, Thorsson V, Akbani R, Bowlby R, Wong CK, Wiznerowicz M, Sanchez-Vega F, Robertson AG, Schneider BG, Lawrence MS, Noushmehr H, Malta TM, Cancer Genome Atlas N, Stuart JM, Benz CC, Laird PW. (2018) Cell-of-Origin Patterns Dominate the Molecular Classification of 10,000 Tumors from 33 Types of Cancer. Cell, 173: 291-304 e296.

[250] Eilers M, Eisenman RN. (2008) Myc's broad reach. Genes Dev, 22: 2755-2766.

[251] Dang CV. (2012) MYC on the path to cancer. Cell, 149: 22-35.

[252] Takahashi K, Yamanaka S. (2006) Induction of pluripotent stem cells from mouse embryonic and adult fibroblast cultures by defined factors. Cell, 126: 663-676.

[253] Smith KN, Lim JM, Wells L, Dalton S. (2011) Myc orchestrates a regulatory network required for the establishment and maintenance of pluripotency. Cell Cycle, 10: 592-597.

[254] Shachaf CM, Kopelman AM, Arvanitis C, Karlsson A, Beer S, Mandl S, Bachmann MH, Borowsky AD, Ruebner B, Cardiff RD, Yang Q, Bishop JM, Contag CH, Felsher DW. (2004) MYC inactivation uncovers pluripotent differentiation and tumour dormancy in hepatocellular cancer. Nature, 431: 1112-1117.

[255] Arvanitis C, Felsher DW. (2006) Conditional transgenic models define how MYC initiates and maintains tumorigenesis. Semin Cancer Biol, 16: 313-317.

[256] Akita H, Marquardt JU, Durkin ME, Kitade M, Seo D, Conner EA, Andersen JB, Factor VM, Thorgeirsson SS. (2014) MYC activates stem-like cell potential in hepatocarcinoma by a p53-dependent mechanism. Cancer Res, 74: 5903-5913.

[257] Van Itallie C, Rahner C, Anderson JM. (2001) Regulated expression of claudin-4 decreases paracellular conductance through a selective decrease in sodium permeability. J Clin Invest, 107: 1319-1327.

[258] Furuse M, Hata M, Furuse K, Yoshida Y, Haratake A, Sugitani Y, Noda T, Kubo A, Tsukita S. (2002) Claudin-based tight junctions are crucial for the mammalian epidermal barrier: a lesson from claudin-1-deficient mice. J Cell Biol, 156: 1099-1111.

[259] Alexandre MD, Lu Q, Chen YH. (2005) Overexpression of claudin-7 decreases the paracellular Cl- conductance and increases the paracellular Na+ conductance in LLC-PK1 cells. J Cell Sci, 118: 2683-2693.

[260] Morita K, Furuse M, Fujimoto K, Tsukita S. (1999) Claudin multigene family encoding four-transmembrane domain protein components of tight junction strands. Proc Natl Acad Sci U S A, 96: 511-516.

[261] Kwon MJ. (2013) Emerging roles of claudins in human cancer. Int J Mol Sci, 14: 18148-18180.

[262] Singh AB, Sharma A, Dhawan P. (2010) Claudin family of proteins and cancer: an overview. J Oncol, 2010: 541957.

[263] Honda H, Pazin MJ, Ji H, Wernyj RP, Morin PJ. (2006) Crucial roles of Sp1 and epigenetic modifications in the regulation of the CLDN4 promoter in ovarian cancer cells. J Biol Chem, 281: 21433-21444.

[264] Chang TL, Ito K, Ko TK, Liu Q, Salto-Tellez M, Yeoh KG, Fukamachi H, Ito Y. (2010) Claudin-1 has tumor suppressive activity and is a direct target of RUNX3 in gastric epithelial cells. Gastroenterology, 138: 255-265 e251-253.

[265] Krishnan M, Singh AB, Smith JJ, Sharma A, Chen X, Eschrich S, Yeatman TJ, Beauchamp RD, Dhawan P. (2010) HDAC inhibitors regulate claudin-1 expression in colon cancer cells through modulation of mRNA stability. Oncogene, 29: 305-312.

[266] Kominsky SL, Argani P, Korz D, Evron E, Raman V, Garrett E, Rein A, Sauter G, Kallioniemi OP, Sukumar S. (2003) Loss of the tight junction protein claudin-7 correlates with histological grade in both ductal carcinoma in situ and invasive ductal carcinoma of the breast. Oncogene, 22: 2021-2033.

[267] Sobel G, Paska C, Szabo I, Kiss A, Kadar A, Schaff Z. (2005) Increased expression of claudins in cervical squamous intraepithelial neoplasia and invasive carcinoma. Hum Pathol, 36: 162-169.

[268] Tokes AM, Kulka J, Paku S, Szik A, Paska C, Novak PK, Szilak L, Kiss A, Bogi K, Schaff Z. (2005) Claudin-1, -3 and -4 proteins and mRNA expression in benign and malignant breast lesions: a research study. Breast Cancer Res, 7: R296-305.

[269] Resnick MB, Konkin T, Routhier J, Sabo E, Pricolo VE. (2005) Claudin-1 is a strong prognostic indicator in stage II colonic cancer: a tissue microarray study. Mod Pathol, 18: 511-518.

[270] Usami Y, Chiba H, Nakayama F, Ueda J, Matsuda Y, Sawada N, Komori T, Ito A, Yokozaki H. (2006) Reduced expression of claudin-7 correlates with invasion and metastasis in squamous cell carcinoma of the esophagus. Hum Pathol, 37: 569-577.

[271] Ueda J, Semba S, Chiba H, Sawada N, Seo Y, Kasuga M, Yokozaki H. (2007) Heterogeneous expression of claudin-4 in human colorectal cancer: decreased claudin-4 expression at the invasive front correlates cancer invasion and metastasis. Pathobiology, 74: 32-41.

[272] Martin TA, Jiang WG. (2009) Loss of tight junction barrier function and its role in cancer metastasis. Biochim Biophys Acta, 1788: 872-891.

[273] Ikenouchi J, Matsuda M, Furuse M, Tsukita S. (2003) Regulation of tight junctions during the epithelium-mesenchyme transition: direct repression of the gene expression of claudins/occludin by Snail. J Cell Sci, 116: 1959-1967.

[274] Lin X, Shang X, Manorek G, Howell SB. (2013) Regulation of the Epithelial-Mesenchymal Transition by Claudin-3 and Claudin-4. PLoS One, 8: e67496.

[275] Suh Y, Yoon CH, Kim RK, Lim EJ, Oh YS, Hwang SG, An S, Yoon G, Gye MC, Yi JM, Kim MJ, Lee SJ. (2013) Claudin-1 induces epithelial-mesenchymal transition through activation of the c-Abl-ERK signaling pathway in human liver cells. Oncogene, 32: 4873-4882.

[276] Philip R, Heiler S, Mu W, Buchler MW, Zoller M, Thuma F. (2015) Claudin-7 promotes the epithelial-mesenchymal transition in human colorectal cancer. Oncotarget, 6: 2046-2063.

[277] Herschkowitz JI, Simin K, Weigman VJ, Mikaelian I, Usary J, Hu Z, Rasmussen KE, Jones LP, Assefnia S, Chandrasekharan S, Backlund MG, Yin Y, Khramtsov AI, Bastein R, Quackenbush J, Glazer RI, Brown PH, Green JE, Kopelovich L, Furth PA, Palazzo JP, Olopade OI, Bernard PS, Churchill GA, Van Dyke T, Perou CM. (2007) Identification of conserved gene expression features between murine mammary carcinoma models and human breast tumors. Genome Biol, 8: R76.

[278] Hennessy BT, Gonzalez-Angulo AM, Stemke-Hale K, Gilcrease MZ, Krishnamurthy S, Lee JS, Fridlyand J, Sahin A, Agarwal R, Joy C, Liu W, Stivers D, Baggerly K, Carey M, Lluch A, Monteagudo C, He X, Weigman V, Fan C, Palazzo J, Hortobagyi GN, Nolden LK, Wang NJ, Valero V, Gray JW, Perou CM, Mills GB. (2009) Characterization of a naturally occurring breast cancer subset enriched in epithelial-to-mesenchymal transition and stem cell characteristics. Cancer Res, 69: 4116-4124.

[279] Prat A, Parker JS, Karginova O, Fan C, Livasy C, Herschkowitz JI, He X, Perou CM. (2010) Phenotypic and molecular characterization of the claudin-low intrinsic subtype of breast cancer. Breast Cancer Res, 12: R68.

[280] Asiedu MK, Ingle JN, Behrens MD, Radisky DC, Knutson KL. (2011) TGFbeta/TNF(alpha)-mediated epithelial-mesenchymal transition generates breast cancer stem cells with a claudin-low phenotype. Cancer Res, 71: 4707-4719.

[281] Liu T, Cheng W, Lai D, Huang Y, Guo L. (2010) Characterization of primary ovarian cancer cells in different culture systems. Oncol Rep, 23: 1277-1284.

[282] Qin W, Ren Q, Liu T, Huang Y, Wang J. (2013) MicroRNA-155 is a novel suppressor of ovarian cancer-initiating cells that targets CLDN1. FEBS Lett, 587: 1434-1439.

[283] Zhang GJ, Xiao HX, Tian HP, Liu ZL, Xia SS, Zhou T. (2013) Upregulation of microRNA-155 promotes the migration and invasion of colorectal cancer cells through the regulation of claudin-1 expression. Int J Mol Med, 31: 1375-1380.

[284] Boylan KL, Misemer B, De Rycke MS, Andersen JD, Harrington KM, Kalloger SE, Gilks CB, Pambuccian SE, Skubitz AP. (2011) Claudin 4 Is differentially expressed between ovarian cancer subtypes and plays a role in spheroid formation. Int J Mol Sci, 12: 1334-1358.

[285] Katsushima K, Shinjo K, Natsume A, Ohka F, Fujii M, Osada H, Sekido Y, Kondo Y. (2012) Contribution of microRNA-1275 to Claudin11 protein suppression via a polycomb-mediated silencing mechanism in human glioma stem-like cells. J Biol Chem, 287: 27396-27406.

[286] Paquet-Fifield S, Koh SL, Cheng L, Beyit LM, Shembrey C, Molck C, Behrenbruch C, Papin M, Gironella M, Guelfi S, Nasr R, Grillet F, Prudhomme M, Bourgaux JF, Castells A, Pascussi JM, Heriot AG, Puisieux A, Davis MJ, Pannequin J, Hill AF, Sloan EK, Hollande F. (2018) Tight Junction Protein Claudin-2 Promotes Self-Renewal of Human Colorectal Cancer Stem-like Cells. Cancer Res, 78: 2925-2938.

[287] Miyamori H, Takino T, Kobayashi Y, Tokai H, Itoh Y, Seiki M, Sato H. (2001) Claudin promotes activation of pro-matrix metalloproteinase-2 mediated by membrane-type matrix metalloproteinases. J Biol Chem, 276: 28204-28211.

[288] Agarwal R, D'Souza T, Morin PJ. (2005) Claudin-3 and claudin-4 expression in ovarian epithelial cells enhances invasion and is associated with increased matrix metalloproteinase-2 activity. Cancer Res, 65: 7378-7385.

[289] Oku N, Sasabe E, Ueta E, Yamamoto T, Osaki T. (2006) Tight junction protein claudin-1 enhances the invasive activity of oral squamous cell carcinoma cells by promoting cleavage of laminin-5 gamma2 chain via matrix metalloproteinase (MMP)-2 and membrane-type MMP-1. Cancer Res, 66: 5251-5257.

[290] de Oliveira SS, de Oliveira IM, De Souza W, Morgado-Diaz JA. (2005) Claudins upregulation in human colorectal cancer. FEBS Lett, 579: 6179-6185.

[291] Soini Y, Kinnula V, Kahlos K, Paakko P. (2006) Claudins in differential diagnosis between mesothelioma and metastatic adenocarcinoma of the pleura. J Clin Pathol, 59: 250-254.

[292] Moldvay J, Fabian K, Jackel M, Nemeth Z, Bogos K, Furak J, Tiszlavicz L, Fillinger J, Dome B, Schaff Z. (2017) Claudin-1 Protein Expression Is a Good Prognostic Factor in Non-Small Cell Lung Cancer, but only in Squamous Cell Carcinoma Cases. Pathol Oncol Res, 23: 151-156.

[293] Cheung ST, Leung KL, Ip YC, Chen X, Fong DY, Ng IO, Fan ST, So S. (2005) Claudin-10 expression level is associated with recurrence of primary hepatocellular carcinoma. Clin Cancer Res, 11: 551-556.

[294] Dhawan P, Singh AB, Deane NG, No Y, Shiou SR, Schmidt C, Neff J, Washington MK, Beauchamp RD. (2005) Claudin-1 regulates cellular transformation and metastatic behavior in colon cancer. J Clin Invest, 115: 1765-1776.

[295] Singh AB, Sharma A, Smith JJ, Krishnan M, Chen X, Eschrich S, Washington MK, Yeatman TJ, Beauchamp RD, Dhawan P. (2011) Claudin-1 up-regulates the repressor ZEB-1 to inhibit E-cadherin expression in colon cancer cells. Gastroenterology, 141: 2140-2153.

[296] Bhat AA, Ahmad R, Uppada SB, Singh AB, Dhawan P. (2016) Claudin-1 promotes TNF-alpha-induced epithelial-mesenchymal transition and migration in colorectal adenocarcinoma cells. Exp Cell Res, 349: 119-127.

[297] Miwa N, Furuse M, Tsukita S, Niikawa N, Nakamura Y, Furukawa Y. (2001) Involvement of claudin-1 in the beta-catenin/Tcf signaling pathway and its frequent upregulation in human colorectal cancers. Oncol Res, 12: 469-476.

[298] Grone J, Weber B, Staub E, Heinze M, Klaman I, Pilarsky C, Hermann K, Castanos-Velez E, Ropcke S, Mann B, Rosenthal A, Buhr HJ. (2007) Differential expression of genes encoding tight junction proteins in colorectal cancer: frequent dysregulation of claudin-1, -8 and -12. Int J Colorectal Dis, 22: 651-659.

[299] Kinugasa T, Huo Q, Higashi D, Shibaguchi H, Kuroki M, Tanaka T, Futami K, Yamashita Y, Hachimine K, Maekawa S, Nabeshima K, Iwasaki H, Kuroki M. (2007) Selective up-regulation of claudin-1 and claudin-2 in colorectal cancer. Anticancer Res, 27: 3729-3734.

[300] Huo Q, Kinugasa T, Wang L, Huang J, Zhao J, Shibaguchi H, Kuroki M, Tanaka T, Yamashita Y, Nabeshima K, Iwasaki H, Kuroki M. (2009) Claudin-1 protein is a major factor involved in the tumorigenesis of colorectal cancer. Anticancer Res, 29: 851-857.

[301] Bezdekova M, Brychtova S, Sedlakova E, Langova K, Brychta T, Belej K. (2012) Analysis of Snail-1, E-cadherin and claudin-1 expression in colorectal adenomas and carcinomas. Int J Mol Sci, 13: 1632-1643.

[302] Kinugasa T, Akagi Y, Ochi T, Tanaka N, Kawahara A, Ishibashi Y, Gotanda Y, Yamaguchi K, Shiratuchi I, Oka Y, Kage M, Shirouzu K. (2012) Increased claudin-1 protein expression in hepatic metastatic lesions of colorectal cancer. Anticancer Res, 32: 2309-2314.

[303] Matsuoka T, Mitomi H, Fukui N, Kanazawa H, Saito T, Hayashi T, Yao T. (2011) Cluster analysis of claudin-1 and -4, E-cadherin, and beta-catenin expression in colorectal cancers. J Surg Oncol, 103: 674-686.

[304] Nakagawa S, Miyoshi N, Ishii H, Mimori K, Tanaka F, Sekimoto M, Doki Y, Mori M. (2011) Expression of CLDN1 in colorectal cancer: a novel marker for prognosis. Int J Oncol, 39: 791-796.

[305] Higashi Y, Suzuki S, Sakaguchi T, Nakamura T, Baba S, Reinecker HC, Nakamura S, Konno H. (2007) Loss of claudin-1 expression correlates with malignancy of hepatocellular carcinoma. J Surg Res, 139: 68-76.

[306] Holczbauer A, Gyongyosi B, Lotz G, Torzsok P, Kaposi-Novak P, Szijarto A, Tatrai P, Kupcsulik P, Schaff Z, Kiss A. (2014) Increased expression of claudin-1 and claudin-7 in liver cirrhosis and hepatocellular carcinoma. Pathol Oncol Res, 20: 493-502.

[307] Bouchagier KA, Assimakopoulos SF, Karavias DD, Maroulis I, Tzelepi V, Kalofonos H, Karavias DD, Kardamakis D, Scopa CD, Tsamandas AC. (2014) Expression of claudins-1, -4, -5, -7 and occludin in hepatocellular carcinoma and their relation with classic clinicopathological features and patients' survival. In Vivo, 28: 315-326.

[308] Yoon CH, Kim MJ, Park MJ, Park IC, Hwang SG, An S, Choi YH, Yoon G, Lee SJ. (2010) Claudin-1 acts through c-Abl-protein kinase Cdelta (PKCdelta) signaling and has a causal role in the acquisition of invasive capacity in human liver cells. J Biol Chem, 285: 226-233.

[309] Kyuno D, Kojima T, Yamaguchi H, Ito T, Kimura Y, Imamura M, Takasawa A, Murata M, Tanaka S, Hirata K, Sawada N. (2013) Protein kinase Calpha inhibitor protects against downregulation of claudin-1 during epithelial-mesenchymal transition of pancreatic cancer. Carcinogenesis, 34: 1232-1243.

[310] Van Itallie CM, Anderson JM. (2013) Claudin interactions in and out of the tight junction. Tissue Barriers, 1: e25247.

[311] Xin S, Huixin C, Benchang S, Aiping B, Jinhui W, Xiaoyan L, Yu WB, Minhu C. (2007) Expression of Cdx2 and claudin-2 in the multistage tissue of gastric carcinogenesis. Oncology, 73: 357-365.

[312] Ikari A, Sato T, Watanabe R, Yamazaki Y, Sugatani J. (2012) Increase in claudin-2 expression by an EGFR/MEK/ERK/c-Fos pathway in lung adenocarcinoma A549 cells. Biochim Biophys Acta, 1823: 1110-1118.

[313] Dhawan P, Ahmad R, Chaturvedi R, Smith JJ, Midha R, Mittal MK, Krishnan M, Chen X, Eschrich S, Yeatman TJ, Harris RC, Washington MK, Wilson KT, Beauchamp RD, Singh AB. (2011) Claudin-2 expression increases tumorigenicity of colon cancer cells: role of epidermal growth factor receptor activation. Oncogene, 30: 3234-3247.

[314] Kim TH, Huh JH, Lee S, Kang H, Kim GI, An HJ. (2008) Down-regulation of claudin-2 in breast carcinomas is associated with advanced disease. Histopathology, 53: 48-55.

[315] Tabaries S, Dong Z, Annis MG, Omeroglu A, Pepin F, Ouellet V, Russo C, Hassanain M, Metrakos P, Diaz Z, Basik M, Bertos N, Park M, Guettier C, Adam R, Hallett M, Siegel PM. (2011) Claudin-2 is selectively enriched in and promotes the formation of breast cancer liver metastases through engagement of integrin complexes. Oncogene, 30: 1318-1328.

[316] Tabaries S, Dupuy F, Dong Z, Monast A, Annis MG, Spicer J, Ferri LE, Omeroglu A, Basik M, Amir E, Clemons M, Siegel PM. (2012) Claudin-2 promotes breast cancer liver metastasis by facilitating tumor cell interactions with hepatocytes. Mol Cell Biol, 32: 2979-2991.

[317] Morin PJ. (2005) Claudin proteins in human cancer: promising new targets for diagnosis and therapy. Cancer Res, 65: 9603-9606.

[318] Hewitt KJ, Agarwal R, Morin PJ. (2006) The claudin gene family: expression in normal and neoplastic tissues. BMC Cancer, 6: 186.

[319] Oshima T, Kunisaki C, Yoshihara K, Yamada R, Yamamoto N, Sato T, Makino H, Yamagishi S, Nagano Y, Fujii S, Shiozawa M, Akaike M, Wada N, Rino Y, Masuda M, Tanaka K, Imada T. (2008) Reduced expression of the claudin-7 gene correlates with venous invasion and liver metastasis in colorectal cancer. Oncol Rep, 19: 953-959.

[320] Shang X, Lin X, Alvarez E, Manorek G, Howell SB. (2012) Tight junction proteins claudin-3 and claudin-4 control tumor growth and metastases. Neoplasia, 14: 974-985.

[321] Michl P, Buchholz M, Rolke M, Kunsch S, Lohr M, McClane B, Tsukita S, Leder G, Adler G, Gress TM. (2001) Claudin-4: a new target for pancreatic cancer treatment using Clostridium perfringens enterotoxin. Gastroenterology, 121: 678-684.

[322] Kominsky SL, Vali M, Korz D, Gabig TG, Weitzman SA, Argani P, Sukumar S. (2004) Clostridium perfringens enterotoxin elicits rapid and specific cytolysis of breast carcinoma cells mediated through tight junction proteins claudin 3 and 4. Am J Pathol, 164: 1627-1633.

[323] Walther W, Petkov S, Kuvardina ON, Aumann J, Kobelt D, Fichtner I, Lemm M, Piontek J, Blasig IE, Stein U, Schlag PM. (2012) Novel Clostridium perfringens enterotoxin suicide gene therapy for selective treatment of claudin-3- and -4-overexpressing tumors. Gene Ther, 19: 494-503.

[324] Chen JS, Chen KT, Fan CW, Han CL, Chen YJ, Yu JS, Chang YS, Chien CW, Wu CP, Hung RP, Chan EC. (2010) Comparison of membrane fraction proteomic profiles of normal and cancerous human colorectal tissues with gel-assisted digestion and iTRAQ labeling mass spectrometry. FEBS J, 277: 3028-3038.

[325] de Souza WF, Fortunato-Miranda N, Robbs BK, de Araujo WM, de-Freitas-Junior JC, Bastos LG, Viola JP, Morgado-Diaz JA. (2013) Claudin-3 overexpression increases the malignant potential of colorectal cancer cells: roles of ERK1/2 and PI3K-Akt as modulators of EGFR signaling. PLoS One, 8: e74994.

[326] Ahmad R, Kumar B, Chen Z, Chen X, Muller D, Lele SM, Washington MK, Batra SK, Dhawan P, Singh AB. (2017) Loss of claudin-3 expression induces IL6/gp130/Stat3 signaling to promote colon cancer malignancy by hyperactivating Wnt/beta-catenin signaling. Oncogene, 36: 6592-6604.

[327] Jiang L, Yang YD, Fu L, Xu W, Liu D, Liang Q, Zhang X, Xu L, Guan XY, Wu B, Sung JJ, Yu J. (2014) CLDN3 inhibits cancer aggressiveness via Wnt-EMT signaling and is a potential prognostic biomarker for hepatocellular carcinoma. Oncotarget, 5: 7663-7676.

[328] Lodi C, Szabo E, Holczbauer A, Batmunkh E, Szijarto A, Kupcsulik P, Kovalszky I, Paku S, Illyes G, Kiss A, Schaff Z. (2006) Claudin-4 differentiates biliary tract cancers from hepatocellular carcinomas. Mod Pathol, 19: 460-469.

[329] Nichols LS, Ashfaq R, Iacobuzio-Donahue CA. (2004) Claudin 4 protein expression in primary and metastatic pancreatic cancer: support for use as a therapeutic target. Am J Clin Pathol, 121: 226-230.

[330] Michl P, Barth C, Buchholz M, Lerch MM, Rolke M, Holzmann KH, Menke A, Fensterer H, Giehl K, Lohr M, Leder G, Iwamura T, Adler G, Gress TM. (2003) Claudin-4 expression decreases invasiveness and metastatic potential of pancreatic cancer. Cancer Res, 63: 6265-6271.

[331] Ding L, Lu Z, Foreman O, Tatum R, Lu Q, Renegar R, Cao J, Chen YH. (2012) Inflammation and disruption of the mucosal architecture in claudin-7-deficient mice. Gastroenterology, 142: 305-315.

[332] Darido C, Buchert M, Pannequin J, Bastide P, Zalzali H, Mantamadiotis T, Bourgaux JF, Garambois V, Jay P, Blache P, Joubert D, Hollande F. (2008) Defective claudin-7 regulation by Tcf-4 and Sox-9 disrupts the polarity and increases the tumorigenicity of colorectal cancer cells. Cancer Res, 68: 4258-4268.

[333] Kuhn S, Koch M, Nubel T, Ladwein M, Antolovic D, Klingbeil P, Hildebrand D, Moldenhauer G, Langbein L, Franke WW, Weitz J, Zoller M. (2007) A complex of EpCAM, claudin-7, CD44 variant isoforms, and tetraspanins promotes colorectal cancer progression. Mol Cancer Res, 5: 553-567.

[334] Nakayama F, Semba S, Usami Y, Chiba H, Sawada N, Yokozaki H. (2008) Hypermethylation-modulated downregulation of claudin-7 expression promotes the progression of colorectal carcinoma. Pathobiology, 75: 177-185.

[335] Bornholdt J, Friis S, Godiksen S, Poulsen SS, Santoni-Rugiu E, Bisgaard HC, Lothe IM, Ikdahl T, Tveit KM, Johnson E, Kure EH, Vogel LK. (2011) The level of claudin-7 is reduced as an early event in colorectal carcinogenesis. BMC Cancer, 11: 65.

[336] Sauer T, Pedersen MK, Ebeltoft K, Naess O. (2005) Reduced expression of Claudin-7 in fine needle aspirates from breast carcinomas correlate with grading and metastatic disease. Cytopathology, 16: 193-198.

[337] Soini Y, Takasawa A, Eskelinen M, Juvonen P, Karja V, Hasegawa T, Murata M, Tanaka S, Kojima T, Sawada N. (2012) Expression of claudins 7 and 18 in pancreatic ductal adenocarcinoma: association with features of differentiation. J Clin Pathol, 65: 431-436.

[338] Kwak PB, Iwasaki S, Tomari Y. (2010) The microRNA pathway and cancer. Cancer Sci, 101: 2309-2315.

[339] Georges R, Bergmann F, Hamdi H, Zepp M, Eyol E, Hielscher T, Berger MR, Adwan H. (2012) Sequential biphasic changes in claudin1 and claudin4 expression are correlated to colorectal cancer progression and liver metastasis. J Cell Mol Med, 16: 260-272.

[340] Kaihara T, Kawamata H, Imura J, Fujii S, Kitajima K, Omotehara F, Maeda N, Nakamura T, Fujimori T. (2003) Redifferentiation and ZO-1 reexpression in liver-metastasized colorectal cancer: possible association with epidermal growth factor receptor-induced tyrosine phosphorylation of ZO-1. Cancer Sci, 94: 166-172.

DOI:10.14753/SE.2019.2291

10. LIST OF PUBLICATIONS

Cumulative impact factor (IF): 85.654

Publications related to the doctoral thesis (IF: 16.329):

- **Holczbauer Á**, Factor VM, Andersen JB, Marquardt JU, Kleiner D, Raggi C, Kitade M, Seo D, Akita H, Durkin M, Thorgeirsson SS. (2013) Modeling pathogenesis of primary liver cancer in lineage-specific mouse cell types. Gastroenterology, 145: 221-231. **IF: 13.926**

- **Holczbauer Á***, Gyöngyösi B*, Lotz G, Szijártó A, Kupcsulik P, Schaff Z, Kiss A. (2013) Distinct claudin expression profiles of hepatocellular carcinoma and metastatic colorectal and pancreatic carcinomas. J Histochem Cytochem, 61: 294-305. **IF: 2.403** (*These authors contributed equally)

Publications unrelated to the doctoral thesis (IF: 69.325):

- Vermulst M, Denney AS, Lang MJ, Hung CW, Moore S, Moseley MA, Thompson JW, Madden V, Gauer J, Wolfe KJ, Summers DW, Schleit J, Sutphin GL, Haroon S, **Holczbauer A**, Caine J, Jorgenson J, Cyr D, Kaeberlein M, Strathern JN, Duncan MC, Erie DA. (2015) Transcription errors induce proteotoxic stress and shorten cellular lifespan. Nat Commun, 6: 8065. **IF: 11.329**

- **Holczbauer Á***, Gyöngyösi B*, Lotz G, Törzsök P, Kaposi-Novák P, Szijártó A, Tátrai P, Kupcsulik P, Schaff Z, Kiss A. (2014) Increased expression of claudin-1 and claudin-7 in liver cirrhosis and hepatocellular carcinoma. Pathol Oncol Res, 20: 493-502. **IF: 1.855** (*These authors contributed equally)

- Raggi C, Factor VM, Seo D, **Holczbauer Á**, Gillen MC, Marquardt JU, Andersen JB, Durkin M, Thorgeirsson SS. (2014) Epigenetic reprogramming modulates malignant properties of human liver cancer. Hepatology, 59: 2251-2262. IF: **11.055**

- Kitade M, Factor VM, Andersen JB, Tomokuni A, Kaji K, Akita H, **Holczbauer Á**, Seo D, Marquardt JU, Conner EA, Lee SB, Lee YH, Thorgeirsson SS. (2013) Specific fate decisions in adult hepatic progenitor cells driven by MET and EGFR signaling. Genes Dev, 27: 1706-1717. **IF: 12.639**

- Lee SB, Seo D, Choi D, Park KY, **Holczbauer Á**, Marquardt JU, Conner EA, Factor VM, Thorgeirsson SS. (2012) Contribution of hepatic lineage stage-specific donor memory to the differential potential of induced mouse pluripotent stem cells. Stem Cells, 30: 997-1007. **IF: 7.701**

- Marquardt JU, Raggi C, Andersen JB, Seo D, Avital I, Geller D, Lee YH, Kitade M, **Holczbauer Á**, Gillen MC, Conner EA, Factor VM, Thorgeirsson SS. (2011) Human hepatic cancer stem cells are characterized by common stemness traits and diverse oncogenic pathways. Hepatology, 54: 1031-1042. **IF: 11.665**

- Nemes B, Doros A, **Holczbauer Á**, Sárváry E, Nagy P, Lengyel G, Kiss A, Schaff Z. (2009) Expression pattern of molecular chaperones after liver transplantation in hepatitis C positive recipients. Relation to serum HCV-RNA titers. Interv Med Appl Sci, 1: 35-40. **IF: -**

- Szabó E, Korpos E, Batmunkh E, Lotz G, **Holczbauer Á**, Kovalszky I, Deák F, Kiss I, Schaff Z, Kiss A. (2008) Expression of matrilin-2 in liver cirrhosis and hepatocellular carcinoma. Pathol Oncol Res, 14: 15-22. **IF: 1.260**

- Batmunkh E, Tátrai P, Szabó E, Lódi C, **Holczbauer Á**, Páska C, Kupcsulik P, Kiss A, Schaff Z, Kovalszky I. (2007) Comparison of the expression of agrin, a basement membrane heparan sulfate proteoglycan, in cholangiocarcinoma and hepatocellular carcinoma. Hum Pathol, 38: 1508-1515. **IF: 3.034**

- Halász J*, **Holczbauer Á***, Páska C, Kovács M, Benyó G, Verebély T, Schaff Z, Kiss A. (2006) Claudin-1 and claudin-2 differentiate fetal and embryonal components in human hepatoblastoma. Hum Pathol, 37: 555-561. **IF: 2.810** (*These authors contributed equally)

- Lódi C, Szabó E, **Holczbauer Á**, Batmunkh E, Szijártó A, Kupcsulik P, Kovalszky I, Paku S, Illyés G, Kiss A, Schaff Z. (2006) Claudin-4 differentiates biliary tract cancers from hepatocellular carcinomas. Mod Pathol, 19: 460-469. **IF: 3.753**

- Győrffy H*, **Holczbauer Á***, Nagy P, Szabó Z, Kupcsulik P, Páska C, Papp J, Schaff Z, Kiss A. (2005) Claudin expression in Barrett's esophagus and adenocarcinoma. Virchows Arch, 447: 961-968. **IF: 2.224** (*These authors contributed equally)

DOI:10.14753/SE.2019.2291

11. ACKNOWLEDGEMENTS

I would like to thank all the colleagues and friends in Hungary and in the United States of America who helped me during my research.

I wish to express my sincere gratitude to Professor Dr. Zsuzsa Schaff, former director of the 2nd Department of Pathology, Semmelweis University, who gave me the opportunity to work at the Department, encouraged and supported me during the whole time, and introduced me to Dr. Snorri S. Thorgeirsson.

I would like to express my special appreciation and gratitude to my enthusiastic Ph.D. advisor Professor Dr. András Kiss, director of the 2nd Department of Pathology, Semmelweis University, for the continuous support of my Ph.D. study and related research, and for supporting me academically and emotionally through the rough road to finish this thesis.

I wish to express my gratitude to Dr. Snorri S. Thorgeirsson, director of the Laboratory of Experimental Carcinogenesis, National Institutes of Health, for providing me with the opportunity to work in his laboratory, encouraging me to step out of my comfort zone and allowing me to grow as a research scientist.

I deeply thank my dear friend and former colleague at the National Cancer Institute, a true modern day renaissance man, Dr. Chi-Ping Day, who was always ready to guide and encourage me, and engaged me in discussions ranging from fundamental concepts in cancer biology to evolution of Chinese characters.

I would also like to thank my mentor at the National Cancer Institute, Dr. Suresh Arya who taught me about the beauty of conducting good science, and the art and elegance of a great experiment.

I am grateful to my former colleagues at the 2nd Department of Pathology for their valuable contribution and help. My special thanks to Dr. Benedek Gyöngyösi, Dr. Hajnalka

DOI:10.14753/SE.2019.2291

Győrffy, Dr. Judit Halász, Dr. Erzsébet Szabó, Dr. Csaba Lódi, Dr. Enkhjargal Bathmunkh, and Dr. Gábor Lotz.

I also express my gratitude to my former colleagues at the Laboratory of Experimental Carcinogenesis for their kind help, especially to Dr. Chiara Raggi, Tanya Hoang, Anita Ton, Dr. Marian Durkin, Dr. Hirofumi Akita, Dr. Mitsuteru Kitade, Dr. Daekwan Seo, Dr. Jens U. Marquardt, Dr. Jesper B. Andersen, and Dr. Elizabeth A. Conner.

Finally, I would like to express my deepest gratitude to my family for unconditional support.